

INFORMATION TO USERS

The most advanced technology has been used to photograph and reproduce this manuscript from the microfilm master. UMI films the text directly from the original or copy submitted. Thus, some thesis and dissertation copies are in typewriter face, while others may be from any type of computer printer.

The quality of this reproduction is dependent upon the quality of the copy submitted. Broken or indistinct print, colored or poor quality illustrations and photographs, print bleedthrough, substandard margins, and improper alignment can adversely affect reproduction.

In the unlikely event that the author did not send UMI a complete manuscript and there are missing pages, these will be noted. Also, if unauthorized copyright material had to be removed, a note will indicate the deletion.

Oversize materials (e.g., maps, drawings, charts) are reproduced by sectioning the original, beginning at the upper left-hand corner and continuing from left to right in equal sections with small overlaps. Each original is also photographed in one exposure and is included in reduced form at the back of the book.

Photographs included in the original manuscript have been reproduced xerographically in this copy. Higher quality 6" x 9" black and white photographic prints are available for any photographs or illustrations appearing in this copy for an additional charge. Contact UMI directly to order.

U·M·I

University Microfilms International
A Bell & Howell Information Company
300 North Zeeb Road, Ann Arbor, MI 48106-1346 USA
313. 761-4700 800'521-0600

Order Number 9107019

**Composition and distribution of carbonates, sulfates, and
hydrates on the Martian surface from earth-based spectroscopy
between 3 μm –5 μm**

Blaney, Diana Lee, Ph.D.

University of Hawaii, 1990

U·M·I
300 N. Zeeb Rd.
Ann Arbor, MI 48106

COMPOSITION AND DISTRIBUTION OF CARBONATES, SULFATES,
AND HYDRATES ON THE MARTIAN SURFACE FROM EARTHBASED
SPECTROSCOPY BETWEEN 3 μm - 5 μm

A DISSERTATION SUBMITTED TO THE GRADUATE DIVISION OF THE
UNIVERSITY OF HAWAII IN PARTIAL FULFILLMENT
OF THE REQUIREMENTS FOR THE DEGREE

DOCTOR OF PHILOSOPHY

IN GEOLOGY AND GEOPHYSICS

AUGUST 1990

By

Diana L. Blaney

Dissertation Committee

Thomas B. McCord, Chairperson

Fraser P. Fanale

Bernard Ray Hawke

John Mahoney

William M. Sinton

Acknowledgments

I would like to thank the following people without whom this dissertation would not have been possible: Tom McCord -who gave guidance throughout the last five years and let me explore different directions; Fraser Fanale -who provided guidance in the perilous world of Martian volatiles; Susan Postawko and Aaron Zent -who acted as sounding boards for various ideas on Martian surface evolution (some of which even made it into this dissertation); Paul Lucey -who gave me advice on almost every facet of my graduate experience; Pam Owensby -who showed me the nuts and bolts of observing; the engineering and computer staff at PGD, Karl Hink, Tim Williams, Jeff Bosel, Terry Friedman, and Julianna Lo -who helped me cope with packing for observing runs, building instruments, keeping the lab spec running, specpr, GARP, ect. ect. ect.; Cass Combs and Beth Clark -who worked during the long nights at Mauna Kea during the opposition and helped keep me awake, sane, and functioning; the staff at both the IRTF and UH88" -who helped keep things working (with a special thanks to Alan Tokunaga and Kris Selgren); the PGD faculty, B. Ray Hawke, Lionel Wilson, Jeff Bell, Johnathon Gradie, Stan Zisk, Peter Mougini-Mark -who gave advice throughout the last five years ; John Mahoney and Bill Sinton, who provided balance and insight during my defense; the other graduate students during my graduate student career, Ed Cloutis, Lisa Gaddis, Ted Roush, Eileen Roush, Joan Hayashi-Smith, Pam Blake, Marcia Nelson, Duncan Munro, Bruce Campbell, Jim Bell, Barb Bruno, and Jill Mahoney -who made Wednesday afternoons a crucial part of my education.

And to my parents- Without whom this would not have happened. Their encouragement, belief in me, and love provided the inner core of strength I needed to pursue my dreams.

Abstract

Earth-based telescopic data provides information on the mineralogy of the Martian surface. Data was collected during the 1986 and 1988 Earth-Mars oppositions between 3 μm and 5 μm to study carbonates, sulfates, and hydrates. The 1986 data was at 3% spectral resolution with a spatial spot diameter of 2000 km and covered a wavelength region between 2.5 μm and 4.2 μm . The 3 μm bound water band was clearly observed and an upper limit of 3 - 5 wt% carbonate was established for the regions measured based on comparisons with laboratory mixtures of carbonates and Mauna Kea palagonite, a Martian soil analog.

The 1988 data had $1/3$ % spectral resolution between 3.2 μm and 5.1 μm with a 900 km spatial resolution. These data indicate that there is substantial variation (20 %) in the depth of the 3 μm bound water band which is not correlated with atmospheric absorptions. Faint (<1%) atmospheric absorptions caused by isotopically heavy CO₂ were detected at 3.6 μm and 3.81 μm . An upper limit of 1 - 3 wt% carbonate was made for these regions. The implications of low carbonate abundance for climate change and weathering is explored and several models suggested. An absorption at 4.5 μm was also detected. This absorption is consistent with sulfates in mineral structure that preserves tetrahedral symmetry.

Table of Contents

Acknowledgements.....	iii.
Abstract.....	iv.
List of Tables.....	viii.
List of Figures	ix.
Chapter 1. Introduction	1.
I. Abstract.....	1.
II. Volatiles on the Martian Surface.....	2.
III. Carbonates.....	2.
IV. Sulfates.....	7.
V. Hydrates.....	8.
VI. Summary.....	10.
References.....	11.
Chapter 2. Infrared Spectroscopy of Molecules.....	15.
I. Introduction.....	15.
II. Vibrational Absorptions.....	15.
III. Bound Water.....	18.
IV. Carbonates.....	18.
V. Sulfates.....	19.
References.....	20.
Chapter 3. An Observational Search for Carbonates on Mars.....	32.
I. Abstract.....	33.
II. Review of Support for Carbonates on Mars.....	34.
III. Review of Previous Measurements	38.
IV. New Mars Observations.....	39.
V. Supporting Laboratory Measurements.....	41.

VI. Thermal Modeling.....	43.
VII. Interpretation	44.
Acknowledgments.....	46.
References.....	47.
Note	59.

Chapter 4. Constraints on the Climatic and Weathering Histories of Mars

From Earth-Based Near Infrared Spectroscopy between 3.2 and 4.2 μm.....	60.
I. Abstract.....	61.
II. Introduction.....	61.
III. Previous Measurements	62.
III. Observations.....	64.
IV. Description of the Spectra.....	65.
A. General Characteristics	65.
B. Isotopically Heavy CO ₂	66.
C. Hydration.....	67.
D. Scapolite.....	69.
E. Carbonates	70.
V. Implications of the Lack of Carbonate Absorption Features	72.
A. Model 1: The observed upper limit on carbonate abundance (i.e. less than 1 wt.%) is representative of the Martian regolith	72.
B. Model 2: Carbonate deposits formed in isolated areas or are located at depth.....	74.
C. Model 3: The low carbonate abundance is the result secondary weathering processes which have removed carbonates from the regolith	76.
D. Model 4: Weathering environments on Mars did not form carbonates.....	78.
VI. Conclusions.....	80.
Acknowledgments.....	83.
References.....	84.

Chapter 5. Spectroscopy of Mars between 4.4 μm and 5.5 μm :	
Indications of Sulfate Minerals.....	102.
I. Introduction.....	102.
II. Observations.....	103.
III. Thermal Modeling.....	104.
IV. Atmospheric Modeling	108.
V. Detection of an Absorption Feature at $\sim 4.5 \mu\text{m}$ -- Indications of Sulfates.....	111.
VI. Spatial Variation in the 4.5 μm Band Depth -- Implications for Sulfate Distribution.....	113.
VII. Conclusions	114.
References.....	115.
Chapter 6. Conclusions	149.
Bibliography	151.

List of Tables

Table 2.1 Sulfate Infrared Absorptions and Symmetry Groups.....	21.
Table 3.1. Observational Parameters for Mars Measurements Taken on September 19, 1986.	50.
Table 4.1. .Observing Information.	89.
Table 4.2. 3.81 μm Band Depth	90.
Table 4.3. Slope between 3.2 μm and 3.6 μm	91.
Table 4.4. Thermodynamically stable weathering products of a basalt with the same composition as Shergotty weathered on Mars.....	92.
Table 5.1. Observing Information	118.
Table 5.2. 3.81 μm Band Depth	119.
Table 5.3. Slope between 3.2 μm and 3.6 μm (Hydration state) as compared to 4.5 μm band strength.....	120.

List of Figures

Figure 2.1. Normal mode of vibration of a ball and spring model of a diatomic molecule such as HCl	22.
Figure 2.2. Plots of mass displacement versus time for harmonic and anharmonic vibrations.....	23.
Figure 2.3. Symmetry elements of the C_{2v} point group	24.
Figure 2.4. Normal modes of vibrations of water molecules.....	25.
Figure 2.5. Symmetry elements of the D_{3h} point group	26.
Figure 2.6. Normal modes of vibration of planar XY_3 molecules such as CO_3^{-2}	27.
Figure 2.7. Symmetry elements of the a) D_3 and b) C_s point groups.....	28.
Figure 2.8. Symmetry elements of the T_d point group	29.
Figure 2.9. Normal modes of vibration of tetrahedral XY_4 molecules.....	30.
Figure 2.10. Types of sulfate complexes, their symmetry groups, and vibrational degeneracy	31.
Figure 3.1. Locations of the four areas observed on Mars on September 19, 1986. Base map from U.S. Geologic Survey I-1535, (1985).....	51.
Figure 3.2. Ratios of the spectra of the four Mars regions (numerator) designated Hellas, Arabia, Syrtis and North East Highlands and the star Tau Sagittarius (denominator).....	52.

Figure 3.3. Reflectance spectra from 0.6 to 4.4 μm of reagent grade calcite, 20, 10, 5, and 3 weight percent mixture of calcite in Mauna Kea palagonite (MKP), and Mauna Kea palagonite.....	53.
Figure 3.4. Reflectance spectra from .6 to 4.4 μm of Icelandic spar calcite, 20,10, 5, and 3 weight percent calcite in Mauna Kea palagonite (MKP), and Mauna Kea palagonite.....	54.
Figure 3.5. Reflectance spectra from 2.4 to 4.4 μm of magnesite, 20, 10, 5, and 3 weight percent magnesite in Mauna Kea palagonite (MKP), and Mauna Kea palagonite.....	55.
Figure 3.6. Reflectance spectra of magnesite at 300K, phase angle 30°, and at 77°K, phase angle 7° between 2.4 and 4.4 μm	56.
Figure 3.7. Modeled results of a mixture of 5 wt% reagent calcite in Mauna Kea palagonite at temperatures of 210K, 230K, 250K, 270K, and 285K as it would appear if observed on Mars	57.
Figure 3.8. Mars spectra from 3.7 to 4.0 μm for Hellas, Arabia, Syrtis, and North East Highlands with a straight line continuum removed using values at 3.75 and 3.96 μm	58.
Figure 4.1. Locations of the eight regions observed. Base map Scott and Carr (1977) Geologic Map of Mars.....	93.
Figure 4.2. Locations of the eight regions observed. Base map is USGS Map I-1535, (1985) showing shaded relief and surface markings.....	94.
Figure 4.3. Spectra for eight ~900-km diameter regions on Mars reduced using the standard star BS437 and normalized to unity at 3.9133 μm	95.

Figure 4.4. Spectra from Figure 1 with straight line continua removed.....96.

Figure 4.5. Co-added Mars spectra with continuum removed
by fitting a linear least squares fit through all data points
between 3.4 μm and 4.05 μm plotted against an model 2 airmass
Mars atmosphere calculated by Dave Crisp.....97.

Figure 4.6. Spectra with continuum removed in the 4 μm region98.

Figure 4.7. Slope between 3.2 μm and 3.4 μm versus 3.8 μm
band depth.....99.

Figure 4.8. Spectrum of scapolite plotted above spectrum from the
Chryse region of Mars..... 100.

Figure 4.9. Thermal emission for carbonates at 4 μm 101.

Figure 5.1. Locations of the eight regions observed . Base map
Scott and Carr (1977) geologic map of Mars..... 121.

Figure 5.2. Locations of the eight regions observed . Base map is
USGS Map I-1535, (1935) showing shaded relief and surface markings... 122.

Figure 5.3. Spectra for eight ~900-km diameter regions on Mars reduced
using the standard star BS437 and normalized to unity at 4.71 μm 123.

Figure 5.4. Comparison of solar flux and thermal flux at Mars..... 124.

Figure 5.5a. Reflectance and emissivity of basalt grain size <34 μm 125.

Figure 5.5b. Reflectance and emissivity of Mauna Kea palagonite
grain size <34 μm 126.

Figure 5.6a. Flux from a basaltic surface on Mars at temperatures
ranging from 200K - 270K..... 127.

Figure 5.6b. Flux from a palagonite surface on Mars at temperatures ranging from 200K - 270K.....	128.
Figure 5.7a. Flux from a basaltic surface on Mars at temperatures ranging from 200K - 270K normalized to 1.0 at 4.46 μm	129.
Figure 5.7b. Flux from a palagonite surface on Mars at temperatures ranging from 200K - 270K normalized to 1.0 at 4.46 μm	130.
Figure 5.8. Flux from a basalt and a palagonite surface on Mars at temperatures ranging from 200K - 270K normalized to 1.0 at 4.46 μm	131.
Figure 5.9a. Encrenaz model CO ₂ transmission at P = 1, 3, 5, 6, and 7 mbar, T = 240K, airmass = 2.0.....	132.
Figure 5.9b. Encrenaz model CO transmission at P = 1, 3, 5, 6, and 7 mbar, T = 240K, airmass = 2.0, CO / CO ₂ = 0.002.....	133.
Figure 5.9c. Encrenaz model Mars atmospheric transmission at P = 1, 3, 5, 6, and 7 mbar, T = 240K, airmass = 2.0, CO / CO ₂ = 0.002.....	134.
Figure 5.10a. Encrenaz model CO ₂ transmission at P = 7 mbar, T = 230K, 240K, and 250K, airmass = 2.0.....	135.
Figure 5.10b. Encrenaz model CO transmission at P = 7 mbar, T = 230K, 240K, and 250K, airmass = 2.0, CO / CO ₂ = 0.002.....	136.
Figure 5.10c. Encrenaz model Mars atmospheric transmission at P = 7 mbar, T = 230K, 240K, and 250K, airmass = 2.0, CO / CO ₂ = 0.002.....	137.
Figure 5.11a. Encrenaz model CO ₂ transmission at P = 7 mbar, T = 240K, airmass = 1.0, 1.75, 2.0, and 4.0.....	138.

Figure 5.11b. Encrenaz model CO transmission at P = 7 mbar,
T = 240K, airmass = 1.0, 1.75, 2.0, and 4.0, CO / CO₂ = 0.002..... 139.

Figure 5.11c. Encrenaz model Mars atmospheric transmission at P = 7 mbar,
T = 240K, airmass = 1.0, 1.75, 2.0, and 4.0, CO / CO₂ = 0.002..... 140.

Figure 5.12a. Encrenaz model CO₂ transmission at P = 7 mbar,
T = 240K, airmass = 2.0 141.

Figure 5.12b. Encrenaz model CO transmission at P = 7 mbar,
T = 240K, airmass = 2.0, CO / CO₂ = 0.001, 0.002, 0.004 142.

Figure 5.12c. Encrenaz model Mars atmospheric transmission at
P = 7 mbar, T = 240K, airmass = 2.0,
CO / CO₂ = 0.001, 0.002, and 0.004..... 143.

Figure 5.13. Representative spectra (Argyre region) and Mars model
atmosphere of 7 mbar, 2 airmass, 240K, and CO / CO₂ with atmospheric
and surface absorptions labeled..... 144.

Figure 5.14. Reagent MgSO₄, gypsum, and anhydrite reflectance spectra.
Spectra are relative to sulfur and have a grain size of <34 μm. Spectra
measured at 2 cm⁻¹ resolution 145.

Figure 5.15. Reagent MgSO₄, gypsum, and anhydrite reflectance
spectra. Spectra convolved and interpolated to wavelengths of the
telescopic observations..... 146.

Figure 5.16. Gypsum multiplied by model atmospheric transmission
(7 mbar, 240K, 2 airmass, CO / CO₂ 0.002) over Argyre spectra..... 147.

Figure 5.17. Spectra for four regions with similar 3.81 μm band depths ... 148.

Chapter 1.

Introduction

I. Abstract

The surface of Mars has been interacting with the volatiles in the Martian atmosphere and regolith for the last 4.5 billion years. Unlike the earth, where the products of volatile - surface interactions can be determined using analytical geochemical techniques, the mineralogy of weathering products on the Martian surface must currently be determined remotely. Weathering products represent a large storage reservoir for volatiles such as water, carbon dioxide, and sulfur dioxide. Earth-based spectroscopy provides a technique to determine the composition and abundance of minerals on the Martian surface that have absorption features in the wavelengths measured.

The work presented here contains data collected during the 1986 and 1988 Earth-Mars oppositions. The dissertation focuses on three types of minerals that have absorptions in the wavelength region between 3 μm - 5 μm (hydrates, carbonates, and sulfates) and is divided into six chapters. The first deals with the evidence for the presence of carbonates, sulfates and hydrates on Mars. The second chapter discusses spectroscopy as a technique for determining mineralogy. Chapters three, four, and five provide the bulk of the dissertation and are written as stand-alone scientific papers. Chapter three is based on data collected at the University of Hawaii 88" telescope during the 1986 opposition and has been published in the Journal of Geophysical Research. Chapter 4 and 5 are based on data obtained during the 1988 opposition at the NASA Infrared Telescope Facility. Chapter 4 has been submitted to the Journal of Geophysical Research and chapter 5 is in preparation for submittal. The final chapter provides a synthesis of the material and suggestions for future research directions.

II. Volatiles on the Martian Surface

Although Mars is often thought of as a cold arid world, the surface of Mars has clearly undergone geochemical alteration. Though the initial composition of the Martian surface is igneous, the current optical surface of Mars - unlike the Moon and Mercury - is not dominated by a fragmental regolith which preserves the original igneous character of the surface. The red color of Mars, caused by the presence of Fe^{3+} electronic transitions, is perhaps the most obvious example of the altered nature of the surface. The weathering environments that produced the chemically altered Martian materials are unknown. Therefore, the characterization of these alteration products is an important step in identifying Martian weathering environments as well as estimating volatile reservoirs.

III. Carbonates

Reasons for postulating carbonates on the Martian surface are partially linked to the belief in an early, warm, wet Mars. A more clement Mars has been a popular idea since dendritic valley networks were discovered. The morphology of these channels indicate that they formed by near-surface groundwater sapping (Sharp, 1973; Piere, 1980). However, the almost total confinement of these features to areas that are located in the ancient heavily cratered terrain suggests that Mars had a different climate during its first billion or so years. Indeed, Schultz (1986) suggests that a change in the erosion rate and rate of valley network formation occurred about the time the Argyre impact basin was formed. The lack of any evidence for "recent" extensive valley networks indicates that some factor (surface temperature, atmospheric pressure, geothermal gradient, regolith volatile content) about Mars was different early in its history. A warmer climate is strong candidate for this difference between early Mars and the present. If these features indicate

that Mars did indeed have a substantially warmer climate early in its history, the most likely cause is a carbon dioxide induced greenhouse effect.

Estimates of the partial pressure of carbon dioxide needed to raise the average surface temperature to 273 K are about 3-5 bars (Postawko and Kuhn, 1986; Pollack and Black, 1979; Postawko, personal communication 1988) taking into account the reduced solar luminosity early in solar history. Current estimates of the storage capacity of the known reservoirs of carbon dioxide (the atmosphere, regolith, and south polar cap) from Fanale et al. (1982), Fanale and Cannon (1979) and Pollack (1979) account for only about 0.07 to 0.7 bars. For this reason, as for the Earth, carbonates have been invoked as a major reservoir of carbon dioxide that is no longer available to interact with the dynamic reservoirs (e.g. Pollack and Yung, 1980, Toon et. al., 1980, Pollack et al., 1987)

Of course, the amount of carbonates formed depends on the total amount of carbon dioxide available. The estimates of 3 - 5 bars of carbon dioxide needed to raise the temperature above 273 K are only lower limits of the amount of carbon dioxide possibly outgassed (if carbon dioxide greenhouse warming occurred). Cosmochemical arguments comparing the volatile inventories of the Earth, Venus, and Mars indicate that as much as 10 bars of carbon dioxide could have been outgassed from Mars (Pollack and Black 1982).

Carbon dioxide abundance is not the only control on carbonate formation. The availability of water, both to leach cations from rock and to dissolve carbon dioxide, is a critical control on the rate of carbonate formation. Estimates of the volume of water outgassed also can set limits on the amount of carbon dioxide available. Therefore, the phase distribution and abundance of water early in Mars' history is an important control on the evolution of carbon dioxide. Direct estimation of water and carbon dioxide abundances is not possible. However, examination of geomorphic features attributed to water combined with geochemical evidence can set reasonable bounds on the abundance of water. These bounds, though, cannot be used directly to determine the current Martian carbon dioxide/carbonate inventory because of permanent atmospheric loss processes, such as

atmospheric cratering and hydrodynamic escape. Examination of the estimates of water abundances is useful, however, in setting reasonable bounds on the outgassed inventory of carbon dioxide.

There is a large body of evidence supporting the presence of substantial amounts of water on Mars. Ample geomorphic evidence, such as outwash channels, debris aprons, and fretted terrain, exists for the presence of water, but the form and abundance of the water is uncertain. Estimates of the abundance of water on Mars, derived primarily from the volumes of the outwash channels, yield an abundance of outgassed water corresponding to a global liquid layer with depths of 500 to 1,000 m (Carr, 1986). The geochemical evidence, however, is more enigmatic.

Initial consideration of rare gas composition and nitrogen isotope ratios measured by Viking produced estimates of a water layer only 10-100 m thick (Anders and Owen, 1977; Morgan and Anders, 1979; McElroy et al., 1977). The complexities of the rare gas patterns of Mars, the Earth, and Venus prevent construction of a simple picture of volatile acquisition by planets, and the rare gas patterns may have very little to do with the abundance of water and carbon dioxide (Pollack and Black, 1979; Watkins and Lewis, 1986). Nitrogen isotope ratios are affected by nitrate formation rates which are unknown for early Mars (McElroy and Yung, 1977; Yung and McElroy, 1979). Meteorite data from a group of basaltic achondrites thought to originate on Mars has also been used to estimate the volatile content of Mars.

The SNC (S=Shergotty, N=Nahkla, and C=Chassigney after the type meteorites) meteorites are a group of basaltic achondrites thought to originate on Mars due to their young igneous crystallization ages, ~1.3 billion years (Wood and Ashwal 1981) and their nitrogen and argon isotope patterns (Becker and Pepin 1984). Dreibus and Wanke (1984, 1986) concluded, based on the composition of these meteorites and planetary accretion models, that a large portion of the water present during accretion was used largely to oxidize the metallic iron in Mars and that consequently, Mars could have outgassed only

1-50 m of water. Huguenin and Harris (1986) point out that slight changes in the amount of FeO accreting into the planet could lead to a volatile-rich Mars. Although the exact volatile content of Mars is unknown, it is clear that the possibility exists that Mars may be volatile-rich. If the estimates of 500-1000 m of water degassed are correct, then 10-20 bars of carbon dioxide should have been degassed also (Carr, 1986) and perhaps been available for carbonate formation.

Carbonate formation should not be limited to Mars' distant past. Normal weathering processes under current Martian conditions also would tend to produce carbonates and other salts, providing that thermodynamic equilibrium is reached (Gooding, 1978). Fayalite, diopside, augite, and anorthite all weather to calcite and magnesite or dolomite if equilibrium is reached. Siderite could also be a metastable weathering product (Gooding, 1978). Though these deposits would not be as extensive as massive carbonate deposits formed in an era of warm temperatures and abundant surface water, weathering considerations alone indicate that carbonates should exist on the Martian surface regardless of whether there was an early clement climate. Whether the abundance of carbonate formed from this process is sufficient to be detectable at present at the optical surface is unknown.

Carbonate formation from evaporite deposits is another possibility. Variable radar reflectivity in the Solis Lacus region has been interpreted as the melting of near-surface ice (Zisk and Mougini-Mark, 1980). Roth et al. (1985) suggested that the reflectivity may be seasonally variable over a wide range of latitudes. The existence of near-surface water allows the migration of salt-rich solutions toward the surface to form salts. Under present conditions brines are not stable relative to the polar cold-trap (Fanale and Clark, 1983); however, non-equilibrium brines are possible (Zent and Fanale, 1986). In addition, the occurrence of large igneous intrusive events near water/ice-rich layers also should have created ionic aqueous solutions that migrated toward the surface. Thus, salt formation by the evaporation of brines on the surface of Mars could have occurred, but the scale and composition of such salt deposits are unknown.

McKay and Nedell (1988) have proposed that the layered deposits in Valles Marineris formed by carbonate precipitation, similar to the carbonates formed in iced-over Antarctic lakes. The young age of these features rules out any connection with carbonates formed early in Martian history.

Viking lander experiments, though not directly measuring salt content of the surface of Mars, indicate that salts are present. Results from the X-ray fluorescence (XRF) spectrometer experiment (Clark et al. 1976, 1982) and the gas-chromatograph mass spectrometer (Biemann et al., 1977) were especially informative. Interpretation of these results, combined with laboratory and theoretical work, has led to estimates of 5-7 weight percent of carbonates and 10-13 weight percent of sulfates in the samples measured (Baird et al., 1976; Toulmin et al., 1977). The uniformity of the material collected at the two lander sites (Clark et al., 1976, 1982; Biemann et al., 1977) suggests that carbonates may be a component of the global dust.

Direct detection of carbonates and sulfates in a SNC meteorite has also been made. Gooding et al. (1987) identified two types of Ca-carbonate and of Ca-sulfate in the SNC meteorite EETA79001. The carbonates found do not appear to be a terrestrial weathering product and thus are thought to originate on Mars.

Warren (1987) used petrologic arguments involving the ratios of $(Mg + Fe)/Si$ and of Ca/Si combined with the abundances of K_2O and Zr in the SNC meteorites compared to the Viking Lander XRF analysis to conclude that a large amount of calcium was "missing" in the Viking fines. Although other mechanisms were discussed to account for the low calcium abundance, they seemed to be less probable than the formation of calcium carbonates. The "missing calcium" requires a carbonate abundance equivalent to a global layer of carbonates 20 m thick.

Many lines of evidence thus lead to the conclusion that carbonates should be present on the surface of Mars. Furthermore the abundance and location of these carbonates have major implications for the evolution of Martian volatiles.

IV. Sulfates

Unlike the circumstantial evidence for carbonates, sulfates are known to exist on the Martian surface. Sulfur was measured directly at both Viking Lander sites in abundances of 5 - 9 wt% SO₃ (Clark et. al. 1976, 1982). The elemental analysis of the red fine-grained material that dominated the surface at both sites were nearly identical for most elements, except sulfur which displayed a high degree of variation. The variation in sulfur abundance correlated with the amount of duracrust in the sample measured, indicating that sulfates were cementing the fines together. The composition of the duracrust at both Lander sites was remarkably similar (Clark et. al. 1979, 1982). Theories for the origin of the sulfate and the duracrust fall in two camps - upward migration of water containing the sulfate anion or deposition of sulfate from volcanic aerosols.

Baird et al. (1976) and Toulmin et al. (1977) proposed that the sulfates were deposited by the upward migration of soluble salts. More recently, Burns (1988) suggested that acidic ground water, produced from the interactions of massive iron sulfide deposits (associated with komatiitic magmas) and neighboring groundwater may be the source of the sulfate deposits at the surface. Mobile sulfuric acid-rich fluids would migrate to the surface to form gossans (iron sulfate deposits). Recent work on the weathering of olivine by sulfuric acid (Fisher and Burns, 1989) indicates that the sulfuric acid oxidizes the iron in the olivine to goethite. Acidic solutions could be a major modifier of the Martian surface. Groundwater migration as a mechanism for forming sulfate deposits implies that the similarities in sulfur abundance at both Lander sites are a coincidence because sulfate abundance locally would depend on the availability of water, the permeability of the regolith and the composition of the source region.

Settle (1979) proposed that the sulfates are the result of volcanic aerosols that were transported into the upper atmosphere by synoptic convergence of lower level winds in the

Tharsis region. These sulfates would settle out of the atmosphere as sulfuric acid droplets and react with the surface to form a cemented surface. This process currently is occurring in the interior portions of Antarctica, where sulfate and nitrate deposits form from the deposition of stratospheric anions that react with local rocks, which provide the necessary cations (Campbell and Claridge,1987).

As mentioned previously, Ca-sulfate was detected in the meteorite EETA79001 by Gooding et al. (1987). The mineralogy of the sulfate (i.e. gypsum, anhydrite or something more exotic) has not been determined owing to the small amount of material present.

V. Hydrates

As mentioned in section III, water is relatively abundant in the near-surface regions on Mars. Evidence for the presence of hydrated minerals on the Martian surface comes primarily from spectroscopic observations in the 3 μm region.

The first measurements between 3 μm and 4 μm were reported by Sinton (1957) and covered the wavelength region from 3.3 μm to 3.6 μm , but stopped well short of the 4 μm carbonate absorption. During the opposition of 1963, Moroz used two autocollimating infrared spectrometers with lead sulfide detectors to make measurements between 1.1 and 4.1 microns (Moroz, 1964). Moroz suggested that the spectrum of Mars was similar to that of limonite, with discrepancies at wavelengths longer than 2.5 microns between limonite and Mars caused by differences in the amount of water of crystallization and thermal emission. During the 1963 opposition, Sinton (1967) observed a strong bound-water absorption band and pointed out that thermal emission is not a major factor controlling the slope between 3 and 4 microns at reasonable Martian temperatures. Sinton further pointed out that many minerals have strong bound-water absorptions and the presence of a 3 μm band is not definitive evidence for limonite. Beer et al. (1971)

confirmed the presence of the bound-water band and set detection limits on the presence of many proposed molecular species on Mars such as H₂S, NO₂, COS, and C₃O₂.

Though the previous studies assumed that bound-water was causing the absorption near 3 μm, they were not definitive, as telluric atmospheric water absorptions between 2.5 and 3.0 microns made observations of the band center of any bound-water feature impossible. To avoid terrestrial atmospheric water absorptions, Houck et. al (1973) used an airborne telescope to make measurements above most of the Earth's atmosphere (the amount of water present above the aircraft was less than 15 precipitable microns). The resultant spectra covered the region between 2 and 4 microns. The measurements showed an 80% absorption depth with a band minimum at about 2.85 microns. This feature is similar to the bound-water feature found in terrestrial minerals. Estimates by Houck et al. (1973) on the amount of bound water present based on albedo, particle size, and modeling of terrestrial hydrated material, indicated about 1% water by weight.

Mariners 6 and 7 were the only U.S. spacecraft to carry spectrometers for measurements in the near infrared wavelength region. The IRS spectrometers aboard collected data between 1.9 and 14.4 microns. An initial report of the 3 μm absorption feature was made by Herr et al. (1969) shortly after the first data return. Detailed interpretation with respect to hydrated minerals and solid water was published by Pimentel et al. (1974). They examined variations in signal level inside and outside the water band as represented by the ratios of intensity at 3.1 μm/2.2 μm and at 2.9 μm/3.1 μm, and found that variations in the 3.1/2.2 ratio changed systematically with albedo (especially in the equatorial region). Variations due to particle size and the extent and nature of hydration of material could not be separated. The 2.9/3.1 ratio was determined to be diagnostic of the presence of ice, allowing discrimination between bound water and ice.

VI. Summary

Carbonates, sulfates, and hydrates are all important in understanding the weathering history of the Martian surface. A combination of direct and circumstantial evidence led to the expectation that these minerals should be present in abundances that are detectable by earth-based telescopic measurements. Determination of the mineralogy, abundance and distribution of these volatile bearing species is necessary in order to determine the processes by which the Martian surface evolved and is the subject of this dissertation.

References

- Anders, E., and T. Owen, Mars and Earth: Origin and abundance of volatiles, *Science*, **198**, 453-465, 1977.
- Baird, A.K., P. Toulmin, B.C. Clark, H.J. Rose, K. Keil, R.P. Christian, and J.L. Gooding, Mineralogic and petrologic implications of Viking geochemical results from Mars: Interim report, *Science*, **194**, 1288-1293, 1976.
- Beer, R., R.H. Norton, and J.V. Martonchik, Astronomical infrared spectroscopy with a Connes-type interferometer: II. Mars, 2500-3500 cm⁻¹, *Icarus*, **15**, 1-10, 1971.
- Biemann, K., J. Oro, P. Toulmin, L.E. Orgel, O. Nier, P.M. Anderson, P.G. Simmonds, D. Floy, A.V. Diaz, R. Rushneck, J.E. Biller, and A.L. Lafleur, The search for organic substances and inorganic volatile compounds in the surface of Mars, *J. Geophys. Res.*, **82**, 4641-4658, 1977.
- Burns, R.G., Gossans on Mars, *Proc. of the 18th Lunar and Planetary Sci. Conf.*, 713-721, 1988.
- Campbell, I.B., and G.G.C. Claridge, *Antarctica: Soils, Weathering Processes and Environment, Developments in soil science 16*, Elsevier Science Pub. B.V., New York, N.Y., 1987.
- Carr, M.H., Mars: A Water-Rich Planet?, *Icarus*, **82**, 187-216, 1986.
- Clark, B.C., A.K. Baird, P. Toulmin, H.J. Rose, K. Keil, A.J. Castro, W.C. Kelliher, C.D. Rowe, and P.H. Evans, Organic analysis of martian surface samples at the Viking landing sites, *Science*, **194**, 1283-1288, 1976.
- Clark, B.C., A.K. Baird, R.J. Weldon, D.M. Tsusaki, L. Schrabel, and M.P. Candelaria, Chemical Composition of Martian Fines, *J. Geophys. Res.*, **87**, 10,059-10,068, 1982.
- Dreibus, G., and H. Wanke, Accretion of the earth and inner planets, *Proc. 27th Int. Geol. Congr. Moscow*, **11**, 1-11, 1984.
- Dreibus, G., and H. Wanke, Comparison of Cl/Br and Br/I ratio in terrestrial samples and SNC meteorites, *Proc. Workshop on The Evolution of the Martian Atmosphere*, Technical Report, 86-07, 13-14, Lunar and Planetary Institute, Houston, TX, 1986.
- Fanale, F.P., and W.A. Cannon, Mars: CO₂ absorption and capillary condensation on clays--Significance for volatile storage and atmospheric history, *J. Geophys. Res.*, **84**, 8404-8415, 1979.

- Fanale, F.P., and R.N. Clark, Solar System ices and Mars permafrost, *Permafrost: Fourth International Conference Proceedings*, 289-294, National Academy Press, Washington, DC, 1983.
- Fanale, F.P., J.R. Salvail, W.B. Banerdt, and R.S. Saunder, The regolith-atmosphere-cap system and climate change, *Icarus*, 50, 381-407, 1982.
- Gooding, J.L., Chemical Weathering on Mars. Thermodynamic Stability of Primary Minerals (and their Alteration Products) from Mafic Igneous Rocks, *Icarus*, 33, 483-513, 1978.
- Gooding, J.L., S.J. Wentworth, and M.E. Zolensky, Calcium Carbonate and sulfate of possible extraterrestrial origin in the EETA 79001 meteorite, *Geochim. et. Cosmochim. Acta*, 52, 909-915, 1988.
- Herr K.C. and G.C. Pimental, Infrared absorptions near three microns recorded over the polar cap of Mars, *Science*, 166, 496-498, 1969.
- Houck, J.R., J.B. Pollack, C. Sagan, P. Schack, and J.A. Pecker, High altitude infrared spectroscopic evidence for bound water on Mars, *Icarus*, 18, 3, 470-479, 1973.
- Huguenin, R.L., and L. Harris, Accreted H₂O inventory on Mars, *Proc. Workshop on the Evolution of the Martian Atmosphere*, Honolulu, *Technical Report*, 86-07, 19-22, Lunar and Planetary Institute, Houston, TX, 1986.
- Masursky, H., J.M. Boyce, A.L. Dial, G.G. Schaber, and M.E. Strobell, Formation of martian channels, *J. Geophys. Res.*, 82, 4016-4038, 1977.
- McElroy, M.B., T.Y. Kong, and Y.L. Yung, Photochemistry and evolution of Mars' atmosphere: A Viking perspective, *J. Geophys. Res.*, 82, 4379-4388, 1977.
- McKay, C.P., and S.S. Nedell, Are there carbonate deposits in the Valles Marineris, Mars?, *Icarus*, 73, 142-148, 1988.
- Morgan, J.W., and E. Anders, Chemical composition of Mars, *Geochim. Cosmochim. Acta.*, 43, 60-76, 1979.
- Moroz, V.I., The Infrared Spectrum of Mars (1.1 - 4.1 μ), *Soviet Astronomy*, 8, 273-281, 1964.
- Piere, D.C., Martian Valleys: Morphology, distribution, age, and origin, *Science*, 210, 895-897, 1980.
- Pimentel G. C., P.B. Forney, and K.C. Herr, Evidence about Hydrate and Solid Water in the Martian Surface from the 1969 Mariner Infrared Spectrometer, *J. Geophys. Res.*, 79, 1623-1634, 1974.
- Pollack, J.B., Climate change on the terrestrial planets, *Icarus*, 37, 479-533, 1979.

- Pollack, J.B., and D.C. Black, Implications of the gas compositional measurements of Pioneer Venus for the origin of planetary atmospheres, *Science*, 205, 56-59, 1979.
- Pollack, J. B., and Yung, Y. L., Origin and evolution of planetary atmospheres. *Ann. Rev. Earth Planet. Sci.* 8, 425-487, 1980.
- Pollack, J. B., Kasting, J. F., Richardson, S. M., and Poliakoff, K., The case for a wet warm climate on early Mars. *Icarus*, 71, 203-224, 1987.
- Postawko S.E., and W.R. Kuhn, Effects of the greenhouse gases (CO₂, H₂O, and SO₂) on Martian paleoclimate, *J. Geophys. Res.*, 82, 4635-4639, 1986.
- Roth, L.E., R.S. Saunders, and G. Schubert, Mars: Seasonally variable radar reflectivity (abstract), *Lunar and Planetary Science XVI*, 712-713, Lunar and Planetary Institute, Houston, TX, 1985.
- Schultz, P., The Martian atmosphere before and after the Argyre impact, *Proc. Workshop on The Evolution of the Martian Atmosphere*, Honolulu, Tech. Report 86-07, 38-39, Lunar and Planetary Institute, Houston, TX, 1986.
- Settle, M., Formation and deposition of volcanic sulfate aerosols on Mars, *J. Geophys. Res.*, 84, 8,343-8,354, 1979.
- Sharp, R.P., Mars: Fretted and chaotic terrains, *J. Geophys. Res.*, 78, 4073-4083, 1973a.
- Sharp, R.P., Mars Troughed terrain, *J. Geophys. Res.*, 78, 4063-4072, 1973b.
- Sharp, R.P., Mars: South polar pits and etche terrain, *J. Geophys. Res.*, 78, 4222-4230, 1973c.
- Sinton, W.M., On the composition of the Martian surface materials, *Icarus*, 6, 222-228, 1967.
- Sinton, W.M., Spectroscopic evidence for Vegetation on Mars, *Astrophys. J.*, 126, p.231-238, 1957.
- Toulmin, P., A. K. Baird, B. C. Clark, K. Keil, H.J. Rose, R. P. Christian, P. H. Evans, and W.C. Kelliher, Geochemical and mineralogical interpretation of the Viking inorganic chemical results, *J. Geophys. Res.*, 82, 4625-4634, 1977.
- Warren, P.H., Mars regolith versus SNC meteorites: Possible evidence for abundant crustal carbonates, *Icarus*, 70, 153-161, 1987.
- Watkins, G.H., and J.S. Lewis, Evolution of the atmosphere of Mars as the result of asteroidal and cometary impacts, *Proc. Workshop on the Evolution of the Martian Atmosphere*, Honolulu, Technical Report, 86-07, 46-47, Lunar and Planetary Institute, Houston, TX, 1986.

- Yung, Y.L., and M.B. McElroy, Fixation of nitrogen in the prebiotic atmosphere, *Science*, 203, 1002-1004, 1979.
- Zent, A.P., and F.P. Fanale, Possible Mars brines: Equilibrium and kinetic considerations, *J. Geophys. Res.*, 91, D439-D445, 1986.
- Zisk, S.H., and P.J. Mouginis-Mark, Anomalous region on Mars: Implications for near-surface liquid water, *Nature*, 44, 735-738, 1980.

Chapter 2.

Infrared Spectroscopy of Molecules

I. Introduction

Infrared spectroscopy provides unique opportunities to study the composition and abundances of carbonates and sulfates on the Martian surface. Although actual samples of the Martian surface would provide much more detailed geochemical information, such samples are currently unavailable. What is readily measured is the light from the optical surface of Mars. Optical spectroscopy measures the light reflected and emitted from a surface at specific wavelengths. This restricts the information that can be obtained in two ways: 1) information is available for only the topmost level of the surface so that compositional differences at depth are not detectable, and 2) only certain types of minerals in relatively large abundances (a few weight percent) can be detected.

The anions such OH^- , CO_3^{2-} and SO_4^{2-} , and the water molecule absorb specific wavelengths of light. These absorption features allow mineralogic identifications and abundances to be determined. A general discussion on the theory of vibrational absorptions and specific information on hydrate, carbonate, and sulfate absorptions follows.

II. Vibrational Absorptions

Anions such as CO_3^{2-} and SO_4^{2-} and molecules such as O_2 , N_2 , CO_2 , CO , and H_2O can be thought of as simple harmonic oscillators. The simple harmonic oscillator analogy is commonly used to explain vibrational and rotational absorption. Atoms belonging to the molecule are pictured as "masses" on the end of a spring. The covalent bonds connecting

these atoms are the "springs" holding the molecules together. The strength of the bond determines the "stiffness" of the spring. A displacement of one of the masses from its rest position results in a restoring force, pulling it back toward its equilibrium position. This restoring force is linearly proportional to the distance the mass is displaced.

Like regular simple harmonic oscillators, the masses of the atoms and the bond strengths (spring stiffness) control the behavior of the system and produce natural frequencies at which the system prefers to vibrate, called normal modes (see basic physics text or Colthrup et. al., 1975 for derivation). In a normal mode the center of mass of the molecule does not move or rotate and all molecules pass through their equilibrium positions simultaneously although the relative vibrational amplitudes of each atom may be different. A schematic illustration of a diatomic molecule in a normal mode is shown in figure 2.1. The relative displacement of each atom from the center of mass of the system as a function of time forms a sine or cosine wave. Note that the "larger" atom has a smaller amplitude of displacement than the "small" atom and that the phases of the amplitude are 180° from each other so that the center of mass of the system is constant.

In the case of the vibration of molecules, the driving force causing the oscillation is electromagnetic radiation. Quantum theory shows that the energy of a photon at a specific wavelength (or frequency) of light is given by the equation:

$$E = hc/\lambda \quad (2.1)$$

or

$$E = h\nu \quad (2.1 \text{ b}).$$

Where E is the energy of the photon, h is Planck's constant, λ is the wavelength of the photon, c is the velocity of light, and ν is the frequency of the photon.

When a photon of the same energy as the frequency of the normal mode of the molecule strikes, it is absorbed and the molecule accounts for its greater energy by oscillating with

greater amplitude. Energy at nonresonant frequencies (i.e. frequencies at other than the normal modes) is not absorbed efficiently. The energy associated with the resonant frequencies is located in the infrared wavelength region.

The strength of an absorption at a resonant frequency is dependent on the change in the dipole moment. The dipole moment expresses the change in electric field of the molecule induced by changes in the spacing between atoms during vibration. Diatomic molecules such as O₂ and N₂ do not undergo any change in their dipole moment when they vibrate and are thus do not have infrared absorption features.

Most molecules are not perfect vibrators. Anharmonicity occurs when the restoring force is not linear with displacement and imparts a positional dependence of vibrational amplitude. Figure 2.2 shows an anharmonic oscillator. Note that the anharmonic function is periodic and thus can be expressed as a Fourier series with the first term representing the harmonic portion of the oscillations and given by: $A \cdot \cosine(\nu t)$ or $A \cdot \sine(\nu t)$, where A is the total amplitude of the vibration under harmonic conditions, ν is the dominant frequency (also called the fundamental), and t is time. Deviations from harmonic behavior are expressed by a series of sine or cosine functions with the frequency an integral multiple of the fundamental frequency. These integral multiples of the fundamental frequency are called overtones. If the molecule has an anharmonic component the dipole moment of the molecule will vibrate at the fundamental and at the overtone frequencies. Absorptions therefore occur at the fundamental frequency and the overtone frequencies. The strength of an overtone absorption depends on the degree of anharmonicity.

The analogy of aharmonic oscillator with an anharmonic component is an idealized physical model for a molecular process. In practice the molecules do not behave in a "perfect" manner. Overtones are often found offset from the integral multiples of the fundamental frequencies due to the quantum - mechanical nature of the energy levels

(Colthrup et al., 1975). Absorption features, called combination bands, are also found at frequencies that are a sum of the frequencies of fundamental frequencies (Colthrup et al., 1975).

The vibrational modes of specific minerals can be determined by examining their structure and planes of symmetry and assigning them to a "point group" of minerals which have the same structure. Minerals within the same point group exhibit similar vibrational behavior (Farmer, 1974).

III. Bound Water

Water is a planar molecule belonging to the point group C_{2v} (shown in figure 2.3). The three normal modes for water are shown in figure 2.4. All three are infrared active (i.e. the vibrational mode also produces a change in the dipole moment). These fundamental modes occur at 3220 cm^{-1} ($3.106\text{ }\mu\text{m}$), 1645 cm^{-1} ($6.08\text{ }\mu\text{m}$), and 3445 cm^{-1} ($2.903\text{ }\mu\text{m}$) (Hunt and Salisbury 1970). The presence of both the ν_1 and ν_3 fundamentals in the $3\text{ }\mu\text{m}$ region tends to depress the continuum and individual bands are not identifiable. Instead, one strong, broad absorption feature dominates if water is present. Water depresses the continuum to almost as far as $4\text{ }\mu\text{m}$. Therefore, whereas the measurements discussed in Chapter 4 do not cover the entire wavelength region of interest (the measurements start at $3.2\text{ }\mu\text{m}$) they do provide information on the distribution of hydrated materials on Mars.

IV. Carbonates

The CO_3^{-2} anion has a point symmetry group of D_{3h} (shown in figure 2.5) and four normal modes of vibrations (shown in figure 2.6). The ν_2 , ν_3 , and ν_4 fundamentals are all

infrared active and occur at 879 cm^{-1} ($11.4\ \mu\text{m}$), 1415 cm^{-1} ($7.07\ \mu\text{m}$), and 680 cm^{-1} ($14.7\ \mu\text{m}$), respectively (Farmer 1974). The CO_3^{-2} anion has extremely strong covalent bonds and consequently, little variation in the infrared spectra of these materials exists. Calcite has symmetry of D_3 and aragonite has a symmetry of C_s (figure 2.7). The lower symmetry of the aragonite group causes the ν_1 fundamental to be infrared active. Work by Walsh (1989) shows that the $4\ \mu\text{m}$ carbonate absorption feature caused by the $\nu_1 + \nu_3$ combination band is independent of the mineralogy of the mineral and an extremely sensitive indication of the presence of carbonate compounds. Chapters 3 and 4 detail work in the $4\ \mu\text{m}$ region to detect carbonates on the Martian surface

V. Sulfates

The SO_4^{-2} anion has tetrahedral symmetry (T_d) and four normal modes of vibrations, shown in figures 2.8 and 2.9 respectively, two of which are infrared active -- the ν_3 and ν_4 modes. The ν_3 fundamental is located at 1104 cm^{-1} ($9.06\ \mu\text{m}$), and the ν_4 at 613 cm^{-1} ($16.3\ \mu\text{m}$) (Nakamoto 1963). When a metal cation complexes with the SO_4^{-2} anion the symmetry is usually lowered. The lower symmetry causes splitting of the degenerate modes (the ν_3 and ν_4) and the appearance of the ν_1 and ν_2 which are not infrared active under tetrahedral symmetry. The various metal - SO_4 coordination structures, their symmetry groups, and their subsequent splitting are shown in figure 2.10. Lattice effects on the symmetry are usually of lesser importance than complexing. Common sulfate minerals such as anhydrite, gypsum, bassanite, and MgSO_4 are shown with their site symmetry and fundamental frequencies in table 2.1.

Chapter 5 deals with a search of the $4.5\ \mu\text{m}$ region for the $2\nu_3$ overtone sulfate absorption feature in telescopic data of the Martian surface.

References

- Colthrup, N. B., L. H. Daly, and S. E. Wiberley, *Introduction to Infrared and Raman Spectroscopy*, Academic Press, Inc., New York, New York, 523p., 1975.
- Farmer V.C. (ed.), *The Infrared Spectral of Minerals*, Mineralogical Society of London, Monograph 4, London England, 539p., 1974.
- Hunt, G.R., and J. W. Salisbury, Visible and Near Infrared Spectra of Minerals and Rocks: I. Silicate Minerals, *Mod. Geol. 1*, p. 283-300, 1977.
- Nakamoto, Kuzuo, *Infrared Spectra of Inorganic and Coordination Compounds*, John Wiley and Sons, Inc., New York, New York, 328p., 1963.
- Walsh, P.A., *A Spectroscopic Study of Mars Surface Analogs*, master thesis, University of Hawaii at Manoa, defense pending 1989.

Table 2.1 Sulfate Infrared Absorptions and Symmetry Groups adapted from Farmer (1974, pages 427 - 430).

Compound	Mineral	Site Symmetry	v1	v2	v3	v4
CaSO ₄	Anhydrite	C _{2v}	1013	512	1149 1126 1095	671 612 592
CaSO ₄ ·½H ₂ O	Bassanite	D ₂ , C ₂ , or C ₁	1012	465, 420	1158 1120 1100	667 634 605
CaSO ₄ ·2H ₂ O	Gypsum	C ₂	1006	492 413	1144 1138 1117	669 624 621
MgSO ₄		C _{2v}	1020	505 430	1235 1175 1155 1110 1085	705 615

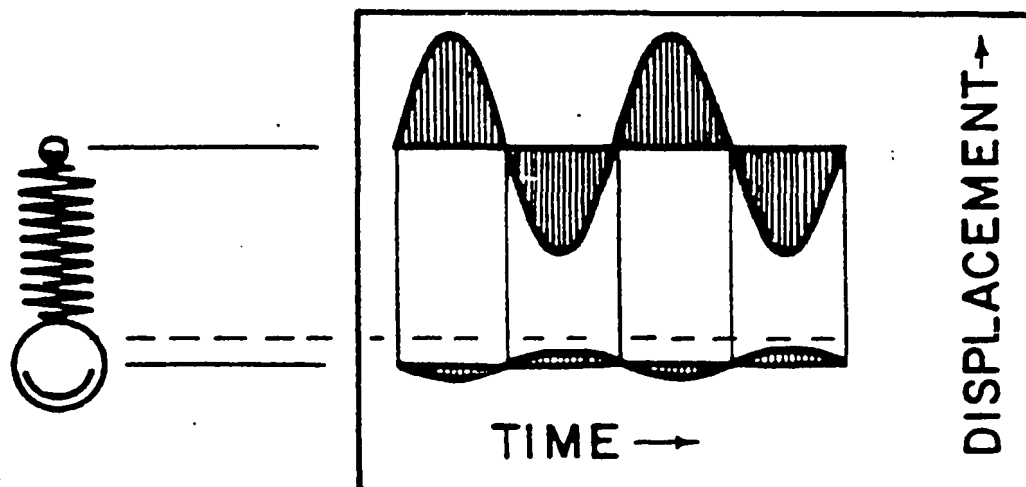


Figure 2.1 Normal mode of vibration of a ball and spring model of a diatomic molecule such as HCl. The displacement versus time plot for each mass is a sine wave and the center of gravity (dashed line) is motionless. From Colthup et al. (1974, page 4).

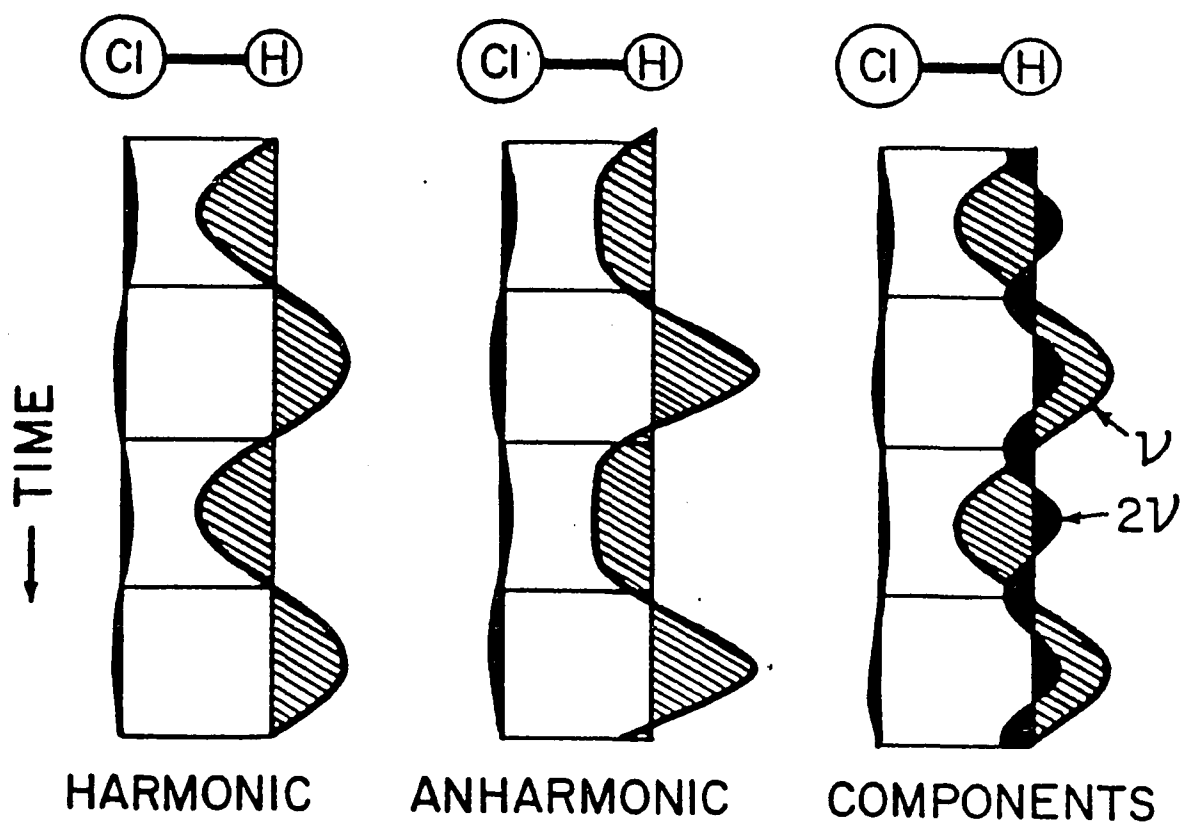


Figure 2.2 Plots of mass displacement versus time for harmonic and anharmonic vibrations with a fundamental vibrational frequency of ν and a second overtone of 2ν . On the right are the main components of the anharmonic curve in the middle. From Colthrup et al. (1974, page 13).

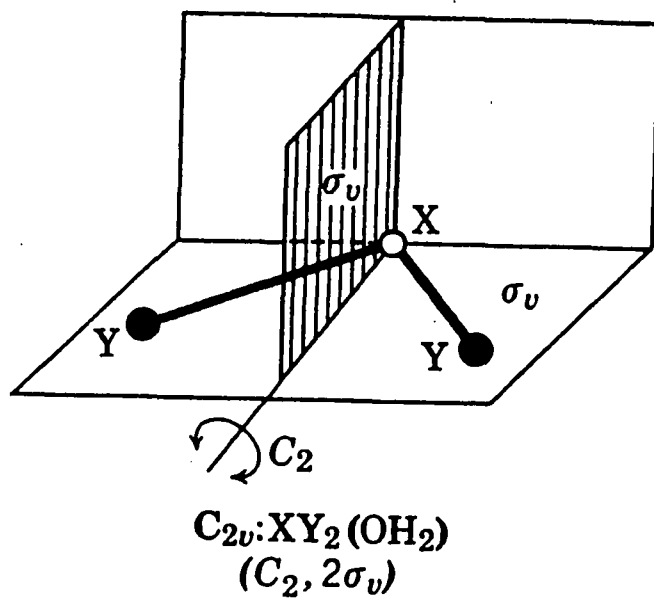


Figure 2.3 Symmetry elements of the C_{2v} point group (σ_v , σ_h , and σ_d denote vertical, horizontal, and diagonal planes of symmetry, respectively). From Nakamoto (1963, page 16).

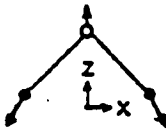
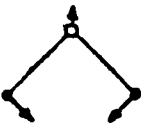


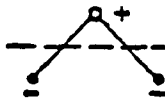
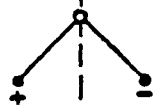


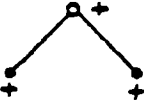
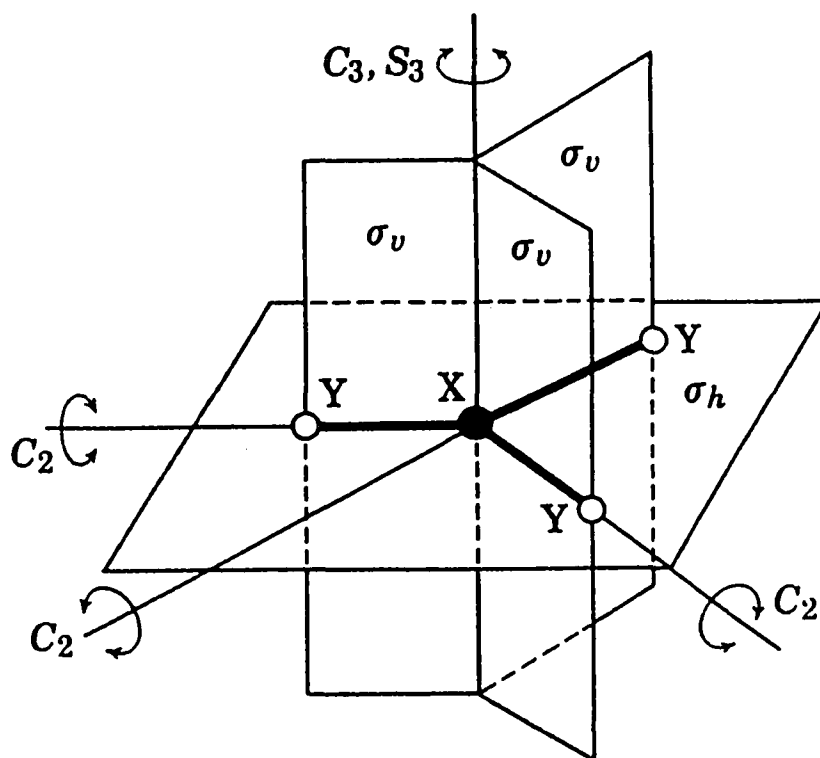
Species (C_{2v})	A_1	B_1	B_2	A_2
Internal vibrations	 ν_1	 ν_2	 ν_3	
Libration vibrations		 R_y	 R_x	 R_z
Translation vibrations	 T_z	 T_x	 T_y	

Figure 2.4 Normal modes of vibrations of water molecules. From Farmer (1974, page 161).



$D_{3h}:XY_3$ (CO_3^{2-} ion)
 ($C_3 \approx S_3, 3C_2, 3\sigma_v, \sigma_h$)

Figure 2.5 Symmetry elements of the D_{3h} point group (σ_v , σ_h , and σ_d denote vertical, horizontal, and diagonal planes of symmetry respectively). From Nakamoto (1963, page 18).

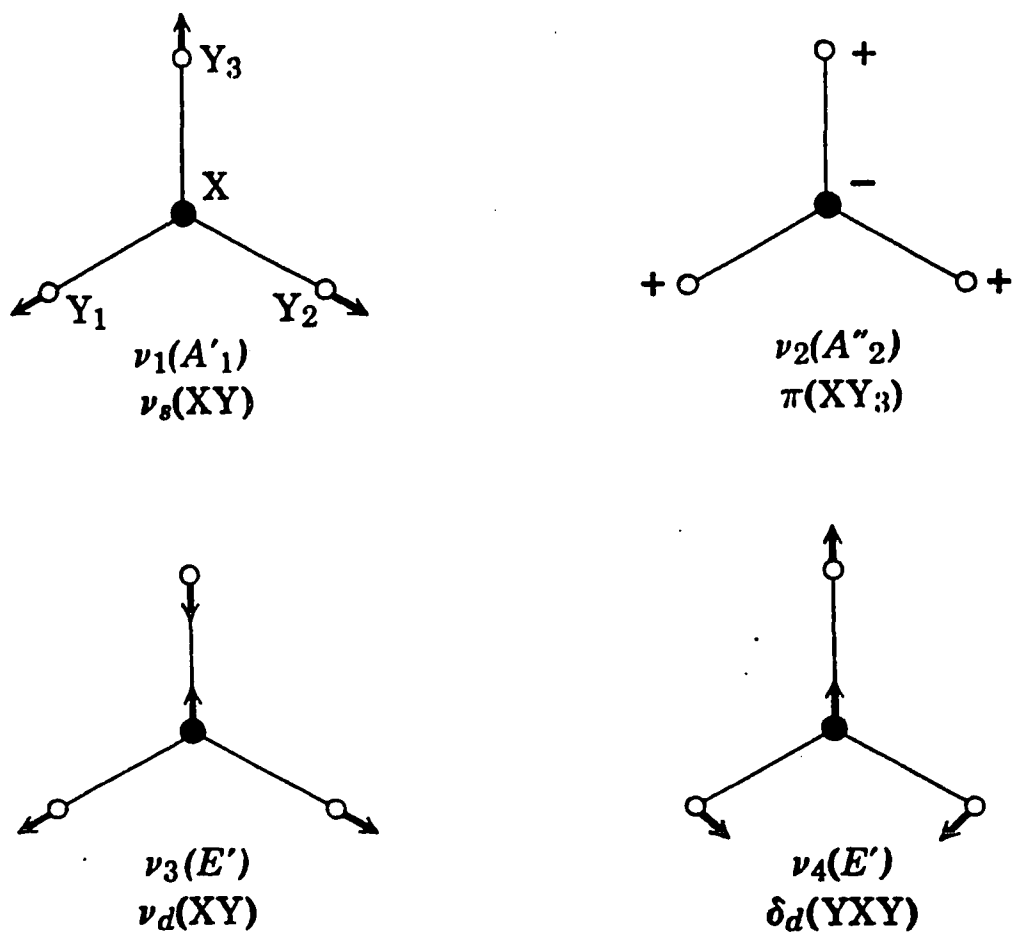


Figure 2.6 Normal modes of vibration of planar XY_3 molecules such as CO_3^{-2} . From Nakamoto (1963, page 123).

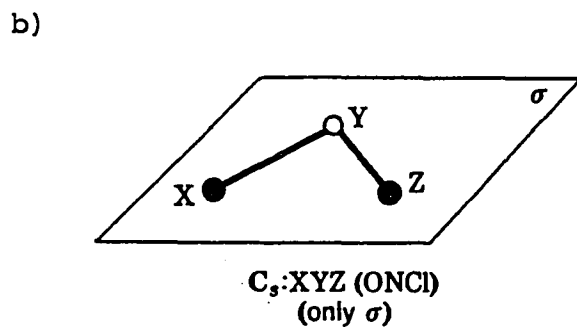
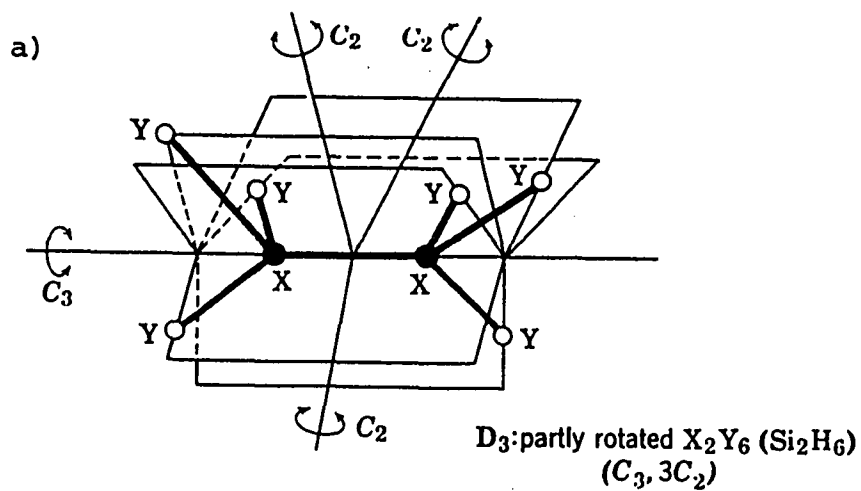


Figure 2.7 Symmetry elements of the a) D_3 and b) C_s point groups (σ_v , σ_h , and σ_d denote vertical, horizontal, and diagonal planes of symmetry respectively). From Nakamoto (1963, pages 16 and 17).

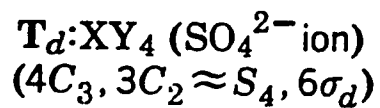
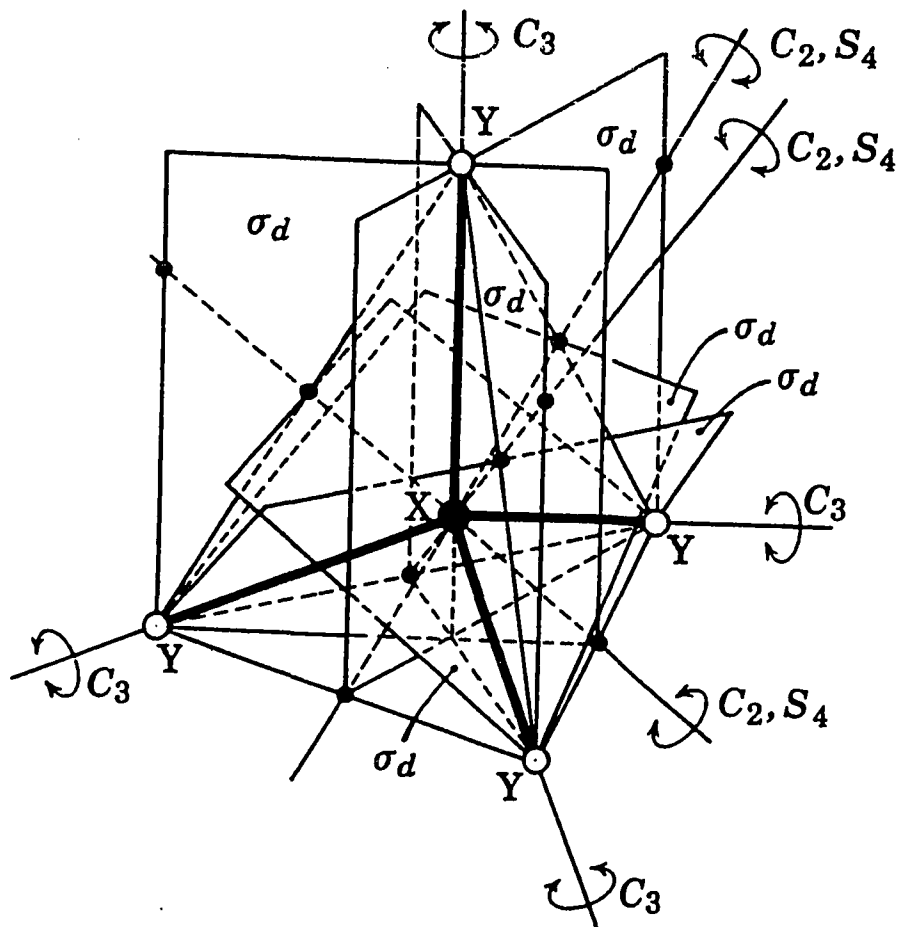


Figure 2.8 Symmetry elements of the T_d point group (σ_v , σ_h , and σ_d denote vertical, horizontal, and diagonal planes of symmetry respectively). From Nakamoto (1963, page 21).

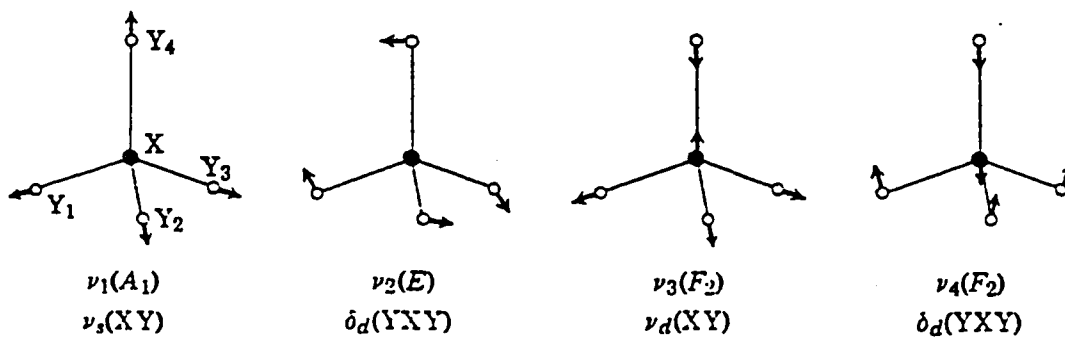


Figure 2.9 Normal modes of vibration of tetrahedral XY_4 molecules. From Nakamoto (1963, page 103).

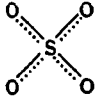
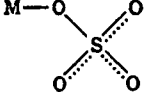
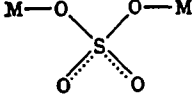
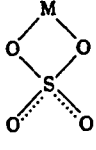
Sulfate Complex	Symmetry	Degeneracy of Normal Mode of Vibration			
		v1	v2	v3	v4
 Free ion (T_d)	T_d	—	—	1	1
 Unidentate complex (C_{3v})	C_{3v}	1	1	2	2
 Bridged bidentate complex (C_{2v})	C_{2v}	1	1	3	3
 Bidentate complex (C_{2v})					

Figure 2.10 Types of sulfate complexes, their symmetry groups, and vibrational degeneracy. Adapted from Nakamoto (1963, page 164).

Chapter 3.

An observational search for carbonates on Mars

Diana L. Blaney and Thomas B. McCord

Planetary Geosciences Division of the

Hawaii Institute of Geophysics

2525 Correa Road

Honolulu, Hawaii 96822

Journal of Geophysical Research, **94**, 10,159-10,166, 1989

I. Abstract

A search for carbonates and other salts exposed on the surface of Mars was undertaken by observing areas of the surface in the 2.6 μm to 4.2 μm spectral region using the University of Hawaii 2.2 m telescope at the Mauna Kea Observatory, Hawaii. Observations of four Martian areas (Syrtis Major, Hellas, Arabia, and an area northeast of Hellas) were made on the night of September 19, 1986. The reflectance spectra for two partially overlapping areas show a weak absorption band in the 3.8 μm to 3.9 μm region, which is in the spectral region where carbonate absorptions appear: 3.8 μm to 4.0 μm . The Mars area of overlap contains Syrtis Planum. The spectral feature (from about 3.76 μm to 3.95 μm) is clearly at a shorter wavelength and broader than the calcium carbonate band (about 3.9 μm to 4.0 μm) and is at a slightly shorter wavelength position than magnesium carbonate (magnesite) bands (about 3.8 μm to 3.96 μm) as measured in this study. Positive identification of this band cannot be made by us at this time. Measurements for two other Mars areas show no evidence of carbonate or other bands. If the band is due to absorptions in the Mars surface material spectrum and if it is due to carbonates, then the results imply about 3 to 5 wt% of a carbonate such as magnesite on average in the upper few millimeters of the Mars surface material over the two areas where the weak spectral feature appears. We can place an upper limit of 3 to 5 wt% calcium carbonate and about 5 wt% magnesite for all areas observed. The interpretations are based on laboratory measurements of the reflectance spectra of calcite and magnesite and their mixtures with palagonite. Effects of thermal emission on the detection of carbonates were also explored for a wide range of temperatures. Thermal effects are not sufficient to mask the presence of calcite in the 3 to 5 wt% range. Theoretical reasoning strongly supporting the presence of carbonates as a component of the Mars surface is reviewed. These and earlier observations do not rule out carbonates below the surface, in other locations, as small outcrops, or in concentrations of less than 3 to 5% of the areas observed.

II. Review of Support for Carbonates on Mars

Reasons for postulating carbonates on the Martian surface are partially linked to the belief in an early, warm, wet Mars. A more clement Mars has been a popular idea since dendritic valley networks were discovered. The morphology of these channels indicate that they formed by near-surface groundwater sapping (Sharp, 1973; Piere, 1980). However, the almost total confinement of these features to areas that are located in the ancient heavily cratered terrain suggests that Mars had a different climate during its first billion or so years. Indeed, Schultz (1986) suggests that a change in the erosion rate and rate of valley network formation occurred about the time the Argyre impact basin was formed. The lack of any evidence for "recent" extensive valley networks indicates that some factor (surface temperature, atmospheric pressure, geothermal gradient, regolith volatile content) about Mars was different early in its history. A warmer climate is strong candidate for this difference between early Mars and the present. If these features indicate that Mars did indeed have a substantially warmer climate early in its history, the most likely cause is a carbon dioxide induced greenhouse effect.

Estimates of the partial pressure of carbon dioxide needed to raise the average surface temperature to 273 K are about 3-5 bars (Postawko and Kuhn, 1986; Pollack and Black, 1979; Postawko, personal communication 1988) taking into account the reduced solar luminosity early in solar history. Current estimates of the storage capacity of the known reservoirs of carbon dioxide (the atmosphere, regolith, and south polar cap) from Fanale et al. (1982); Fanale and Cannon (1979); and Pollack (1979) account for only about 0.07 to 0.7 bars. For this reason, as for the Earth, carbonates have been invoked as a major reservoir of carbon dioxide that is no longer available to interact with the dynamic reservoirs (e.g. Pollack and Yung, 1980; Toon et. al., 1980; Poilack et al., 1987)

Of course, the amount of carbonates formed depends on the total amount of carbon dioxide available. The estimates of 3 - 5 bars of carbon dioxide needed to raise the

temperature above 273 K are only lower limits of the amount of carbon dioxide possibly outgassed (if carbon dioxide greenhouse warming occurred). Cosmochemical arguments comparing the volatile inventories of the Earth, Venus, and Mars indicate that as much as 10 bars of carbon dioxide could have been outgassed from Mars (Pollack and Black 1982).

Carbon dioxide abundance is not the only control on carbonate formation. The availability of water, both to leach cations from rock and to dissolve carbon dioxide, is a critical control on the rate of carbonate formation. Estimates of the volume of water outgassed also can set limits on the amount of carbon dioxide available. Therefore, the phase distribution and abundance of water early in Mars' history is an important control on the evolution of carbon dioxide. Direct estimation of water and carbon dioxide abundances is not possible. However, examination of geomorphic features attributed to water combined with geochemical evidence can set reasonable bounds on the abundance of water. These bounds, though, cannot be used directly to determine the current Martian carbon dioxide/carbonate inventory because of permanent atmospheric loss processes, such as atmospheric cratering and hydrodynamic escape. Examination of the estimates of water abundances is useful, however, in setting reasonable bounds on the outgassed inventory of carbon dioxide.

There is a large body of evidence supporting the presence of substantial amounts of water on Mars. Ample geomorphic evidence, such as outwash channels, debris aprons, and fretted terrain, exists for the presence of water, but the form and abundance of the water is uncertain. Estimates of the abundance of water on Mars, derived primarily from the volumes of the outwash channels, yield an abundance of outgassed water corresponding to a global liquid layer with depths of 500 to 1,000 m (Carr, 1986). The geochemical evidence, however, is more enigmatic.

Initial consideration of rare gas composition and nitrogen isotope ratios measured by Viking produced estimates of a water layer only 10-100 m thick (Anders and Owen, 1977; Morgan and Anders, 1979; McElroy et al., 1977). The complexities of the rare gas

patterns of Mars, the Earth, and Venus prevent construction of a simple picture of volatile acquisition by planets, and the rare gas patterns may have very little to do with the abundance of water and carbon dioxide (Pollack and Black, 1979; Watkins and Lewis, 1986). Nitrogen isotope ratios are affected by nitrate formation rates which are unknown for early Mars (McElroy and Yung, 1977; Yung and McElroy, 1979). Meteorite data from a group of basaltic achondrites thought to originate on Mars has also been used to estimate the volatile content of Mars.

The SNC (S=Shergotty, N=Nahkla, and C=Chassigney after the type meteorites) meteorites are a group of basaltic achondrites thought to originate on Mars due to their young igneous crystallization ages, ~1.3 billion years (Wood and Ashwal 1981) and their nitrogen and argon isotope patterns (Becker and Pepin 1984). Dreibus and Wanke (1984, 1986) concluded, based on the composition of these meteorites and planetary accretion models, that a large portion of the water present during accretion was used largely to oxidize the metallic iron in Mars and that consequently, Mars could have outgassed only 1-50 m of water. Huguenin and Harris (1986) point out that slight changes in the amount of FeO accreting into the planet could lead to a volatile-rich Mars. Although the exact volatile content of Mars is unknown, it is clear that the possibility exists that Mars may be volatile-rich. If the estimates of 500-1000 m of water degassed are correct, then 10-20 bars of carbon dioxide should have been degassed also (Carr, 1986) and perhaps been available for carbonate formation.

Carbonate formation should not be limited to Mars' distant past. Normal weathering processes under current Martian conditions also would tend to produce carbonates and other salts, providing that thermodynamic equilibrium is reached (Gooding, 1978). Fayalite, diopside, augite, and anorthite all weather to calcite and magnesite or dolomite if equilibrium is reached. Siderite could also be a metastable weathering product (Gooding, 1978). Though these deposits would not be as extensive as massive carbonate deposits formed in an era of warm temperatures and abundant surface water, weathering

considerations alone indicate that carbonates should exist on the Martian surface regardless of whether there was an early clement climate. Whether the abundance of carbonate formed from this process is sufficient to be detectable at present at the optical surface is unknown.

Carbonate formation from evaporite deposits is another possibility. Variable radar reflectivity in the Solis Lacus region has been interpreted as the melting of near-surface ice (Zisk and Mouginiis-Mark, 1980). Roth et al. (1985) suggested that the reflectivity may be seasonally variable over a wide range of latitudes. The existence of near-surface water allows the migration of salt-rich solutions toward the surface to form salts. Under present conditions brines are not stable relative to the polar cold-trap (Fanale and Clark, 1983); however, non-equilibrium brines are possible (Zent and Fanale, 1986). In addition, the occurrence of large igneous intrusive events near water/ice-rich layers also should have created ionic aqueous solutions that migrated toward the surface. Thus, salt formation by the evaporation of brines on the surface of Mars could have occurred, but the scale and composition of such salt deposits are unknown.

McKay and Nedell (1988) have proposed that the layered deposits in Valles Marineris formed by carbonate precipitation, similar to the carbonates formed in iced-over Antarctic lakes. The young age of these features rules out any connection with carbonates formed early in Martian history.

Viking lander experiments, though not directly measuring salt content of the surface of Mars, indicate that salts are present. Results from the X-ray fluorescence (XRF) spectrometer experiment (Clark et al., 1976; 1982) and the gas-chromatograph mass spectrometer (Biemann et al., 1977) were especially informative. Interpretation of these results, combined with laboratory and theoretical work, has led to estimates of 5-7 weight percent of carbonates and 10-13 weight percent of sulfates in the samples measured (Baird et al., 1976; Toulmin et al., 1977). The uniformity of the material collected at the two lander sites (Clark et al., 1976, 1982; Biemann et al., 1977) suggests that carbonates may be a component of the global dust.

Direct detection of carbonates and sulfates in a SNC meteorite has also been made. Gooding et al. (1987) identified two types of Ca-carbonate and of Ca-sulfate in the SNC meteorite EETA79001. The carbonates found do not appear to be a terrestrial weathering product and thus are thought to originate on Mars.

Warren (1987) used petrologic arguments involving the ratios of $(Mg + Fe)/Si$ and of Ca/Si combined with the abundances of K_2O and Zr in the SNC meteorites compared to the Viking Lander XRF analysis to conclude that a large amount of calcium was "missing" in the Viking fines. Although other mechanisms were discussed to account for the low calcium abundance, they seemed to be less probable than the formation of calcium carbonates. The "missing calcium" requires a carbonate abundance equivalent to a global layer of carbonates 20 m thick.

Many lines of evidence thus lead to the conclusion that carbonates should be present on the surface of Mars. Furthermore the abundance and location of these carbonates have major implications for the evolution of Martian volatiles.

III. Review of Previous Measurements

A method of detecting salts on Mars is reflectance spectroscopy using groundbased telescopes. Carbonates, nitrates and sulfates have strong molecular absorption bands in the 3.0 to 5.0 μm spectral region, and carbonates have weaker bands in the 2.0 to 2.5 μm region. However, telescopic measurements in the 3.0 to 5.0 μm spectral region have been difficult to acquire, and no evidence of salts has been reported so far.

The first direct measurements which might have detected carbonates and other salts on Mars were groundbased telescope reflectance spectroscopic observations by Sinton (1967), Beer et al. (1971), and by Houck et al. (1973). Sinton (1967) discovered a 3 μm region absorption feature attributed to bound water. Beer et al. (1971) produced spectra in

the 2.0 to 4.0 μm region during a high altitude flight that showed water adsorption in the 3 μm region but no features in the 4 μm region. Houck et al. (1973) obtained a reflectance spectrum of the integral disc of Mars in the 2.1 to 3.9 μm region which also showed a bound water band in the 3 μm region but no evidence of carbonate, sulfate or nitrate bands to at least a band depth of approximately 10% of continuum. Reflectance spectroscopic measurements have been reported in the 2.0 to 2.5 μm region which show no carbonate bands to a percent or two of the continuum (McCord et al., 1982; Singer, 1982; McCord et al., 1978).

The Mariner 6 and 7 spacecraft carried an infrared spectrometer which measured the reflectance spectrum in the 1.9 to 5.0 μm region and longward for areas on Mars. These have been analyzed for salts bands and none were found to a level of a few percent of continuum (Roush et al., 1986). These spectra were examined also by McKay and Nedell (1988), and again no evidence of carbonates was reported.

Thus, in spite of the strong support from theoretical and geochemical arguments for the formation of carbonates on Mars, all known spectroscopic searches have yielded negative results.

IV. New Mars Observations

During the night of September 19, 1986, we used the 2.2 m University of Hawaii telescope at the Mauna Kea Observatory, Hawaii, to observe Mars. A circular variable interference filter (CVF) was used with a cooled InSb detector to measure radiation from Mars with spectral resolution of 0.02 (dl/l) from 2.35 to 4.17 μm . For each observation the CVF was scanned through the spectrum six times over a total period of approximately 15 minutes while the telescope was manually guided on an area of Mars. The signal was digitized and recorded on magnetic disc and transferred to magnetic tape for later analysis. The observing conditions appeared to us to be excellent, with no clouds, low atmospheric

water vapor and good seeing; the quality of the data obtained also reflects these conditions. The observational parameters are shown in Table 1.

A beam splitter was used to send light to the guide camera and to the instrument. A star was used to map out the aperture of the instrument. The image from the guide camera was recorded on video tape along with electronic cross hairs that marked the aperture, and the video tape was used to determine the areas observed (Figure 1). The best measurements are for four overlapping regions on Mars, each with a diameter of approximately 3,000 km. The four locations of the measurement cover approximately the regions of Syrtis Major, Arabia, Hellas, and an area of the southern highlands very slightly north-east of Hellas, which is labeled Northeast Highlands.

The spectrum of the star Tau Sagittarius was observed to calculate and remove atmospheric extinction and instrument response from the Mars data. The Tau Sagittarius measurements were made every thirty minutes and bracketed the Mars observations. Twelve integrations were made each time the instrument returned to observe the star. Tau Sagittarius is a K1 III spectral type with a visible magnitude of 3.32, and was separated from Mars by approximately 20 minutes in right ascension and 1 hour 30 minutes in declination.

The data were reduced by averaging the spectra taken for each location and for the star after removing any spurious data points. The Mars observations were then divided by the measurements of Tau Sagittarius. The star and Mars were close enough in the sky during the measurements that attempts to calibrate for air mass differences using the star data produced no improvement in the Mars spectra, and therefore explicit extinction corrections were not made in the final data analysis. The resultant spectra are shown in Figure 2. To obtain reflectance from the relative flux ratios plotted in Figure 2, the flux ratios should be multiplied by a star/Sun flux ratio, but this is not available. However, the star spectral flux

is close enough to that of the Sun so that the Mars/star flux ratio approximates that of Mars/Sun close enough for identification of carbonate and other absorption features.

V. Supporting Laboratory Measurements

In order to interpret our telescopic reflectance spectra of Mars in terms of the presence or absence of carbonates, the reflectance spectra of the salt in question must be known. A separate program is underway within this research group to provide reflectance spectra of carbonates and sulfates under conditions similar to those on the Mars surface (Blaney et al., 1987; Walsh and McCord, 1988). The study includes mixtures carbonates with various proportions of palagonite, a Mars dust analog. Measurements of palagonite - carbonate mixtures were used to indicate where in 3 μm - 4 μm wavelength region the various absorption bands for different carbonate minerals occur and what the detection levels are.

The samples were prepared by mixing palagonite from Mauna Kea, Hawaii with various amounts of two different calcite samples and a magnesite sample. Palagonite is an amorphous weathering product of basaltic glass and is considered a good spectral analog for Mars dust (Evans and Adams 1980; Singer, 1982). The palagonite used was collected from the 10,000 ft. elevation on Mauna Kea. One of the calcite samples was a reagent grade powder from a chemical supply house. The other calcite sample was ground Icelandic spar, a crystalline mineral sample. The magnesite was also a ground crystalline sample. Black magnetic impurities were removed from the magnesite by magnetic separation. These small, easily removed flecks appeared to be the only impurities in the ground crystalline samples. The materials were sieved to a grain size of less than 35 μm . The amounts (weights) of the materials were measured and mixed together by shaking to produce carbonate mixtures of 3, 5, 10 and 20 weight percent in palagonite. Examination of the mixtures under an optical microscope showed that the samples appeared to be uniform. Surface-adsorbed water was removed by heating the samples in an oven at 135°C

for four hours. The hot samples were immediately transferred into a desiccated environment and allowed to cool. The samples were stored and measured under a purge of dried air and were never exposed to ambient conditions.

Measurements for the carbonate-palagonite mixtures were made using a Nicolet 5SXC Fourier Transform Infrared Spectrometer with diffuse reflectance attachment and a HgCdTe detector. A resolution of 30.9 cm^{-1} was used to duplicate the telescopic measurements as closely as possible. Sulfur was used as a reflectance standard. The instrument provides no phase information. Signal level is extremely sensitive to sample height and cannot be peaked without losing the purge that protects the instrument and sample from the high humidity of ambient conditions. For this reason, we would caution against using the reflectance values as absolute reflectances. The spectra presented in this paper have been scaled multiplicatively to their approximate reflectance levels based on previous work with palagonite (e.g., Singer, 1982; Walsh and McCord, 1988). These problems with absolute reflectances are not critical to this discussion as the internal reflection level is consistent and relative band depth and exact band locations are unaffected. Resultant spectra of the various carbonate-palagonite mixtures are shown in Figures 3, 4, and 5.

The spectra show that at wavelengths shorter than about 3.5 μm none of the carbonates are detectable in quantities under about 10 wt%. However, the 4.0 μm carbonate absorption feature is clearly present in both the 5 wt% calcite and the 10 wt% magnesite measurements and is recognizable in the 3 wt% (5 wt%) calcite (magnesite) sample spectra. The magnesite mixtures' absorption bands appear to be bifurcated, with the large band seeming to split into two adjacent bands. We feel that with this spectral resolution 3% of calcium carbonate and 5% of magnesium carbonate, given high signal-to-noise, can be detected in a Martian soil.

The Martian surface undergoes a wide range of temperatures variations; therefore, one magnesite sample was measured in an environment chamber at liquid nitrogen temperature (77°K) to explore changes in the bands with temperature. Measurements were made using a

circular variable interference filter with a cooled InSb detector and covered the spectral range 2.4 to 4.6 μm (the same instrument used at the telescope). Halon was used as a reflectance standard. Halon is an almost perfect diffuse reflector between 0.33 and 2.6 μm . A correction was made between 2.6 and 4.2 μm for halon absorptions, based on laboratory measurements of the halon standard relative to sulfur and on published work (Nash, 1986). Halon instead of sulfur was used due to changes in sulfur's reflectivity when under vacuum conditions (Nash, 1986). The data collected for each sample were averaged and then divided by the halon reflectance to remove instrumental and light source effect and were finally corrected to reflectance relative to sulfur. The liquid-nitrogen-cooled sample was measured at a phase angle of 7° , owing to the constraints imposed by the environment chamber. The 4.0 μm band became slightly narrower than at room temperature, but the effective wavelength position did not change (Figure 6).

VI. Thermal Modeling

In the 4 μm spectral region, areas on Mars emit thermal radiation which can contribute significantly to the reflected solar component of radiation. A major concern in the interpretation of reflectance measurements made in this region is the masking of weak absorption features by thermal emission. This effect can be critical in setting detection limits for carbonites in the Martian soil.

To explore the influence that thermal emission might have on the detection of carbonates on Mars, the reflectance spectra shown in Figure 3 for a 5 wt% mixture of carbonate and palagonite were multiplied by the flux from a black body at the same effective temperature as the sun, 5770 K, at a distance of 1.523 A.U., the radius of the semi-major axis for Mars' orbit. A correction for absorption effects of the Martian atmosphere was not made because there are no strong absorptions in the wavelength region of interest. The radiated thermal flux for a surface with a wide range of temperatures, from

225 K to 300 K, and an emissivity of 1.0 was then added to the modified solar flux. The combined calculated reflected and emitted flux was then divided by the solar flux at Mars to produce a reflectance spectrum which would also include thermal emission effects.

The spectrum for 5 wt% mixture of icelandic spar calcite in Mauna Kea palagonite with contaminating thermal emission for temperatures of 225, 250, 275 and 300 K is shown in Figure 7. Note that at all temperatures the carbonate band is clearly visible. Only in the 300 K case does the band lose some definition. Thus, for realistic surface temperatures on Mars, $T \leq 270$ K, thermal emission is not likely to mask carbonate absorption features in the 3.5 to 4.0 μm spectral region for carbonate concentrations of 3-5 wt%, but the added slope to the spectrum can appear to shift the band position to shorter wavelengths.

VII. Interpretation

Spectra for the four areas of Mars observed are shown in Figure 8 with a straight line continuum removed using the values at the 3.75 and 3.96 μm channels. Of interest is the shallow depression in the top two spectra between 3.8 and 3.9 μm , which is not present in the lower two spectra. The magnitude these depressions is consistent with the presence of 5 to 10 wt% magnesium carbonate, on the average, in the upper few millimeters of the Martian soil over the areas observed. The depressions are too short in wavelength to be caused by calcium carbonate; they are closer in wavelength to the magnesium carbonate bands, but they are still slightly shorter in wavelength and broader in shape (Figures 3 - 5).

The reflectance spectra for the four areas of Mars are interpreted to indicate an upper limit of no more than ~ 3 wt% on the presence of calcium carbonates and ~ 5 wt% on the presence of magnesium carbonate in the upper few millimeters of Mars soil at the four areas measured. Two areas near Syrtis Major show weak spectral features similar in strength to those exhibited by 5-10 wt% magnesium carbonate in palagonite but at a shorter wavelength than magnesium carbonate so the identification of a specific carbonate species

has not been made. The overlapping nature of the regions involved limits the location of the material causing the feature to the region formed by the union of the Syrtis and North-East Highlands spots minus areas of the Arabia and Hellas spots. This region encompasses most of Syrtis Major Planum. Viking images of this dark region reveal a high concentration of bright wind-streaks indicating that a high degree of differential erosion is occurring which may expose material responsible for the absorption.

While the material causing the absorption feature is not yet identified, it seems to be on the Martian surface, and the region where it exists in sufficient abundance to be detected spectroscopically is of limited extent, specifically at Syrtis Major Planum. As noted earlier there are strong theoretical reasons for believing that carbonates are present on Mars. Our observations do not limit the presence of carbonates in general on Mars because they cover only a small area of the planets surface. Nor do they put any limits on the presence of carbonates at depth on Mars, say, below tens to hundreds of meters where they would not have been extensively exposed by meteorite impact since formation. Also, there may be outcrops or deposits of carbonates but over a sufficiently small portion (a few percent) of the areas observed so as not to affect the spectrum measured. The measurements do, however, argue strongly against a large concentration of carbonates in the windblown dust of Mars.

Hopefully, the evidence presented here will stimulate future improved groundbased observations during the Mars opposition. Emphasis should be placed on high spatial resolution and high signal-to-noise measurements in areas that have little dust accumulation. Even more important, the Mars Observer Mission should place a visible and infrared mapping spectrometer, the VIMS, in orbit around Mars in 1993. With its 600 m spatial resolution and the necessary spectral coverage (0.4 to 5.0 μm) and spectral resolution (about 1 %), area deposits as small as 10^4 m^2 or 100 m on a side (two U.S. football fields side by side) should be detected, if present.

Acknowledgments

We thank the University of Hawaii 2.2 m telescope support staff for assisting with our observations. These data were acquired as part of a larger observation project in which other people from the authors' organization participated, and they helped make possible the subset of observations reported here. These others were: Pamela Owensby, Paul Lucey, Jeffrey Bosel, Patti Walsh, and James Bell, who was on summer study from Caltech. We appreciate the helpful discussions with James Pollack, of the Ames Research Center, and Fraser Fanale, of the authors' organization, on the subject of the theoretical basis for expecting salts on Mars.

References

- Anders, E., and T. Owen, Mars and Earth: Origin and abundance of volatiles, *Science*, 198, 453-465, 1977.
- Baird, A.K., P. Toulmin, B.C. Clark, H.J. Rose, K. Keil, R.P. Christian, and J.L. Gooding, Mineralogic and petrologic implications of Viking geochemical results from Mars: Interim report, *Science*, 194, 1288-1293, 1976.
- Beer, R., R.H. Norton, and J.V. Martonchik, Astronomical infrared spectroscopy with a Connes-type interferometer: II. Mars, 2500-3500 cm⁻¹, *Icarus*, 15, 1-10, 1971.
- Biemann, K., J. Oro, P. Toulmin, L.E. Orgel, O. Nier, P.M. Anderson, P.G. Simmonds, D. Floy, A.V. Diaz, R. Rushneck, J.E. Biller, and A.L. Lafleur, The search for organic substances and inorganic volatile compounds in the surface of Mars, *J. Geophys. Res.*, 82, 4641-4658, 1977.
- Blaney, D.L., P.A. Walsh, and T.B. McCord, Laboratory Spectral Measurements of Palagonite-Salt Mixtures in the Visible and Near Infrared- Implications for Mars (abstract), *Lunar and Planetary Science XVIII*, Lunar and Planetary Science Institute, Houston, TX, 1987.
- Carr, M.H., Mars: A Water-Rich Planet?, *Icarus*, 82, 187-216, 1986.
- Clark, B.C., A.K. Baird, P. Toulmin, H.J. Rose, K. Keil, A.J. Castro, W.C. Kelliher, C.D. Rowe, and P.H. Evans, Organic analysis of martian surface samples at the Viking landing sites, *Science*, 194, 1283-1288, 1976.
- Clark, B.C., A.K. Baird, R.J. Weldon, D.M. Tsusaki, L. Schrabel, and M.P. Candelaria, Chemical Composition of Martian Fines, *J. Geophys. Res.*, 87, 10,059-10,068, 1982.
- Dreibus, G., and H. Wanke, Accretion of the earth and inner planets, *Proc. 27th Int. Geol. Congr. Moscow*, 11, 1-11, 1984.
- Dreibus, G., and H. Wanke, Comparison of Cl/Br and Br/I ratio in terrestrial samples and SNC meteorites, *Proc. Workshop on The Evolution of the Martian Atmosphere*, Technical Report, 86-07, 13-14, Lunar and Planetary Institute, Houston, TX, 1986.
- Fanale, F.P., and W.A. Cannon, Mars: CO₂ absorption and capillary condensation on clays--Significance for volatile storage and atmospheric history, *J. Geophys. Res.*, 84, 8404-8415, 1979.
- Fanale, F.P., and R.N. Clark, Solar System ices and Mars permafrost, *Permafrost: Fourth International Conference Proceedings*, 289-294, National Academy Press, Washington, DC, 1983.

- Fanale, F.P., J.R. Salvail, W.B. Banerdt, and R.S. Saunder, The regolith-atmosphere-cap system and climate change, *Icarus*, 50, 381-407, 1982.
- Gooding, J.L., Chemical Weathering on Mars. Thermodynamic Stability of Primary Minerals (and there Alteration Products) from Mafic Igneous Rocks, *Icarus*, 33, 483-513, 1978.
- Gooding, J.L., S.J. Wentworth, and M.E. Zolensky, Calcium Carbonate and sulfate of possible extraterrestrial origin in the EETA 79001 meteorite, *Geochim. Cosmochim. Acta*, 52, 909-915, 1988.
- Houck, J.R., J.B. Pollack, C. Sagan, P. Schack, and J.A. Pecker, High altitude infrared spectroscopic evidence for bound water on Mars, *Icarus*, 18, 3, 470-479, 1973.
- Huguenin, R.L., and L. Harris, Accreted H₂O inventory on Mars, *Proc. Workshop on the Evolution of the Martian Atmosphere*, Honolulu, *Technical Report*, 86-07, 19-22, Lunar and Planetary Institute, Houston, TX, 1986.
- Masursky, H., J.M. Boyce, A.L. Dial, G.G. Schaber, and M.E. Strobell, Formation of martian channels, *J. Geophys. Res.*, 82, 4016-4038, 1977.
- McElroy, M.B., T.Y. Kong, and Y.L. Yung, Photochemistry and evolution of Mars' atmosphere: A Viking perspective, *J. Geophys. Res.*, 82, 4379-4388, 1977.
- McCord, T.B., R.N. Clark, and R.B. Singer, Mars: Near-infrared reflectance spectra of surface regions and compositional implication, *J. Geophys. Res.*, 87, 3021-3032, 1982.
- McKay, C.P., and S.S. Nedell, Are there carbonate deposits in the Valles Marineris, Mars?, *Icarus*, 73, 142-148, 1988.
- Morgan, J.W., and E. Anders, Chemical composition of Mars, *Geochim. Cosmochim. Acta.*, 43, 60-76, 1979.
- Nash, D.B., Mid infrared reflectance spectra (2.3-22 μ m) of sulfur, gold, KBr, and MgO and halon, *Applied Optics*, 25, 2427-2433, 1986.
- Piere, D.C., Martian Valleys: Morphology, distribution, age, and origin, *Science*, 210, 895-897, 1980.
- Pollack, J.B., Climate change on the terrestrial planets, *Icarus*, 37, 479-533, 1979.
- Pollack, J.B., and D.C. Black, Implications of the gas compositional measurements of Pioneer Venus for the origin of planetary atmospheres, *Science*, 205, 56-59, 1979.
- Postawko S.E., and W.R. Kuhn, Effects of the greenhouse gases (CO₂, H₂O, and SO₂) on Martian paleoclimate, *J. Geophys. Res.*, 82, 4635-4639, 1986.
- Roth, L.E., R.S. Saunders, and G. Schubert, Mars: Seasonally variable radar reflectivity (abstract), *Lunar and Planetary Science XVI*, 712-713, Lunar and Planetary Institute, Houston, TX, 1985.

- Roush, T.L., D. Blaney, T.B. McCord, and R.B. Singer, Carbonates on Mars: Searching the Mariner 6 and 7 IRS measurements (abstract), *Lunar and Planetary Science XVII*, 732-733, Lunar and Planetary Institute, Houston, TX, 1986.
- Schultz, P., The Martian atmosphere before and after the Argyre impact, *Proc. Workshop on The Evolution of the Martian Atmosphere*, Honolulu, *Tech. Report 86-07*, 38-39, Lunar and Planetary Institute, Houston, TX, 1986.
- Sharp, R.P., Mars: Fretted and chaotic terrains, *J. Geophys. Res.*, *78*, 4073-4083, 1973a.
- Sharp, R.P., Mars Troughed terrain, *J. Geophys. Res.*, *78*, 4063-4072, 1973b.
- Sharp, R.P., Mars: South polar pits and etched terrain, *J. Geophys. Res.*, *78*, 4222-4230, 1973c.
- Singer, R.B., Spectral evidence for the mineralogy of high albedo soils and dust on Mars, *J. Geophys. Res.*, *87*, 10159-10168, 1982.
- Sinton, W.M., On the composition of the Martian surface materials, *Icarus*, *6*, 222-228, 1967.
- Toulmin, P., A. K. Baird, B. C. Clark, K. Keil, H.J. Rose, R. P. Christian, P. H. Evans, and W.C. Kelliher, Geochemical and mineralogical interpretation of the Viking inorganic chemical results, *J. Geophys. Res.*, *82*, 4625-4634, 1977.
- Warren, P.H., Mars regolith versus SNC meteorites: Possible evidence for abundant crustal carbonates, *Icarus*, *70*, 153-161, 1987.
- Watkins, G.H., and J.S. Lewis, Evolution of the atmosphere of Mars as the result of asteroidal and cometary impacts, *Proc. Workshop on the Evolution of the Martian Atmosphere*, Honolulu, *Technical Report, 86-07*, 46-47, Lunar and Planetary Institute, Houston, TX, 1986.
- Walsh P.A., and T.B. McCord, Spectral studies of salt-palagonite mixtures, in preparation, 1988.
- Yung, Y.L., and M.B. McElroy, Fixation of nitrogen in the prebiotic atmosphere, *Science*, *203*, 1002-1004, 1979.
- Zent, A.P., and F.P. Fanale, Possible Mars brines: Equilibrium and kinetic considerations, *J. Geophys. Res.*, *91*, D439-D445, 1986.
- Zisk, S.H., and P.J. Mouginis-Mark, Anomalous region on Mars: Implications for near-surface liquid water, *Nature*, *44*, 735-738, 1980.

Table 3.1. Observational Parameters for Mars Measurements Taken on September 19, 1986.

<u>Area</u>	<u>Time (UT)</u>	<u>Earth Airmass</u>	<u>#Runs</u>	<u>Central Meridian</u>
Syrtris	6:32-6:46	1.46-1.49	7	302°
Hellas	6:51-7:00	1.49-1.51	7	306°
Arabia	7:37-8:02	1.65-1.70	6	316°
NE High-lands	7:51-8:02	1.72-1.77	6	321°

Observational information for Mars spectra shown in Figure 2. Time is given in hours universal time. Central Meridian given is the value at the halfway point of each set of observations and is given in degrees of west longitude.

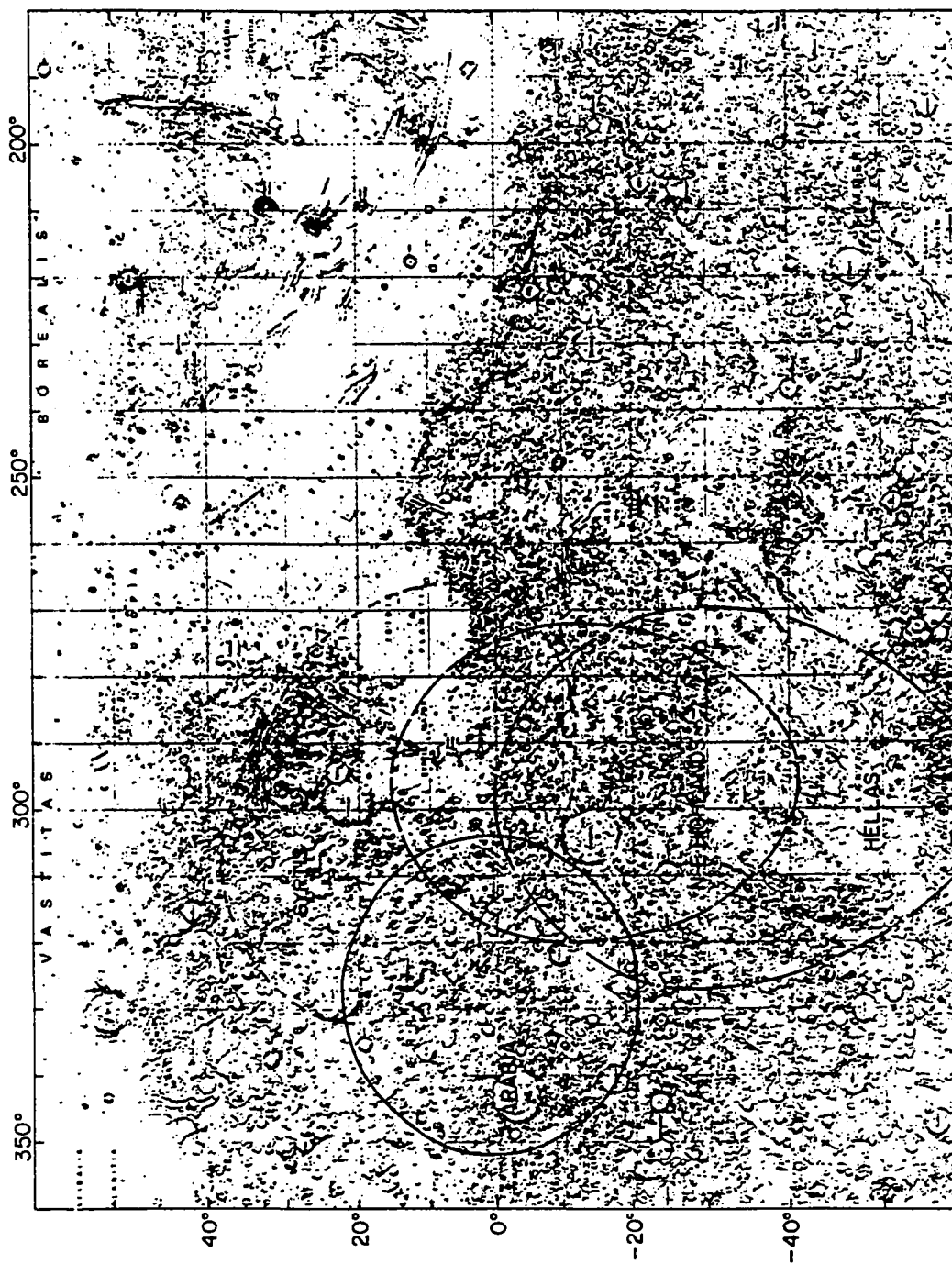


Figure 3.1. Locations of the four areas observed on Mars on September 19, 1986. (Base map from U.S. Geologic Survey.)

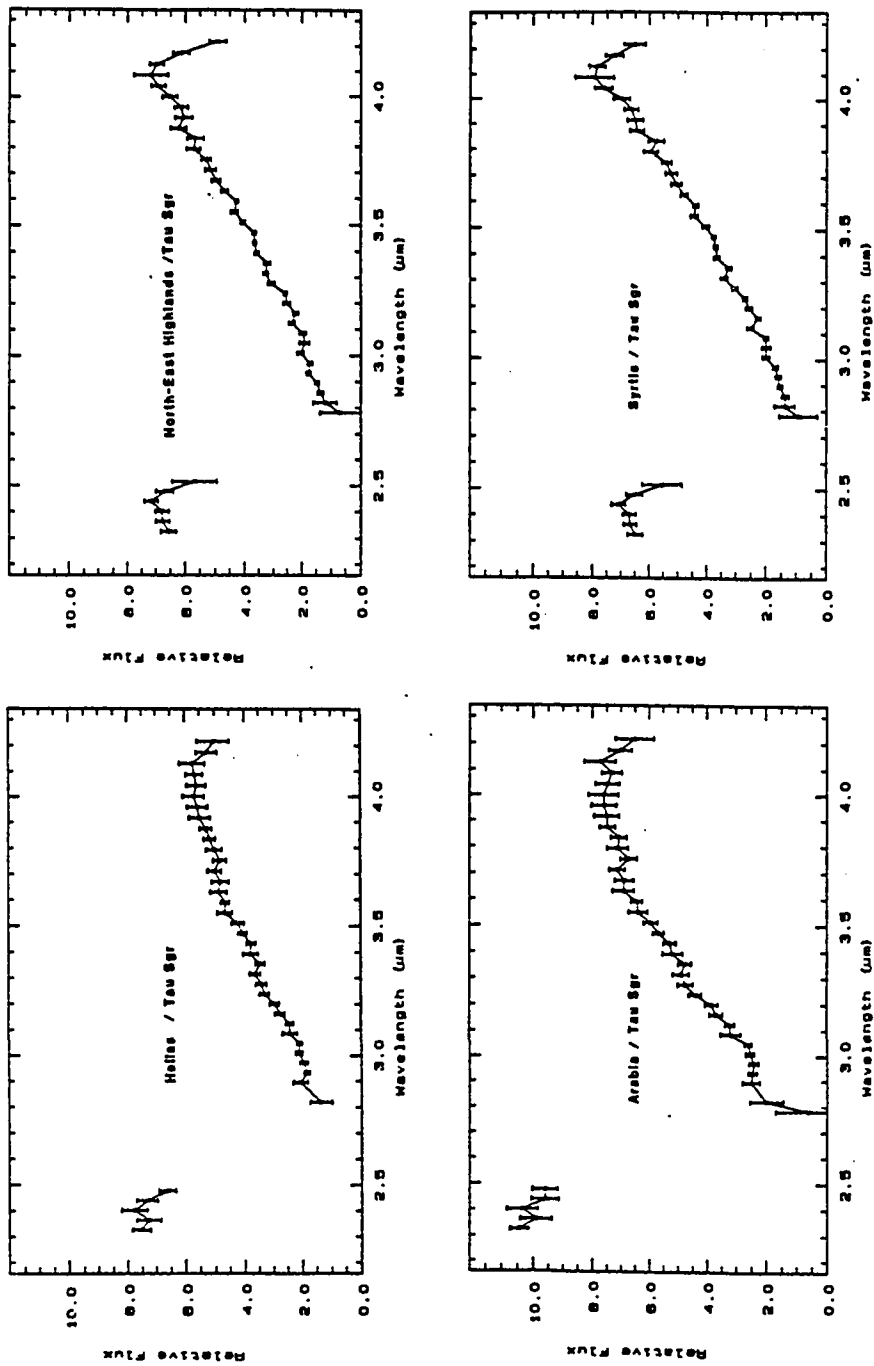


Figure 3.2. Ratios of the spectra of the four Mars regions (numerator) designated Hellas, Arabia, Syrtis and North East Highlands to the star Tau Sagittarius (denominator).

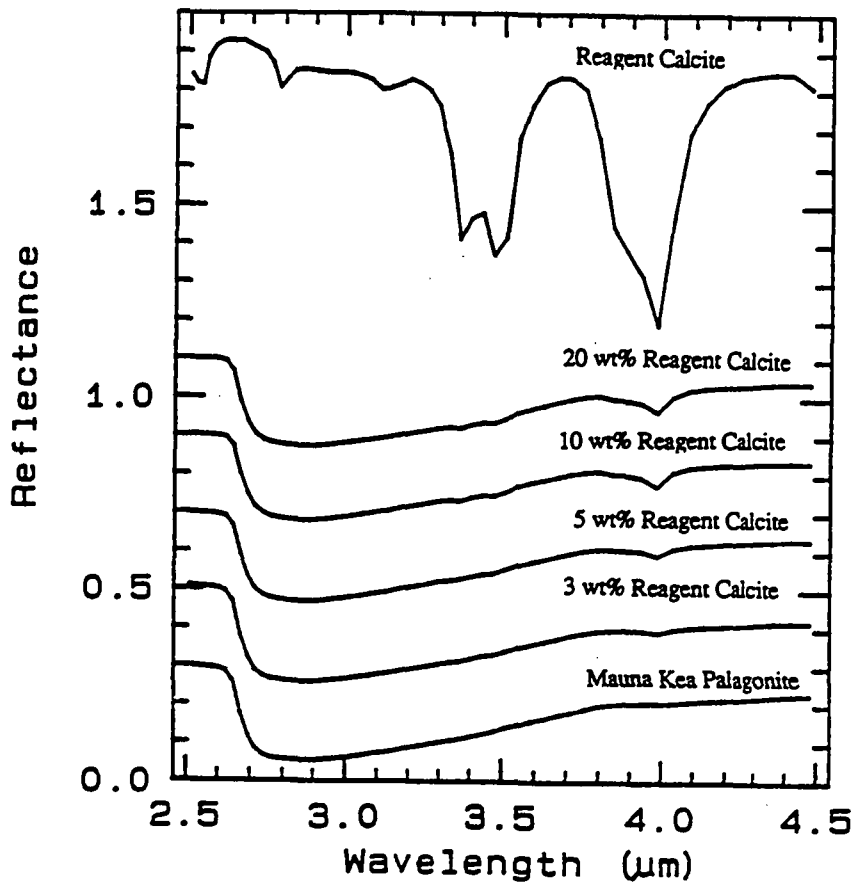


Figure 3.3. Reflectance spectra from 0.6 to 4.4 μm of reagent grade calcite, 20, 10, 5, and 3 weight percent mixtures of calcite in Mauna Kea palagonite, and pure Mauna Kea palagonite. Successive spectra are offset from each other by 0.2.

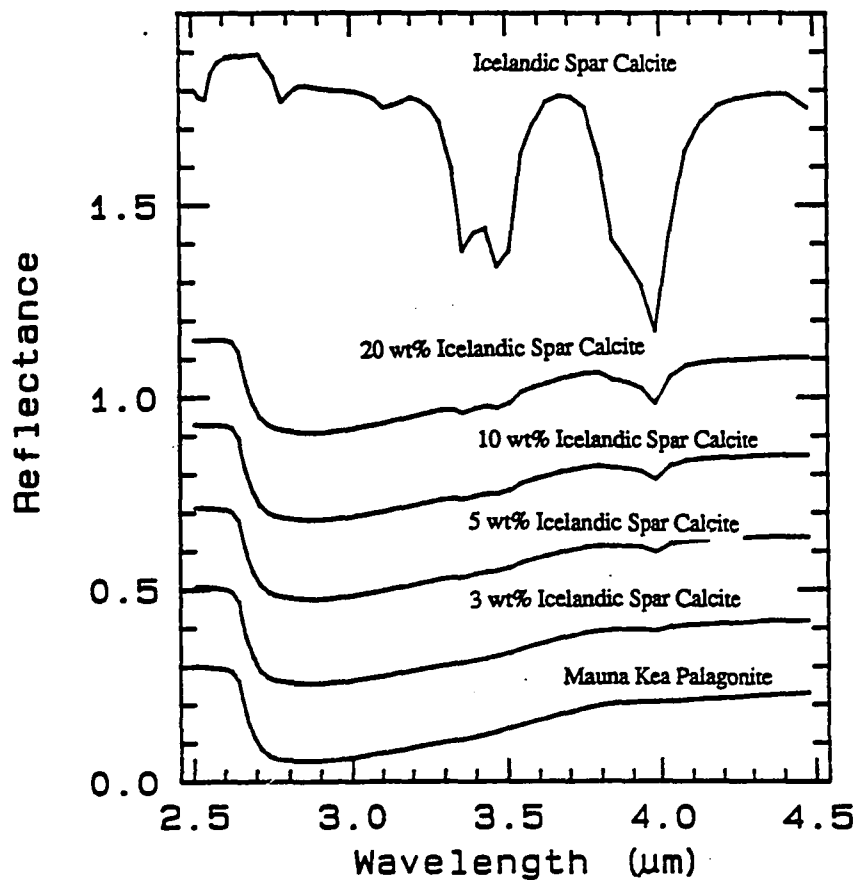


Figure 3.4. Reflectance spectra from .6 to 4.4 μm of Icelandic spar calcite, mixtures of 20, 10, 5, and 3 weight percent calcite in Mauna Kea palagonite, and pure Mauna Kea palagonite. Successive spectra are offset from each other by 0.2.

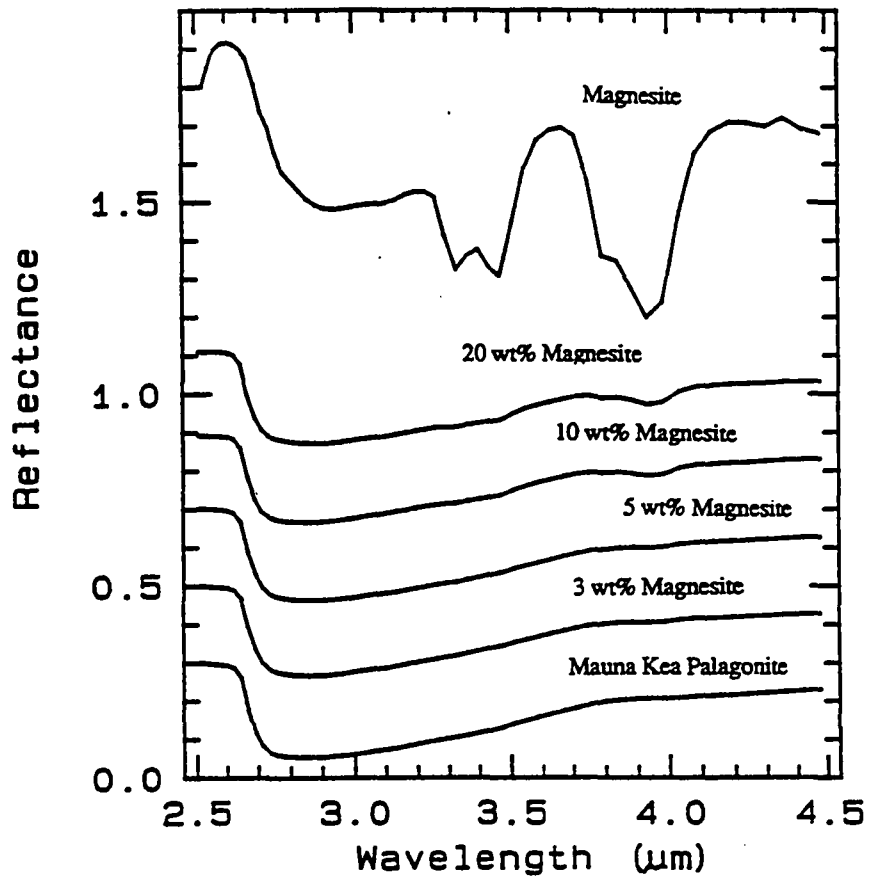


Figure 3.5. Reflectance spectra from 2.4 to 4.4 μm of magnesite, mixtures of 20, 10, 5, and 3 weight percent magnesite in Mauna Kea palagonite, and pure Mauna Kea palagonite. Successive spectra are offset from each other by 0.2.

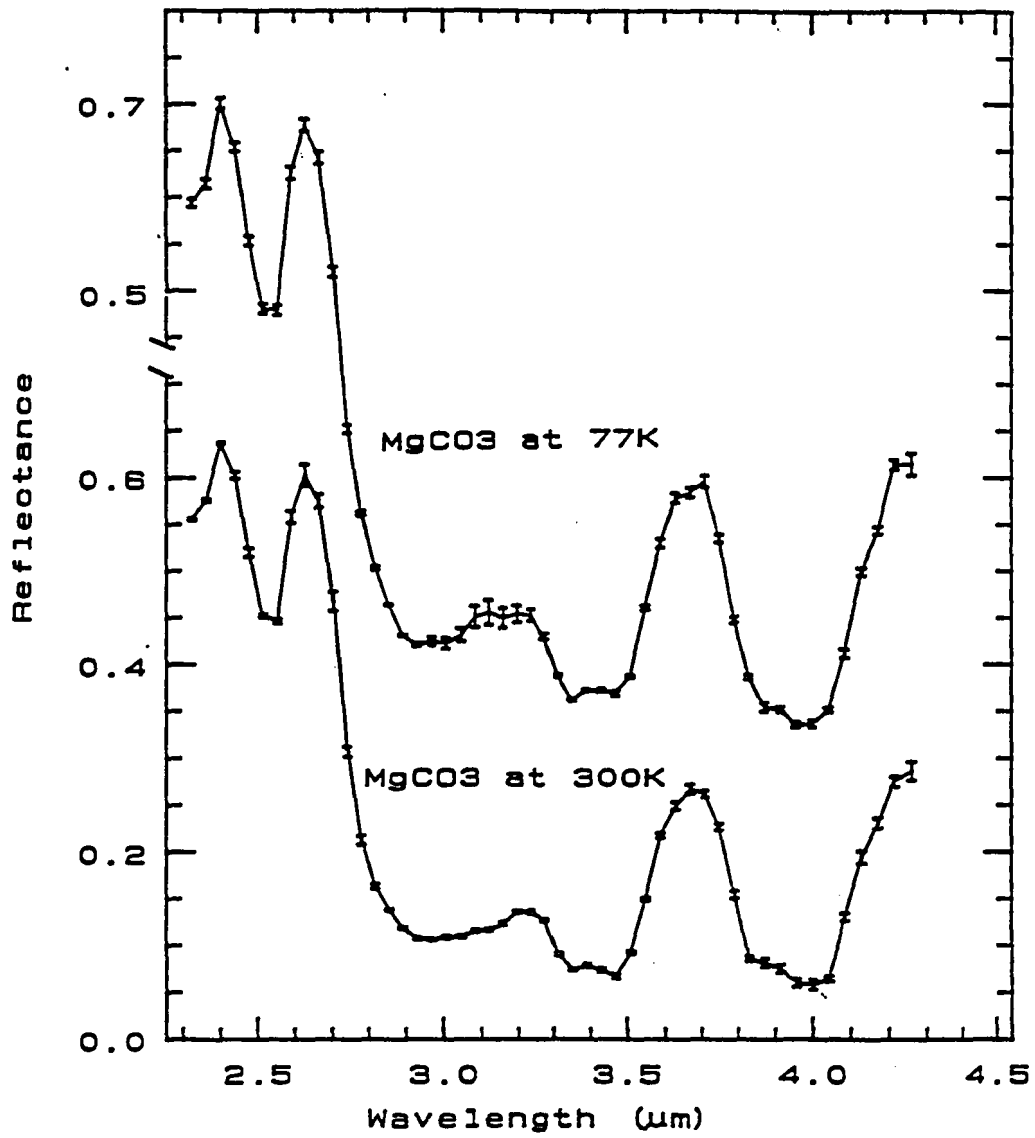


Figure 3.6. Reflectance spectra of magnesite at 300 K, phase angle 30°, and at 77 K, phase angle 7° between 2.4 and 4.4 μm.

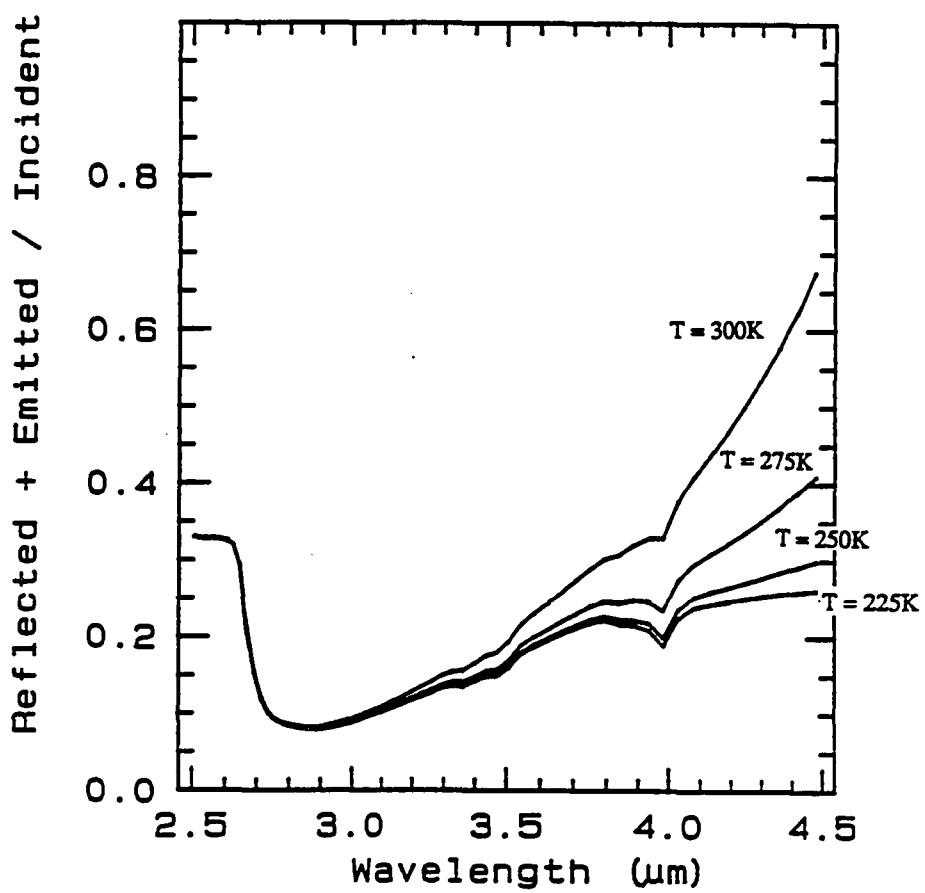


Figure 3.7. Modeled results of a mixture of 5 wt% reagent calcite in Mauna Kea palagonite at temperatures of 210, 230, 250, 270, and 285 K as it would appear if observed on Mars.

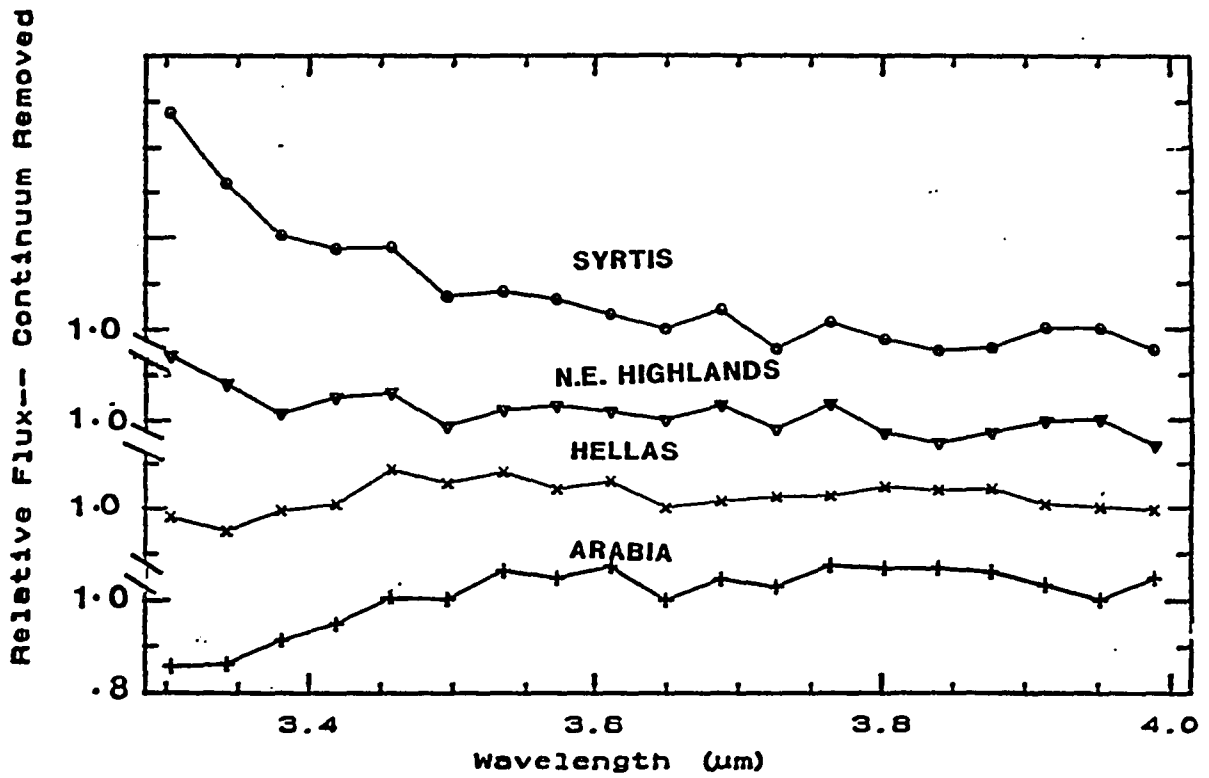


Figure 3.8. Mars spectra from 3.7 to 4.0 μm for Hellas, Arabia, Syrtis, and North East Highlands with a straight line continuum removed using values at 3.75 and 3.96 μm.

Note on Chapter 3.

Since the initial writing of chapter 3 the interpretation of the absorption feature a 3.8 μm has been changed from being due to a surface mineral to being caused by CO_2 with ^{17}O and ^{18}O . This is discussed in detail in Chapter 4. Additionally, the text has been rewritten to read more smoothly. The science discussed has not changed.

Chapter 4.

Constraints on the climatic and weathering histories of Mars from earth based near infrared spectroscopy between 3.2 and 4.2 microns

Diana L. Blaney* and Thomas B. McCord*.

Planetary Geosciences Division of the

Hawaii Institute of Geophysics

2525 Correa Rd.

Honolulu, HI 96822

Submitted to Journal of Geophysical Research, June 1989.

***Visiting Astronomer at the Infrared Telescope Facility which is operated by the University
of Hawaii under contract from the National Aeronautics and Space Administration.**

I. Abstract

Telescopic measurements of Mars were made on August 19, 1988 UT of Mars at the NASA IRTF facility. Spectra were obtained with the Cooled Grating Array Spectrometer (CGAS) with a resolution of $R=300$ with coverage between $3.2 \mu\text{m}$ and $4.2 \mu\text{m}$. The spectra show variations in the steepness of the slope at the longward end of the bound water band. The wavelength coverage of these spectra do not allow us to discriminate between: variations in the hydration; surface frost; or ice clouds. Carbon dioxide with ^{18}O and ^{17}O as one of the oxygen atoms is responsible for absorption features at $3.61 \mu\text{m}$, $3.81 \mu\text{m}$, $3.97 \mu\text{m}$, and $4.05 \mu\text{m}$ (Encranz, 1989). Discrepancies between the observed Mars spectra and the atmospheric models by Encrenaz (1989) and Crisp (personal communication) exist. Whether these differences are indicative of surface components or of the need for further modeling of the Martian atmosphere is undetermined at this point. No evidence of absorptions due to carbonates in the $4 \mu\text{m}$ region was observed in the data. The implications low carbonate abundance in the optical surface for paleo-climate and geochemical weathering models is discussed.

II. Introduction

The Martian surface has been a source of fascination since telescopes first enabled people to see the changing surface albedo features and polar caps. This paper is an initial attempt to use information from earth-based spectroscopic observations in the $3 \mu\text{m}$ to $4 \mu\text{m}$ region in conjunction with other data sources to better understand the climate and weathering evolution of Mars.

Spectroscopy in the near infrared between $3.0 \mu\text{m}$ and $4.2 \mu\text{m}$ provides information on two important potential weathering products on Mars: 1) minerals containing bound water and hydroxyl groups, and 2) carbonates. The $3 \mu\text{m}$ region contains both the symmetrical

and asymmetrical O-H stretching fundamentals of the H₂O molecule at 3.1 μm and 2.9 μm respectively, as well as the 2.78 μm OH⁻ stretching fundamental (Hunt and Salisbury, 1970). The 4 μm region contains carbonate absorptions at 3.5 μm and 4.0 μm . The 4.0 μm band is especially sensitive to the presence of small amounts of carbonates, and the position of the 4.0 μm carbonate band changes little with cation (Walsh, 1987; Blaney and McCord, 1989). The spectra of mixtures of carbonates and Mauna Kea palagonite, an amorphous weathering product of basaltic glass which is a good spectral analog for Mars at low resolution in the visible and near infrared (Evans and Adams, 1979; Singer, 1982), indicate that carbonate abundances on the order of 1-3 wt% should be detectable (Blaney and McCord, 1989; Walsh et al. 1987) depending on the cation and assuming grain sizes similar to fine material measured at both Viking lander sites. The implications of the composition indicated by the telescopic spectra presented here on climate change and weathering processes will be examined.

III. Previous Measurements

Measurements in the 3 μm - 4 μm region have been few and of relatively low resolution both spectrally and spatially, or of low signal-to-noise ratio by current instrumentation standards. The first measurements between 3 μm and 4 μm were reported by Sinton (1957) and covered the wavelength region from 3.3 μm to 3.6 μm , but stopped well short of the 4 μm carbonate absorption. During the opposition of 1963, Moroz used two autocollimating infrared spectrometers with lead sulfide detectors to make measurements between 1.1 and 4.1 microns (Moroz 1964). Moroz suggested that the Mars spectrum was similar to that of limonite, with discrepancies at wavelengths longer than 2.5 microns between limonite and Mars being due to differences in the amount of water of crystallization and thermal emission. During the 1963 opposition, Sinton (1967) observed a strong bound-water band and pointed out that thermal emission is not a major factor

controlling the slope between 3 and 4 microns at reasonable Mars temperatures. Sinton further pointed out that many minerals have strong bound-water absorptions and that the presence of a 3 μm band is not definitive evidence for limonite. Beer et al. (1971) confirmed the presence of the bound-water band and set detection limits on the presence of many proposed molecular species on Mars such as H_2S , NO_2 , COS , and C_3O_2 .

While the previous studies assumed that bound water was causing the absorption near 3 μm , they were not definitive, as telluric water absorptions between 2.5 and 3.0 microns made observations of the band center of any bound water-feature impossible. To avoid terrestrial water absorptions, Houck et. al (1973) used an airborne telescope to make measurements above most of the Earth's atmosphere (the amount of water present was < 15 precipitable microns). The resultant Martian spectra (ratioed to the moon) covered the region between 2 and 4 microns. These spectra showed an 80% absorption depth with a band minimum at about 2.85 microns. This feature is consistent with the bound-water feature found in terrestrial minerals. Estimates by Houck et al. (1973) on the amount of bound water present based on albedo, particle size, and modeling of terrestrial hydrated material, indicated about 1% water by weight.

Mariners 6 and 7 were the only U.S. spacecraft to carry spectrometers to make measurements in the near infrared. The IRS spectrometers collected data between 1.9 and 14.4 microns. An initial report of the 3 μm feature was made by Herr et al. (1969) shortly after the first data return. Detailed interpretation with respect to hydrated minerals and solid water was published by Pimentel et al. (1974). They examined variations in signal level inside and outside the water band as represented by the ratios of intensity at 3.1 μm / 2.2 μm and at 2.9 μm / 3.1 μm , and found that variations in the 3.1/2.2 ratio change systematically with albedo (especially in the equatorial region). Variations due to particle size and the extent and nature of hydration of material could not be separated. The 2.9/3.1 ratio was determined to be diagnostic of the presence of ice, allowing discrimination between bound water and ice. More recent examination by Roush et al. (1986), and by

McKay and Nedel (1988) of the recently restored Mariner 6 and 7 IRS spectrometer data (provided by T. Martin) showed no evidence for carbonate absorptions at 4.0 μm .

IV. Observations

Telescopic measurements of Mars reported here were made on August 19, 1988 UT of Mars at the NASA IRTF facility. Spectra were obtained with the Cooled Grating Array Spectrometer (CGAS) which utilizes a thirty-two element InSb line array as described by Tokunaga et al. (1988). A grating with a resolution of $R=300$ was used. Measurements were made by taking data at three different grating positions, with an eight channel overlap between positions. Segment 1 covered 3.149 μm - 3.603 μm , segment 2, 3.501 μm - 3.958 μm , and segment 3, 3.854 μm - 4.313 μm . Allowing for detector end effects and overlap, the effective total coverage is between 3.2 μm and 4.2 μm .

Location of the aperture on the disc of Mars was accomplished by bore-sighting using a bright star and measuring the half - power points of the signal to locate the center of the aperture in both right ascension and declination. An electronic crosshair was positioned to mark the center of the aperture. The crosshair on the video image of the telescopic focal plane image were video-taped for later reconstruction of the aperture locations on Mars. Bore-sighting was checked roughly every thirty minutes when standard star measurements were made. No noticeable drift in the location of the aperture was observed during the course of the night.

Image locations were derived from the videotapes. The aperture locations are plotted on orthographic maps shown in Figures 1 and 2. Locations are labeled a-h in the figures and called after the dominant geologic feature within the region covered by the aperture. These regions do not coincide with exact locations of the geologic feature named. CGAS has a 2.7 arc-second aperture yielding a spot diameter of 900 km on Mars at the sub-earth point. The regions measured in Figures 1 and 2 show a wide range in both age, and

geological settings based on Viking photogeology. The young Amazonian-age Tharsis volcanic region (areas *f* and *g*), as well as the Noachian-aged heavily cratered terrain (area *c* and *e*), were sampled. Measurements included both equatorial and high latitude locations. Lower Chryse Planitia was included in measurement *h*. Nirgal Valles, a large valley network, was included in *a*. Regions *a* and *b* also included portions of Valles Marineris.

The data were reduced using the spectral data processing system SPECPR (Clark, 1982). The star BS437, a 0.97 magnitude G8III spectral type, was used as a standard. BS 437 followed thirty minutes behind Mars and a measurement scheme of thirty minutes on Mars, thirty on the standard was used. Table 1 shows the measurement sequence and observing information. Each Mars spectrum was reduced using a standard star observation within 0.1 airmass of the observation. Both Martian and standard star spectra were normalized to unity at 3.9133 μm prior to dividing the spectra. Examination of the individual spectra showed that the sky was stable throughout the night and measurements varied smoothly with airmass. The sole exception is a 3.3 μm methane absorption in some spectra which was uncorrelated with extinction. The points affected by this methane absorption have been deleted.

V. Description of the Spectra

A. General Characteristics

The spectra shown in Figure 3 exhibit increasing reflectance between 3.2 μm and 4.1 μm . This is due to absorption from hydrated minerals depressing the continuum level in the 3 μm region and to a slight increase in thermal emission at longer wavelengths. Near 4.1 μm the reflectance decreases owing to Martian atmospheric CO₂ absorptions. Between

3.76 μm and 3.87 μm an absorption feature appears with a double minimum (3.810 μm and 3.854 μm) and a maximum strength of about 4%. This absorption is consistent with the spectra obtained from the 1986 opposition which showed a similar feature observed in the Syrtis region (Blaney and McCord, 1989). Further analysis was done by approximating a continuum with a straight line fitted to the spectrum at 3.751 μm and 3.913 μm and dividing the spectrum by the line to remove the slope. The spectra with the continuum removed are shown in Figure 4. They revealed no variation in the band minima but do show some variation in the band strength. The band depths of each spectra was then measured and used to generate Table 2.

The spectra in Figure 3 also show consistent inflections at about 3.6 μm , and on either side of 4 μm . To investigate these slight inflections, all eight spectra were added together and a least squares fit of a line to all of the data points in the co-added spectrum at wavelengths shorter than the downturn caused by Martian atmospheric CO₂ (4.1 μm) was calculated. The co-added Mars spectrum was divided by the least squares fitted line to produce the lower spectrum shown in Figure 5.

B. Isotopically Heavy CO₂

Encrenaz (personal communication, 1989) points out that these absorptions are correlated with the position that bands would appear in a model CO₂ transmission spectrum including both ¹⁸O and ¹⁷O. Other atmospheric models of the Martian atmosphere also indicate that isotopically heavy CO₂ contributes to the spectrum of Mars in this wavelength region. In Figure 5, (the upper spectrum), a model Martian atmosphere that was generated by David Crisp of the Jet Propulsion Laboratory is shown. The model atmosphere consists of 7 mbar of CO₂ with H₂O and CO also present. An atmospheric depth of 2 airmasses is assumed. Output from the model at 5 cm⁻¹ was convolved through a triangular filter with the same half-width as the CGAS instrument, to produce a synthetic

atmospheric transmission spectrum of the same resolution as the telescopic data. The spectrum was then interpolated to the same wavelengths as the telescopic measurements. Notice that there is good agreement between the positions of the absorption features, and that these slight (1-2 %) bands are clearly recognized in the Mars data. Encrenaz (1989, this issue) has fitted several of the spectra shown in Figure 3 in detail.

Despite the general agreement of the telescope data and the isotopically heavy CO₂ model bands in wavelength, there is a large degree of variation in the band shapes and depths. Neither the Encrenaz (Encrenaz this issue) or the Crisp model does especially well in matching the 3.61 μm feature, particularly the asymmetry of absorption. In addition, the depth of the 3.61 μm feature is too deep when compared to the 3.81 μm feature in both models. The shape of the model absorptions on either side of 4 μm does not match the telescopic data well. This mismatch is due in part to the way the continuum was estimated. Effects from bound water, which control the shape of the curve over most of this wavelength region have declined and contributions from thermal emission begins to be important. A continuum fitted to just the 4 μm region gives a slightly better match between the modeled and the telescopic data, (see Figure 6). Additionally, because these atmospheric transmission spectra are calculated, they depend on assumptions such as the thermal structure of the atmosphere, surface albedo, composition, and line strengths. The preliminary nature of the atmospheric modeling does not permit identification in the telescopic data of surface material absorptions underlying these atmospheric absorptions. A more thorough removal of the atmosphere, with parameters adjusted for each individual spectrum, is necessary.

C. Hydration

The data shown in Figure 3 start at a longer wavelength than is ideal for characterization of hydrates and hydroxyl groups. However, the slopes of the normalized spectra vary systematically owing to the effect of shorter wavelength water absorptions. As a method

for classification, a linear least-squares fit of the values in grating position 1 (covering the wavelength range $3.2\ \mu\text{m}$ - $3.6\ \mu\text{m}$), omitting bad data values caused by variable methane abundances, was performed for each spectrum. Table 3 shows the slope of the spectra for each location. The band depths presented in Table 2, which correlate with the abundance of isotopically heavy CO_2 , as discussed previously, can be thought of as a rough gauge of Martian airmass. Figure 7 shows spectral slope between $3.2\ \mu\text{m}$ and $3.6\ \mu\text{m}$ (Table 3) plotted against $3.81\ \mu\text{m}$ band depth (Table 2) in a scatter diagram. Effects of topography as well as viewing geometry are intermixed. The regions having shallow slope values, Margaritifer Sinus, Valles Marineris, Argyre Basin, Eastern Solis Planum, also have roughly the same Martian airmass and cluster together. Both the Eastern and Western Tharsis spectra have roughly the same intermediate slope although they have different Martian airmass. The difference in airmass between these two regions is due primarily to the western Tharsis region lying at very high altitude. Figure 2 shows the spot location on a topographic map. The western Tharsis region is at an elevation of about 9 km relative to Martian datum with areas in the interior rising to 27 km. The other regions are at much lower elevations. The areas with spectra having steep slope, Chryse and the high-latitude heavily cratered terrain, have roughly the same high Martian airmass.

Separating the effects on the slope of hydration, ice crystals in the atmosphere, and surface frost is difficult given the limited wavelength coverage. Atmospheric water vapor does not contribute to the spectral slope; therefore, if the slight correlation of the slope with airmass is significant, it is due to ground frost or ice clouds. This is plausible as measurements at high Martian airmass were obtained near the limbs and frost could be present. The Chryse measurement is "late" afternoon (Martian time), and the high-latitude heavily cratered terrain is a "morning" measurement. Cool morning temperatures would increase the likelihood of frost. Additionally, higher Mars airmass by definition indicates a longer atmospheric path length, causing the optical thickness of ice clouds in the Martian atmosphere to increase. Equally plausible is that the high-latitude heavily cratered terrain

measurement and the Chryse measurements contain more ground ice or more hydrated material than the other regions measured. High-latitude regions are expected to contain more ground ice (Fanale et al., 1986, Squyres and Carr, 1986). Similarly, several large outflow channels, formed from the catastrophic release of ground water, discharge into Chryse. Water from these events may still be present in the form of permafrost or hydrated minerals. Determination of the reason for the increased spectral slope is thus not possible with the current data.

The similarity of the slopes of the two Tharsis region spectra, despite their different atmospheric column depths, indicates that differences in slope may be caused by variations in the hydration state of the surface that is, the slope measured may be an indication of the degree of hydration of the Tharsis Montes region. The eastern Tharsis spectrum has the same airmass (3.81 μm band depth) as the Argyre, Valles Marineris, and Solis Planum spectra but exhibits a much steeper slope. The Tharsis Montes region is therefore more hydrated than the Argyre, Valles Marineris, and Solis Planum regions measured. More data, collected at a wider spectral range, are needed to resolve questions about distribution and composition of ground ice, surface frosts, atmospheric effects, and hydration variations.

D. Scapolite

Short wavelength data between 2 μm and 2.5 μm collected by Clark et al. (1989) have suggested that meionite, the Ca-rich end member of the scapolite solid solution series, may be a component of the Martian surface. Controversy exists over whether this feature is due to CO or a combination of CO and scapolite (Encrenaz, 1989, Clark et al., 1989). Any mineral with spectral characteristics which account for the short wavelength data must also be consistent with data at longer wavelengths. Figure 8 shows a spectrum of a meionite from Quebec (obtained from Ward's Natural Science Establishment, Inc.) above a spectrum of Chryse between 3.2 μm and 4.2 μm . Although the spectrum of this scapolite

is not typical of most scapolites as scapolite has a wide variation of band positions and strengths that depend on composition (R. N. Clark personal communication, 1989), it does illustrate the point that scapolites have absorption features in the 3.2 μm - 4.2 μm wavelength region. If scapolite is as ubiquitous as the Clark et al. (1989) interpretation of the absorption at 2.36 μm suggests, then an explanation is required to account for the absence of bands in the 3.2 μm - 4.2 μm region. It is possible that some of the deviation between the theoretical atmospheric models and the telescopic observations discussed earlier could be the result of a surface component, such as scapolite but, given the preliminary nature of the atmospheric models, these differences could also be due to an incomplete or incorrect set of assumptions. A considerable amount of work needs to be undertaken before distinctions between these possibilities can be made.

E. Carbonates

No evidence of carbonates in the 4 μm region was observed in the data presented here. The ability to detect atmospheric isotopic features with absorption depths of less than one percent lends confidence to the conclusion that no 4.00 μm feature is present.

To check that the atmospheric isotopic features measured on either side of 4.00 μm were in fact absorptions and not the sides of an emissivity peak at 4.00 μm , a synthetic band with a 10 % absorption feature was created and is shown in Figure 9a. The emissivity of the feature was calculated by using Kirchoff's law ($1 - \text{absorption} = \text{emissivity}$) and the resultant emissivity is given in Figure 9b. The telescope measures both the reflected solar radiation and the thermal energy emitted from the surface. A model of the flux from the surface of Mars from both emitted and reflected light assuming that the surface has the emission and absorption shown in Figures 8a and 8b is given in Figure 9c. Solar flux arriving on the surface is based on 4.0 μm flux values from Allen (1976), scaled to Mars's distance from the sun. Scattering by dust and aerosols, and absorption by the Martian atmosphere were ignored. Emitted flux is from a gray body with emissivity

given in Figure 9b. The combined reflected and emitted flux is shown for three temperatures, 200 K, 250 K, and 300 K. Even at extremes higher than normal Martian temperatures, (i.e. 300 K), the feature is still dominated by absorptions and for reasonable temperatures 200 K - 250 K thermal effects are negligible.

Comparison of the telescopic data to lab data yields an upper limit of carbonate abundance of <1-3 wt% using measurements of carbonate and palagonite mixtures (Blaney and McCord, 1989; Walsh, 1987). If calcite is assumed to be the dominant carbonate form then the carbonate abundance is consistent with the lower limit of less than 1 wt%. The 1 wt% limit is also consistent with longer wavelength measurements by Roush et al. (1989) showing a CO₃ radical feature in an asymmetric site. The strength of this asymmetric CO₃ radical absorption has led to estimates of 1 wt% carbonate in the atmospheric dust component on Mars. Additionally, as calcium carbonate was the carbonate phase measured in the EETA 79001 (Gooding and Wentworth, 1988), the interpretation of 0 - 1 wt% carbonate based on calcite measurements is strengthened further.

The regions measured included large portions of the Valles Marineris (regions a and b in figures 1 and 2). Layered deposits in the central Valles Marineris have been proposed to be composed of carbonates deposited by precipitation in ice covered lakes (McKay and Nedel, 1988). Karst morphology may also be also present in this region (Spencer and Croft, 1987; Spencer et al., 1989). Though no evidence of carbonate was seen at the spatial resolution of this study, the aperture size was too large to isolate specific proposed carbonate-rich regions, or thus to support the idea that the optical surface of Valles Marineris is any more carbonate-rich than other regions.

Although the Martian surface is a mixture of both chemical weathering products (dust) and mafic material, the optical surface in bright regions is thought to be dominated by dust. The regions measured covered a range of albedos, all of which showed no evidence for carbonates. Roush et al. (1989) estimated 1 wt% carbonate specifically for airborne dust.

For purposes of the rest of this paper we assume that no more than 1 wt% carbonate is present in the uppermost part of the Martian regolith.

V. Implications of the Lack of Carbonate Absorption Features

There are two major reasons for expecting carbonates on Mars: 1) if Mars underwent a period of climatic warming due to a thicker CO₂ atmosphere, carbonates would have formed at a rapid rate (Fanale et al., 1982; Pollack et al., 1988) and 2) the thermodynamically stable weathering products of igneous material on Mars under current conditions include carbonates (Gooding, 1978). The absence of abundant carbonates in the optical surface is therefore puzzling. Discussed below are four possibilities which could explain the observations.

A. Model 1: The observed upper limit on carbonate abundance (i.e. less than 1 wt%) is representative of the Martian regolith.

A 1 km mega-regolith with 1 wt% carbonate could at most contain 0.6 bars of CO₂ (Pollack et al., 1987), well short of the 3-5 bars (Pollack et al 1987; Postawko and Kuhn, 1986; Pollack and Black 1979) needed for global warming by a CO₂ greenhouse at average orbital parameters. Optimization of the orbital parameters would lower the amount of CO₂ needed to around a bar (Pollack et. al., 1987), however, this would apply only to the equatorial regions of the planet during perihelion. As valley networks occur over a wide range of latitudes in the heavily cratered terrain (Carr, 1986), much more than 1 bar of CO₂ would be needed to form the channels solely by effects due to a thicker atmosphere.

A consequence of an early, wet, warm Mars is that liquid water would be present to remove CO₂ from the atmosphere by the formation of carbonates. This removal would occur at a rate of approximately 1 bar CO₂ removed every 10⁷ years (Fanale et al., 1982;

Pollack et al., 1987). If the low carbonate abundance observed (0.6 bars), accurately reflects the planetwide inventory, then a 3-5 bar early greenhouse lost most of its CO₂ by other mechanisms and had a duration of a few million years. A short-lived greenhouse contradicts the geomorphic evidence, which shows valley networks (a major geomorphic feature supporting an early greenhouse), forming during throughout the first billion years. Recycling of carbonate to replenish the atmospheric CO₂, whether by volcanic (Pollack, 1988) or by impact (Carr, 1989) processes, may be able to extend the length of the greenhouse, but the last few bars would have to have been stored in the near-surface environment (i.e. if carbonates are formed by surface water, the last carbonates formed must be near the surface).

A major unanswered question is: did valley networks and other features used to invoke a greenhouse originate by other mechanisms operating early in Martian history? The end of widespread valley network formation coincides with a decline in impact rates on Mars (Carr, 1989) and with a decline in the geothermal gradient. Squyres (1989a,b) pointed out that, given the ability of ice covered rivers to flow for distances comparable to those of the valley networks (Wallace and Sagan, 1979; Carr, 1983), triggering the start of valley networks could be the critical control in valley network formation. Differences in the impacting and geothermal rates between the current epoch and early Mars could be the deciding factor in whether valley networks form.

Fanale et al. (1989) discussed the relative importance of atmospheric CO₂ and a higher geothermal gradient at about 3.8 b.y.. Using models to predict the depth to the water table, they showed that a higher geothermal gradient could raise the water table from about 1 km (present value) to 350 m 3.8 b.y. ago with an atmosphere of 1 bar CO₂ (the 1 bar atmosphere raises the surface temperature by only a few degrees). The water table depth estimated is consistent with the depth of the valley networks themselves and could be an important factor in valley network formation.

A low carbonate abundance would also imply that the weathering products observed (i.e. the dust) are not the thermodynamically stable end-members of weathering under current ambient Martian conditions. As an illustration, consider the thermodynamically stable decomposition products from the weathering of basalt of the same composition as Shergotty. Shergotty is a basaltic achondrite from the SNC (S=Shergotty, N=Nakhla, and C=Chassigny) group of meteorites. SNC meteorites are thought for a variety of reasons to come from Mars (e.g. Wood and Ashwall 1980, McSween 1985). The Shergotty composition from Stolper and McSween (1979) was used in the calculations below. The weathering products of a Shergotty-like basalt which has reached thermodynamic equilibrium by gas-solid interactions at 240°K and current Mars atmospheric conditions, based on calculations by Gooding (1978), are shown in Table 4A. Note a total carbonate abundance of 32.48 wt% is expected. If the 1 wt% carbonate in the dust is a reasonable upper limit, then about only about 3% of the dust could have formed by gas-solid reactions carried to equilibrium. The majority of the dust would have formed by other processes. Similarly, if liquid water containing dissolved CO₂ and O₂ from the current Martian atmosphere were involved, again based on Gooding (1978), the end products would contain 18.07 wt% carbonate (see Table 4B), leaving 5.5 wt% of the dust to form by this process. Clearly, either the majority of the dust formed by processes other than surface weathering under current ambient conditions, or the formation process has been halted mid-way by kinetic barriers, leaving metastable products.

B. Model 2: Carbonate deposits formed in isolated areas or are located at depth

These Earth-based spectra lack the spatial resolution to detect small localized deposits. A potential problem with localized carbonate deposits is that they may not be able to store the amount of CO₂ needed for an early greenhouse. Such small carbonate deposits reflect

special local conditions such as short term equatorial warming during high obliquity, precipitating carbonates beneath iced-over lakes (McKay and Nedel, 1988), or transient water from geothermal melting or brines.

Carbonate deposits at depth are impossible to detect with spectroscopy, as spectroscopy looks only at the optical surface. Previous models calling for the recycling of carbonates to sustain an early greenhouse (Pollack et al.,1988; Carr,1989) assumed that carbonates are well mixed in the regolith. Carbonate recycling rates from both impact and volcanic burial are too slow to replenish the carbon dioxide fixed as carbonates in liquid water (Carr,1989). Carr (1989) suggested that the rate of carbonate fixation may have been overestimated. If liquid water was not continuously present on the surface, then carbonate formation would have preceded at a much slower rate. Temperatures, though warmer than in the current epoch, would have remained just below the point at which liquid water could exist. Ground water would be close to the surface and under proper hydrostatic conditions would break out and form valley networks. Even with the slower carbon dioxide fixation rates, carbonates would form in the near surface environment where they should be detectable. Thus, a mechanism for depositing carbonates at depth is needed.

An alternative hypothesis calls for stratified carbonate layers. If carbonates exist at depth in stratigraphically localized deposits a possible formation scenario could be: a) early Mars is warm, valley networks form; b) carbonates form rapidly, decreasing the atmospheric CO₂ pressure until temperatures drop below the level needed to maintain liquid water; c) carbonate formation ceases and volcanic and impact processes bury the carbonates; d) carbonates are buried to a depth where rapid decrepitation occurs, releasing a pulse of CO₂; e) the released CO₂ causes another episode of greenhouse warming and valley network formation, and carbonates begin to form with the cycle repeating. If a carbonate decrepitation depth of about 17 km, as suggested by Carr (1989), is valid then the cycle of rapid carbonate formation followed by burial could repeat itself about 10 times

in the first billion years according to liquid stirring models by Carr (1989). Declining impact rates would then slow the burial rates, leaving the carbonate layer stratified somewhere in the Martian crust. There is some geomorphic evidence for a strength discontinuity at about 1 km depth (interpreted as a fossil ice-water interface)(Soderblom and Wenner, 1978) which could be a carbonate layer. Geochemical arguments advanced by Warren which focus on the calcium deficiency of the Viking fines when compared to SNC meteorites (1986) also indicate that a carbonate layer may be present at depth. Further support for early episodic warming comes from the fact that erosion rates inferred for the ancient cratered terrains do not show evidence of prolonged periods of warmer, wetter climates (Carr, 1988). Additionally, the valley networks do not exhibit mature drainage systems (Carr and Clow, 1981), suggesting that fluvial action occurred only intermittently (Carr, 1989).

C. Model 3: The low carbonate abundance is the result of secondary weathering processes which have removed carbonates from the regolith

The presence of the sulfates in the fine grained material measured by Viking Landers 1 and 2 (Clark et al.,1976; Clark et al.,1982), may have major implications for carbonate abundance. Sulfate deposit formation models lie in three classes: a) ground water evaporite deposits; b) volcanic aerosol models; and c) an intrinsically high sulfur abundance. Implications of the second mechanism, involving volcanic aerosols, are discussed below.

The stability of carbonates in the presence of gaseous SO₂ has been addressed by Clark et al. (1979) and Sidorov and Zolotov (1986) with differing results. Clark et. al (1979) performed laboratory experiments which indicated that carbonates decompose readily in the presence of SO₂, leaving sulfates. Sidorov and Zoltov (1986) examined kinetic constraints and showed that the reaction encounters a kinetic barrier which would

make this reaction negligible. Understanding the possible role of SO₂ in destroying carbonates is critical in understanding the composition and evolution of the fines at the Martian surface. Alteration of the surface by airborne reactive components may be a major process in the formation of salts on Mars. For example, sulfate and nitrate deposits form in Antarctica from the deposition of stratospheric anions, which react with local rocks which in turn provide the cations to form these deposits (Campbell and Claridge, 1987).

Settle (1979) proposed a sulfate aerosol model for the formation of the sulfate duracrust at the Viking sites. The acidic nature of these aerosols would tend to decompose carbonates readily. If carbonates do decompose in the presence of SO₂ vapor or sulfate aerosols, CO₂ would be released from the decomposed carbonates back into the Martian atmosphere.

Current estimates of the CO₂ inventories for the atmosphere - polar cap - regolith storage, in the absence of carbonates, are at most ~ 0.7 bars (Fanale et al., 1982). Therefore, the amount of CO₂ liberated from the surface by SO₂ interactions after carbonated formation stopped must be less than 0.7 bars. The SO₂ would have been converted to sulfates. A Martian regolith assumed to contain 10 wt% sulfate, as suggested by the modeling of Toulmin et al. (1982) and Clark and Van Hart (1984), would, if all the sulfate began as carbonate plus SO₂, have started with a composition of 7.3 wt% calcite (with calcium as the anion), or 7.0 wt % magnesite (with magnesium as the anion). The entire inventory of CO₂ present in the atmosphere - cap - regolith system would be provided by depleting the first 170 m of the regolith. It is extremely doubtful that all of the present Martian atmosphere is provided by the decrepitation of carbonates by sulfates so the 170 m figure remains a limit on the extent to which this mechanism operated since carbonate formation ceased.

Carbonates and sulfates must be considered together. If carbonates are absent from the surface due to interactions with volcanic aerosols, then the rate of SO₂ released by

volcanoes on Mars must be greater than the rate of regolith overturn which exposes new carbonates. Fresh craters which have occurred after the height of volcanism would be expected to show evidence of carbonates brought up from depth, if carbonates exist at depth. Both volcanism and cratering occurred at higher rates during the early portion of Martian history than at the present (e.g. Greeley and Spudis 1978, Neukum and Hiller 1982). If the sulfur in the Martian regolith is the result of sulfate aerosol deposition throughout Martian history, then the release of CO₂ by sulfate aerosols may have played a critical role in the rapid recycling of CO₂ throughout Martian history. The expected weathering products under current conditions may also need to be revised. Previous thermodynamic calculations with carbon dioxide, water, and oxygen as the principle reactants may not be valid with sulfur dioxide playing a major role.

D. Model 4: Weathering environments on Mars did not form carbonates

The majority of materials examined on the Martian surface are weathering products formed by unknown mechanisms. As discussed previously, the expected carbonates from surface atmospheric interactions do not seem to be present in large quantities in the optical surface of Mars. Processes unique to Mars may have formed the observed dust. Two weathering mechanisms which may have created the dust are: 1) impact ejecta from volatile rich targets (Kieffer and Simonds, 1980), and 2) alteration of basaltic rocks by acidic ground waters (Fisher and Burns, 1989). The minerals formed in any of these processes are not well understood, however, and may preclude the formation of carbonates.

Impacts into sedimentary rocks do not produce the melt sheets associated with impacts into a crystalline basement; instead suevite deposits are found in stratigraphically equivalent positions (Kieffer and Simonds, 1980). Suevites, as defined by Gary et al. (1974) are "grayish or yellowish fragmental rock (depositional breccias) associated with meteoritic

craters that contain both shock metamorphosed rock fragments and glassy inclusions that occur typically as aerodynamically shaped bombs". Suevites are often composed of a clay matrix and contain evidence of hot volatiles mixed with fragmental material during or shortly after the impact event. Degassing vents are found in suevite deposits at the Ries crater in Germany, indicating that hot steam escaped from the interior of the deposit. Evidence of hydrothermal alteration is found in the suevite deposits at Ries (Staile and Ottermann, 1977; Stoffler et al. 1977) and at West Clearwater (Phinney et al., 1978). Excavation of this hydrothermally altered material would occur during subsequent impacts. Allen et al. (1982) investigated the mineralogy and abundance of hydrothermally altered impact melt and breccia and concluded that the clays produced by impact-induced hydrothermal alteration would contribute to but not dominate the chemistry of the fine grained material on Mars.

In addition to the hydrothermal alteration of material in throughout sheets, Kieffer and Simonds (1980) also proposed that a fine ash deposit formed by the rapid expansion of silicate melt/vapor by superheated steam from pore water or by carbon dioxide from decrepitated carbonates would exist. The ash formed by the interaction of melt and vapor would be widely distributed and occur at the top of the crater's stratigraphic sequence. Erosion has removed this ash layer from terrestrial craters which, by analogy with melt sheets from impacts into crystalline rock would comprise 1-5% of the volume excavated. Impacts into volatile-rich rocks provide a way of producing a large volume of fine grained material of unknown composition. The alteration of the melt in the vapor cloud would be controlled by the dominant volatile propelling the expansion of the melt-vapor cloud. Thus, if water was the principal volatile, oxidation and hydration products would dominate and little if any carbonate would form. Owing to the speed with which this event would occur, the altered material would be poorly crystalline or crystalline on a small scale. It is more difficult to estimate what would happen in an impact into material rich in carbonate and water. Given the lower vaporization point of water, products created by steam-melt

interaction might be expected to dominate. The composition of products from a silicate melt-steam cloud and in silicate melt-steam-CO₂ cloud remains to be examined.

Ash deposits from impacts would comprise most of the mobile material on the surface of the planet. Low erosion rates on Mars, (Arvidson et. al. (1979) estimated a rock breakdown rate of 10^{-3} $\mu\text{m}/\text{yr}$), would prevent competent rock from making up a large fraction of the fine grained material. Therefore, the ash created in an impact event could dominate the optical surface of the planet.

Another weathering process that may occur on Mars which may prevent carbonate formation involves acidic ground water. Burns (1988) proposed that acidic ground water produced from the interactions of massive iron sulfide deposits, associated with komatiitic magmas, and ground water may be the source of the sulfate deposits at the surface. Mobile sulfuric acid-rich fluids would migrate to the surface creating gossans (iron sulfate deposits) to form. Recent work on the weathering of olivine by sulfuric acid (Fisher and Burns, 1989) indicates that oxidation of the iron in the olivine to goethite occurs. This type of acid reaction would also operate in the weathering of the surface by sulfate aerosols. A highly acidic environment would inhibit the formation of carbonates.

The weathering processes discussed above are all plausible given the present lack of knowledge. They involve geological processes that could reasonably occur on Mars. All may have occurred, and the relative importance of each in producing the fines on the surface is unknown.

VII. Conclusions

Our conclusions fall into two categories: 1) observational and 2) interpretive. The spectra show variations in the steepness of the slope at the long wavelength end of the bound-water band. The wavelength coverage of these spectra do not allow us to discriminate between variations in hydration; surface frost; or ice clouds. Carbon dioxide

with ^{18}O and ^{17}O as one of the oxygen atoms is responsible for absorption features at 3.61 μm , 3.81 μm , 3.97 μm , and 4.05 μm (Encrarnaz, 1989). Discrepancies exist between the observed Mars spectra and the atmospheric models by Encrarnaz (1989) and Crisp (personal communication, 1989). Whether these differences are indicative of surface components or of the need for further modeling of the Martian atmosphere is undetermined at this point, but it would be surprising if the only absorption features on the surface coincided with isotopic atmospheric absorptions. No evidence of absorptions caused by carbonates in the 4 μm region was observed in the data presented here. Additionally, no evidence for ubiquitous scapolite was found. The ability to detect atmospheric isotopic features with absorption depths of less than one percent lends confidence to the conclusion that no 4.00 μm feature is present to a 1% band depth.

The scenarios discussed in section 5 represent a range of models that may explain the lack of carbonate features found in our data. The different models are not exclusive and may have worked in conjunction. Of the possibilities discussed previously, we feel that insufficient data exist to rule out any of these possibilities definitively, let alone chose combinations of processes to arrive at a unique solution. However, the lack of abundant carbonates in the optical surface is an important piece of evidence that must be accounted for in paleo-climate and geochemical weathering models.

High spatial resolution imaging spectroscopy from spacecraft is critical to addressing these questions. Recent impact craters can act as probes into the Martian crust in a similar way that telescopic data of lunar craters provides information on crustal inhomogeneities (Hawke et. al., 1989; Pieters, 1989). Lateral variations and temporal variations can be investigated on a small scale and direct evidence for carbonates at depth, in localized deposits, or in dust-free regions can be observed.

More geochemical and geophysical modeling also is needed. The alteration products created by the interactions of silicate melt and steam in an expanding vapor cloud produced by an impact into a water-rich target should be determined, and the similarity of such a

deposit to the spectral signature of Martian dust evaluated. Given the high sulfur content of the fines at both Viking Lander sites, carbonates must be considered in relationship with sulfates. The stability of carbonates in the presence of SO₂ or sulfate aerosols is a major unanswered question that must be addressed as well.

Acknowledgments

We would like to thank the scientists and staff at the NASA Infrared Telescope Facility for their assistance. In particular Alan Tokunaga and Kris Selgren provided advice and support in operating CGAS so as to optimize these measurements. Discussions with Fraser Fanale and Susan Postawko were invaluable in synthesizing the carbonate section. This work was supported by NASA grants NSG7312 and NSG7323. This is Planetary Geosciences Division publication #574.

References

- Allen C. C., J. L. Gooding, M. Jercinovic, and K. Keil, Altered basaltic glass: a terrestrial analog to the soil of Mars, *Icarus*, 45, 347-369, 1981.
- Allen C. C., J. L. Gooding, and K. Keil, Hydrothermally altered impact melt rock and breccia: contributions to the soil of Mars, *J. Geophys. Res.*, 87, 10,083-10101, 1982.
- Allen C.W., *Astrophysical Quantities*. London: University of London Athlone Press, 1976.
- Arvidson, R.E., E.A. Guinness, S.W. Lee, Differential aeolian redistribution rate on Mars, *Nature*, 278, 533-555, 1979.
- Ashwal, L.D., J.L. Warner, and C.A.Wood, SNC meteorites: Evidence against asteroidal origin, *Proc. Lunar and Planet. Sci. Conf. 13th, Part 1, J. Geophys. Res.* 87, suppl., A393-A400, 1982.
- Becker, R.H., and R.O. Pepin, The case for a Martian origin of the shergottites: Nitrogen and noble gases in EETA 79001, *Earth and Planet. Sci. Lett.*, 69, 225-242, 1984.
- Beer, R., R.H. Norton, and J.V. Martonchik, Astronomical infrared spectroscopy with a Connes-type interferometer: II. Mars, 2500-3500 cm⁻¹, *Icarus*, 15, 1-10, 1971.
- Biemann, K., J. Oro, P. Toulmin, L.E. Orgel, O. Nier, P.M. Anderson, P.G. Simmonds, D. Floy, A.V. Diaz, R. Rushneck, J.E. Biller, and A.L. Lafleur, The search for organic substances and inorganic volatile compounds in the surface of Mars, *J. Geophys. Res.*, 82, 4641-4658, 1977.
- Blaney D.B., and T.B. McCord, An observational search for carbonates on Mars, *J. of Geophys. Res.*, 94, 10,159-10,166, 1989.
- Burns, R.G., Ferric sulfates on Mars. *Proc. Seventeenth Lunar Planet. Sci. Conf., Part 2, J. Geophys. Res.*, 92, E570-E574, 1987.
- Burns, R.G., Gossans on Mars, *Proc. of the 18th Lunar and Planetary Sci. Conf.*, 713-721, 1988.
- Campbell, I.B., and G.G.C. Claridge, *Antarctica: Soils, Weathering Processes and Environment, Developments in soil science 16*, Elsevier Science Pub. B.V., New York, N.Y., 1987.
- Carr, M. H., Stability of streams and lakes on Mars. *Icarus* , 56, 476-495, 1983.
- Carr, M. H., Mars: A water-rich planet? *Icarus* ,68, 187-216, 1986.
- Carr, M. H., Recharge of the early atmosphere of Mars by impact-induced release of CO₂. *Icarus*, in press, 1989.

- Carr, M. H., and Clow, G. D., 1981. Martian channels and valleys: Their characteristics, distribution and age. *Icarus*, 48, 91-117, 1981.
- Clark B.C., S.L. Kenley, D.L. O'Brien, G.R. Huss, R. Mack, and A.K. Baird, Heterogeneous phase reactions of Martian volatiles with putative regolith minerals. *J. Mol. Evol.*, 14, 91-102, 1979.
- Clark, B.C., A.K. Baird, P. Toulmin, H.J. Rose, K. Keil, A.J. Castro, W.C. Kelliher, C.D. Rowe, and P.H. Evans, Organic analysis of martian surface samples at the Viking landing sites, *Science*, 194, 1976.
- Clark, B.C. and P.C. Van Hart, The salts of Mars, *Icarus*, 45, 370-378, 1981.
- Clark, B.C., A.K. Baird, R.J. Weldon, D.M. Tsusaki, L. Schrabel, and M.P. Candelaria, Chemical Composition of Martian Fines, *J. Geophys. Res.*, 87, 10,059-10,068, 1982.
- Clark, R.N., A large scale interactive one dimensional array processing system, *Pub. A.S.P.*, 92, 221-224, 1980.
- Clark, R.N., R.B. Singer, and G.A. Swayze, Discovery of Globally-distributed Scapolite on Mars, 4th International Conference on Mars, 82-83, 1989.
- Encranaz, T., On the atmospheric origin of weak absorption features in the infrared spectrum of Mars, submitted to *J. Geophys. Res.*, 1989.
- Evans, D.L. and J.B. Adams, Amorphous gels as possible analogs to Martian weathering products, Proc. Lunar Planet. Sci. Conf. 11th, 757-763, 1980.
- Fanale, F.P., Martian volatiles; Their degassing history and geochemical fate. *Icarus*, 28, 179-202, 1976.
- Fanale, F.P., and W.A. Cannon, Mars: CO₂ absorption and capillary condensation on clays--Significance for volatile storage and atmospheric history, *J. Geophys. Res.*, 84, 8404-8415, 1979.
- Fanale, F.P., J.R. Savail, W.B. Banerdt, and R.S. Saunder, The regolith-atmosphere-cap system and climate change, *Icarus*, 50, 381-407, 1982.
- Fanale, F.P., J.R. Savail, A.P. Zent, and S.E. Postawko, Global distribution and migration of subsurface ice on Mars, *Icarus*, 67, 1-18, 1986.
- Fanale, F.P., J. B. Pollack, M. H. Carr, R. O. Pepin, and S. E. Postawko, Epochal climate change on Mars, *Mars Book*, University of Arizona Press, submitted 1989.
- Gary, M., R. McAfee, and C.L. Wolf (Eds), *Glossary of Geology*, American Geologic Institute, Washington, D. C., 1974.
- Goetz, A.F.H., B.N. Rock, and L.C. Rowan, Remote sensing for exploration: An overview, *Econ. Geol.* 78, 573-590, 1983.

- Gooding, J.L., Chemical Weathering on Mars. Thermodynamic Stability of Primary Minerals (and their Alteration Products) from Mafic Igneous Rocks, *Icarus*, 33, 483-513, 1978.
- Gooding, J.L., S.J. Wentworth, and M.E. Zolensky, Calcium Carbonate and sulfate of possible extraterrestrial origin in the EETA 79001 meteorite, *Geochim. et. Cosmochim. Acta*, 52, 909-915, 1988.
- Greeley, R. and P. Spudis, Volcanism on Mars, *Rev. of Geophys. and Space Phys.*, 19, 13-41, 1981.
- Hawke, B. R., P. G. Lucey, P. D. Spudis, P. D. Owensby, Impact structures as crustal probes, (abstract), *Lunar and Planetary Science XX*, 389-390, Lunar and Planetary Institute, Houston, Texas, March 1989.
- Herr K.C. and G.C. Pimental, Infrared absorptions near three microns recorded over the polar cap of Mars, *Science*, 166, 496-498, 1969.
- Houck, J.R., J.B. Pollack, C. Sagan, P. Schack, and J.A. Pecker, High altitude infrared spectroscopic evidence for bound water on Mars, *Icarus*, 18, 3, 470-479, 1973.
- Hunt, G.R. and J.W. Salisbury, Visible and near-infrared spectra of minerals and rocks, I, Silicate minerals, *Mod. Geol.* 1, 283-300 (1970).
- Kieffer, S.W., and C.H. Simonds, The role of volatiles and lithology in the impact cratering process, *Rev. of Geophys. and Space Phys.*, 18, 143-181, 1980.
- McKay, C.P., and S.S. Nedell, Are there carbonate deposits in the Valles Marineris, Mars?, *Icarus*, 73, 142-148, 1988.
- McSween, H.Y., SNC Meteorites: Clues to Martian petrologic evolution?, *Rev. Geophys.*, 23, 391-416, 1985.
- Moroz, V.I., The Infrared Spectrum of Mars (1.1 - 4.1 μ), *Soviet Astronomy*, 8, 273-281, 1964.
- Neukum, G. and K. Hiller, Martian Ages, *J. Geophys. Res.*, 86, 3097-3121, 1982.
- Phinney, W.C., C.H. Simonds, A. Cochran, and P.E. McGee, West Clearwater, Quebec impact structure II, Petrology, *Proc. Lunar Sci. Conf. 9th.*, 2659-2693, 1978.
- Pieters, C. M., Stratigraphy of the lunar crust, (abstract), *Lunar and Planetary Science XX*, 848-849, Lunar and Planetary Institute, Houston, Texas, March 1989.
- Pimentel G. C., P.B. Forney, and K.C. Herr, Evidence about Hydrate and Solid Water in the Martian Surface from the 1969 Mariner Infrared Spectrometer, *J. Geophys. Res.*, 79, 1623-1634, 1974.
- Pollack, J. B., Climate change on the terrestrial planets. *Icarus* 37, 479-553, 1979.
- Pollack, J.B., and D.C. Black, Implications of the gas compositional measurements of Pioneer Venus for the origin of planetary atmospheres, *Science*, 205, 56-59, 1979.

- Pollack, J. B., and Yung, Y. L., Origin and evolution of planetary atmospheres. *Ann. Rev. Earth Planet. Sci.* 8, 425-487, 1980.
- Pollack, J. B., Kasting, J. F., Richardson, S. M., and Poliakov, K., The case for a wet warm climate on early Mars. *Icarus* ,71, 203-224, 1987.
- Postowko S.E. and W.R. Kuhn, Effects of the greenhouse gases (CO₂, H₂O, and SO₂) on Martian paleoclimate. *J. Geophys. Res.*, 82, 4635-4639, 1986.
- Roush, T.L., D. Blaney, T.B. McCord, R.B. Singer, Carbonates on Mars: Searching the Mariner 6 and 7 IRS measurements (abstract), *Lunar and Planetary Science XVII*, 732-733, Lunar and Planetary Institute, Houston, Texas, 1986.
- Roush, T., J. Pollack, C. Stoker, F. Witteborn, J. Bregman, D. Wooden, and D. Rank (1989b) CO₃(2-)- and SO₄(2-)-Bearing Anionic Complexes Detected in Martian Atmospheric Particulates, Presented at the Fourth International Conference on Mars, Tucson, Arizona, January, 1989.
- Roush, T., J. Pollack, C. Stoker, F. Witteborn, J. Bregman, D. Wooden, and D. Rank (1989b) CO₃(2-)- and SO₄(2-)-Bearing Anionic Complexes Detected in Martian Atmospheric Dust, Submitted to 20th Lunar and Planetary Science Conference, Lunar and Planetary Institute, Houston, Texas, March, 1989.
- Scott, D. H., and M. H. Carr, *Geologic Map of Mars*, U. S. Geol. Survey, Misc. Inv. Map I-1083, 1978.
- Settle, M., Formation and deposition of volcanic sulfate aerosols on Mars, *J. Geophys. Res.*, 84, 8,343-8,354, 1979.
- Sidorov Yu. I. and M. Yu Zolotov, Weathering of Martian surface rocks. In S.K. Saxena (ed.), *Chemistry and Physics of Terrestrial Planets*, Adv. Geochem. Vol. 6, Springer-Verlag, New York, p. 191-223, 1986.
- Singer,R.B. Spectral evidence for the mineralogy of high-albedo soils and dust on Mars, *J. Geophys. Res.* 87, 10159-1016, 1982.
- Sinton, W.M., Spectroscopic evidence for Vegetation on Mars, *Astrophys. J.*, 126, p.231-238, 1957.
- Sinton, W.M., On the Composition of the Martian Surface Materials, *Icarus*, 6, 222-228, 1967.
- Soderblom, L. S., Kriedler, T. J., and Masursky, H., 1973. Latitudinal distribution of a debris mantle on the martian surface. *J. Geophys. Res.* 78, 4117-4122.
- Soderblom L.A. and D.B. Wenner (1978) Possible fossil water liquid-ice interfaces in the martian crust, *Icarus*, 34, 622-637.

- Spencer and Croft, *MECA Workshop on the Evolution of the Martian Atmosphere*, LPI Technical Report 86-07, p.40-41, 1986.
- Spencer, J.R. , F.P. Fanale, and J.E. Tribble, Karst on Mars? Origin of Closed Depressions in Valles Marineris by Solution of Carbonates in Groundwater Sulfuric Acid, in *Fourth Int. Conf. on Mars, Tuscon Az, Jan 10-13*, p.193-194, 1989.
- Squyres, S. W., Early Mars: Wet and warm, or just wet? (abstract). *Fourth International Conference on Mars. Tucson, AZ., Tuscon Az, Jan 10-13*, p.193-194, 1989a.
- Squyres, S. W., Early Mars: Wet and warm, or just wet? (abstract), *Lunar and Planetary Science XX*, 1044-1045, Lunar and Planetary Institute, Houston, Texas, March 1989b.
- Squyres, S. W., and Carr, M. H., 1986. Geomorphic evidence for the distribution of ground ice on Mars. *Science*, 231, 249-252.
- Stahle, V., and J. Ottemann, Ries-Forschungsbohrung 1973: Zeolithisierung der glaser in suevit und petrographic der Beckensuevite und gangbreccian, *Geol. Bavarica*, 75, 191-217, 1977.
- Stoffler, D., U. Ewald, R. Ostertag, and W.U. Reimold, Research drilling Nordlingen 1973, (Ries) composition and texture of polymict impact breccias, *Geol. Bavarica*, 75, 163-190, 1977.
- Stolper, E.M., and H.Y. McSween Jr., Petrology and origin of the shergottite meteorites, *Geochim. Cosmochim. Acta.*, 43, 1475-1498, 1979.
- Tokunaga, A.T., R.G. Smith, E. Irwin, Use of a 32-element reticon array for 1-5 micrometer spectroscopy, *Infrared Astronomy with Arrays*, Wynn-Williams and Becklin eds., p. 367-378, 1987.
- Toulmin, P., A.K. Baird, B.C. Clark, K. Keil, H.J. Rose, R.P. Christian, P.H. Evans, and W.C. Kelliher, Geochemical and mineralogical interpretation of the Viking inorganic chemical results, *J. Geophys. Res.*, 82, 4625-4634, 1977.
- U.S. Geol. Survey, *Shaded Relief Map of Eastern Mars*, U.S. Geol. Survey Map I-1535, 1985.
- Wallace, D., and C. Sagan, Evaporation of ice in planetary atmospheres: Ice covered rivers on Mars, *Icarus*, 39, 385-400, 1979.
- Walsh, P.A., D.L. Blaney, and T.B. McCord, martian surface analogs: Laboratory spectral studies in the mid infrared. (Abstract) *Mars Evolution of Volcanism, Tectonism and Volatiles Meeting*, Napa Valley, CA, December, 93-84, 1987.
- Warren, P.H., Mars Regolith versus SNC Meteorites: Possible Evidence for Abundant Crustal Carbonates, *Icarus*, 70, 153-161, 1987.

Table 4.1. Observing Information.

Observation No.	Segment	Object	Region on Mars	Time (UT)	Airmass
1	1	Mars	Margaritifer	9:23	2.17
2	1	Mars	Margaritifer	9:27	2.09
3	2	Mars	Margaritifer	9:31	2.06
4	3	Mars	Margaritifer	9:34	2.01
5	1	Mars	Chryse	9:54	1.77
6	2	Mars	Chryse	9:56	1.75
7	3	Mars	Chryse	9:59	1.72
8	3	BS437		10:28	1.64
9	3	BS437		10:32	1.61
10	2	BS437		10:36	1.57
11	2	BS437		10:39	1.55
12	1	BS437		10:42	1.58
13	3	Mars	Valles Mariner.	11:09	1.29
14	2	Mars	Valles Mariner.	11:11	1.28
15	1	Mars	Valles Mariner.	11:13	1.27
16	1	Mars	Argyre	11:16	1.26
17	2	Mars	Argyre	11:18	1.26
18	3	Mars	Argyre	11:20	1.25
19	3	BS437		11:57	1.17
20	2	BS437		12:04	1.15
21	1	BS437			1.14
22	3	Mars	Solis Planum		1.11
23	2	Mars	Solis Planum	12:19	1.11
24	1	Mars	Solis Planum	12:23	1.09
25	1	Mars	E. Tharsis	12:41	1.09
26	2	Mars	E. Tharsis	12:43	1.08
27	3	Mars	E. Tharsis	12:45	1.08
28	2	BS437		13:14	1.03
29	1	BS437		13:19	1.02
30	3	BS437		13:40	1.01
31	2	Mars	S. Highlands	14:10	1.09
32	2	Mars	S. Highlands	14:12	1.09
33	1	Mars	S. Highlands	14:15	1.09
34	1	Mars	S. Highlands	14:17	1.09
35	1	Mars	W. Tharsis	14:19	1.10
36	2	Mars	W. Tharsis	14:21	1.10
37	3	Mars	W. Tharsis	14:23	1.10
38	3	BS437		15:11	1.04
39	2	BS437		15:15	1.04
40	1	BS437		15:17	1.05

Table 4.2. 3.81 μm Band Depth

<u>Location</u>	<u>Band Depth</u>
a) Margaritifer Sinus	3.3%
b) Valles Marineris	3.1%
c) Argyre Basin	3.2%
d) Eastern Solis Planum	3.2%
e) Heavily Cratered Terrain	3.9%
f) Eastern Tharsis	3.3%
g) Western Tharsis	2.5%
h) Southern Chryse	4.0%

Table 4.3. Slope between 3.2 μm and 3.6 μm

Location	Slope (normalized reflectance/ μm)
a) Margaritifer Sinus	0.76
b) Valles Marineris	0.71
c) Argyre Basin	0.73
d) Eastern Solis Planum	0.75
e) Heavily Cratered Terrain	1.01
f) Eastern Tharsis	0.88
g) Western Tharsis	0.89
h) Southern Chryse	0.99

Table 4.4. Thermodynamically stable weathering products of a basalt with the same composition as Shergotty weathered on Mars. Shergotty composition based on Stolper and McSween (1979). Reactions used developed by Gooding (1978). Weathering products given in order of their mass percentage.

Conditions A. 240°K Solid -Vapor Interactions		Conditions B. Liquid Water with Dissolved CO ₂ and O ₂ at 273°K.	
Mineral	wt.%	Mineral	wt.%
Quartz	31.75	Quartz	25.93
Magnesite	17.16	Goethite	17.63
Calcite	15.32	Talc	15.22
Ca-Beidellite	12.90	Calcite	13.78
Hematite	11.03	Na-Beidellite	10.47
Albite	8.67	Ca-Beidellite	10.41
Whitlockite	1.68	Sodium Carbonate	4.19
Corundum	0.83	Whitlockite	0.66
Iron Sulfate	0.57	Corundum	0.36
Orthoclase	0.35	K-Beidellite	0.20
Ilmenite	0.25	Ilmenite	0.20
		Potassium Carbonate	0.10
		Sulfur	0.10

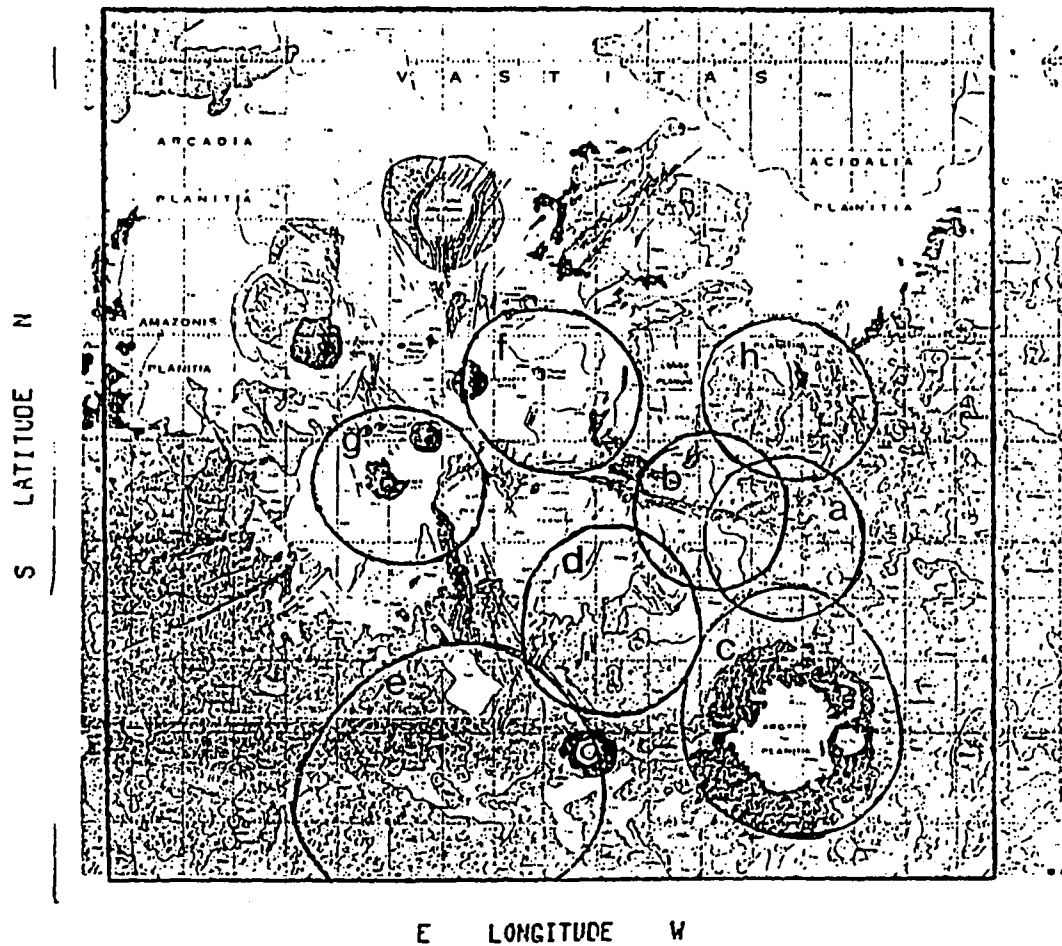


Figure 4.1. Locations of the eight regions observed . Aperture location was determined by measurement of bore sited cross-hairs video taped during the measurement then geometrically transformed to a mercator projection. Base map is Scott and Carr (1977) geologic map of Mars.

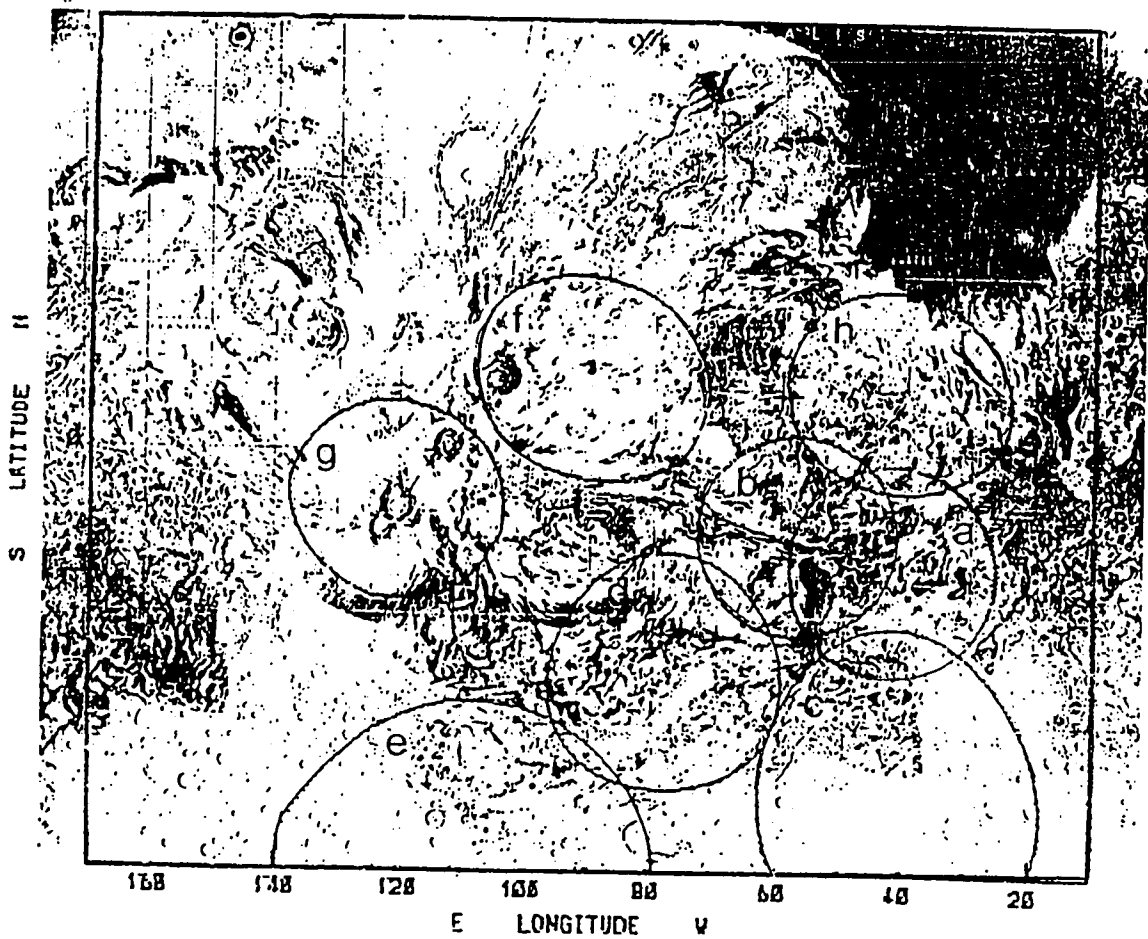


Figure 4.2. Locations of the eight regions observed . Aperture location was determined by measurement of bore sited cross-hairs video taped during the measurement then geometrically transformed to a mercator projection. Base map is USGS Map I-1535, (1985) showing shaded relief and surface markings.

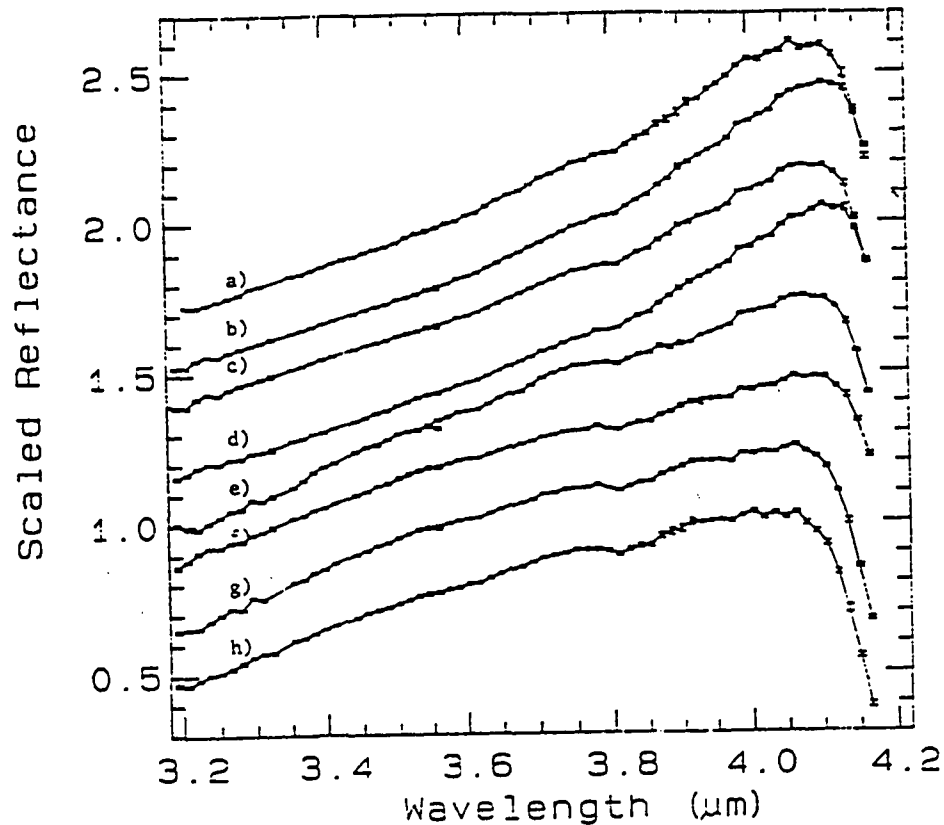


Figure 4.3. Spectra for eight ~900-km diameter regions on Mars reduced using the standard star BS437 and normalized to unity at 3.9133 μm . The rough geographic locations are a) Margaritifer Sinus, Nirgal Valles, and Eastern Valles Marineris, b) Central Valles Marineris and Surroundings, c) Argyre Basin, d) Eastern Solis Planum, Ridged Plains, Heavily Cratered Terrain, e) Mid to High Latitude Heavily Cratered Terrain, f) Eastern Tharsis, g) Western Tharsis Montes, h) Southern Chryse and Outflow Channels. Locations of apertures are shown in Figures 1 and 2. Subsequent spectra are offset from each other by 0.2 units.

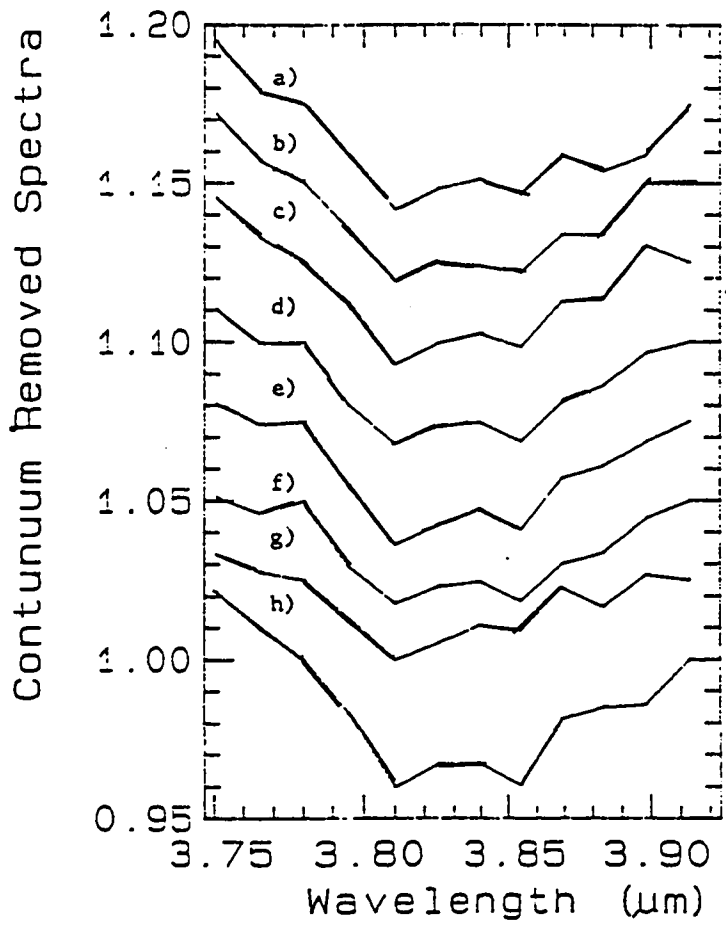


Figure 4.4. Spectra from Figure 1 with straight line continua removed. The continua were calculated using values at 3.75095 μm and 3.913 μm. Subsequent spectra are offset from each other by 0.025 units.

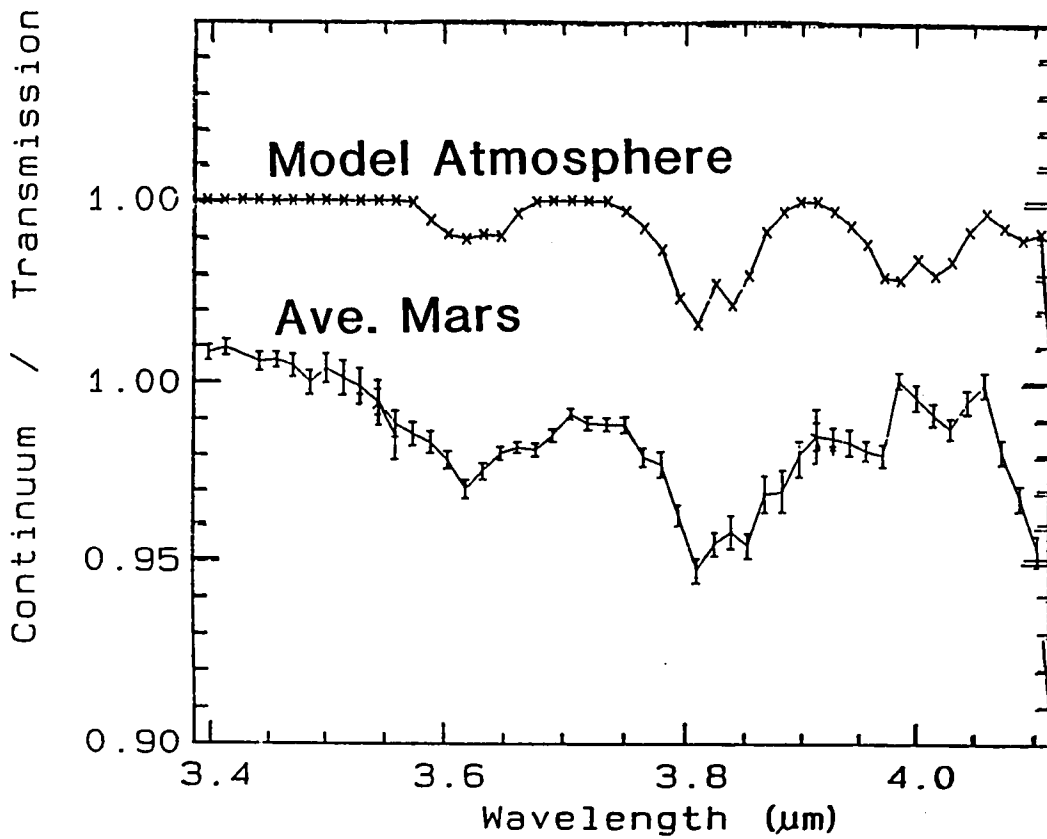


Figure 4.5. Co-added Mars spectrum with continuum removed by fitting a linear least squares fit through all data points between 3.4 μm and 4.05 μm plotted against a model 2 airmass Mars atmosphere calculated by Dave Crisp (personal communication, 1989).

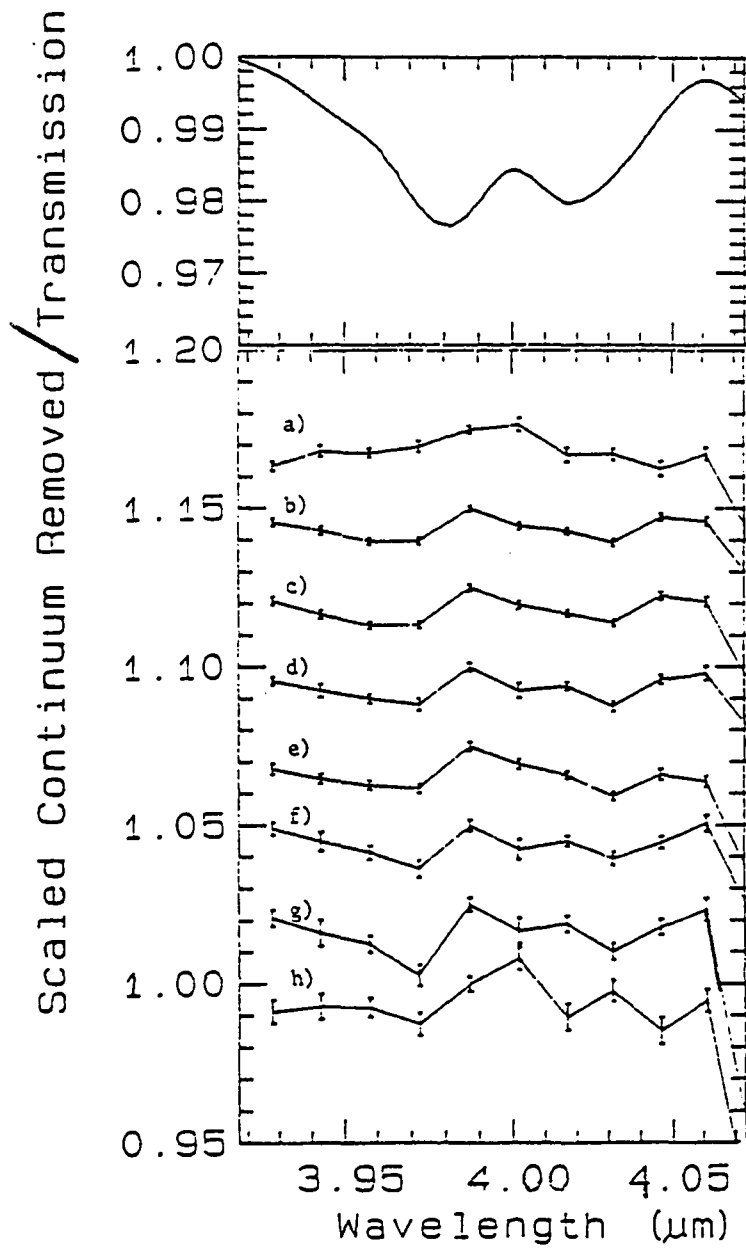


Figure 4.6. Crisp atmospheric model in the 4 μm region (personal communication, 1989) and spectra of Mars with continuum removed in the 4 μm region.

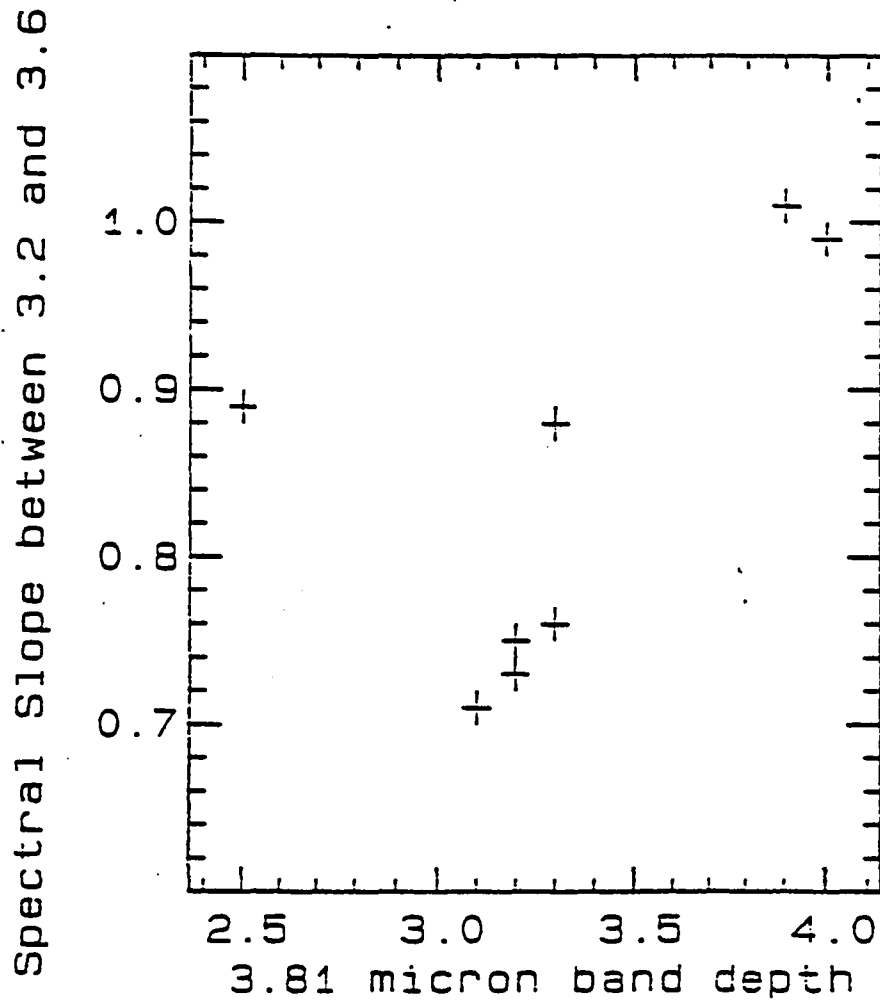


Figure 4.7. Plot of slope in the 3.2 μm to 3.6 μm wavelength region versus 3.8 μm band depth for each spectra measured. Data taken from tables 2 and 3.

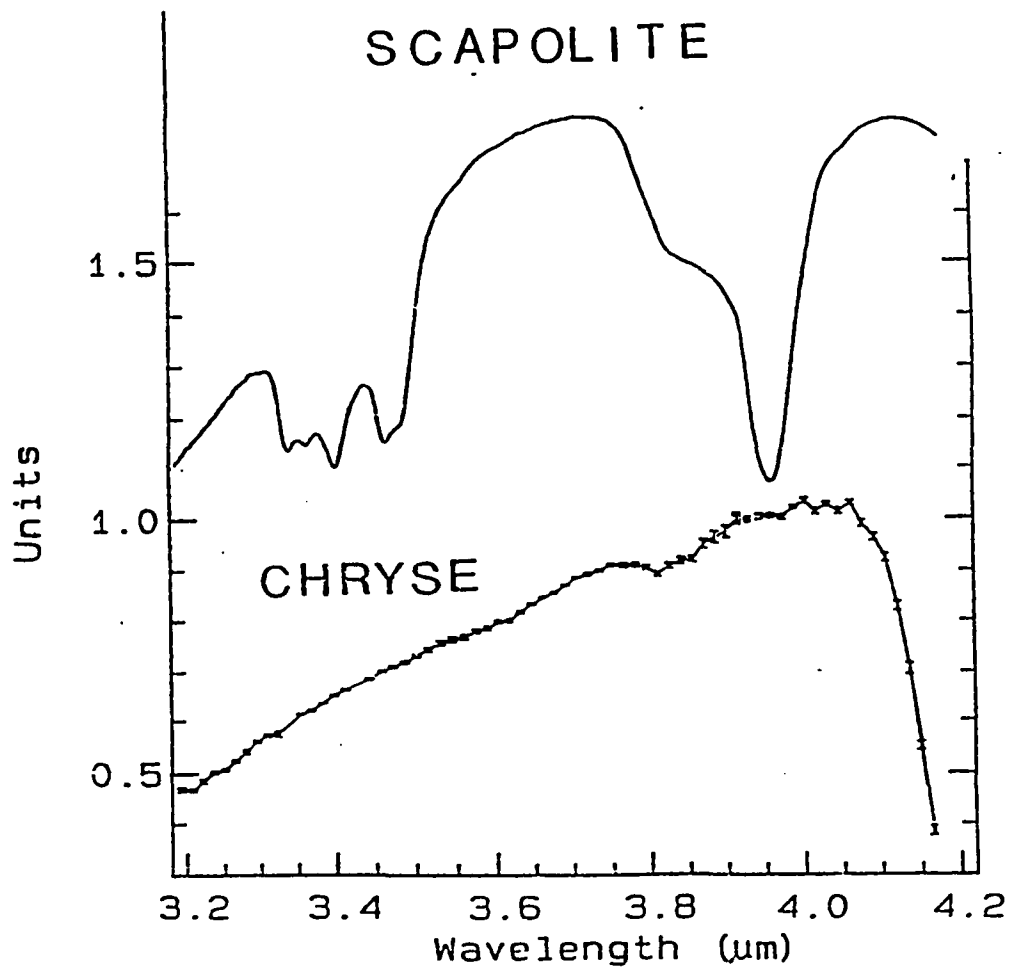


Figure 4.8. Spectrum of scapolite overlying spectrum from the Chryse region of Mars. Chryse spectrum is scaled to 1.0 at 3.913 μm . Scapolite spectrum is unscaled and dimensionless.

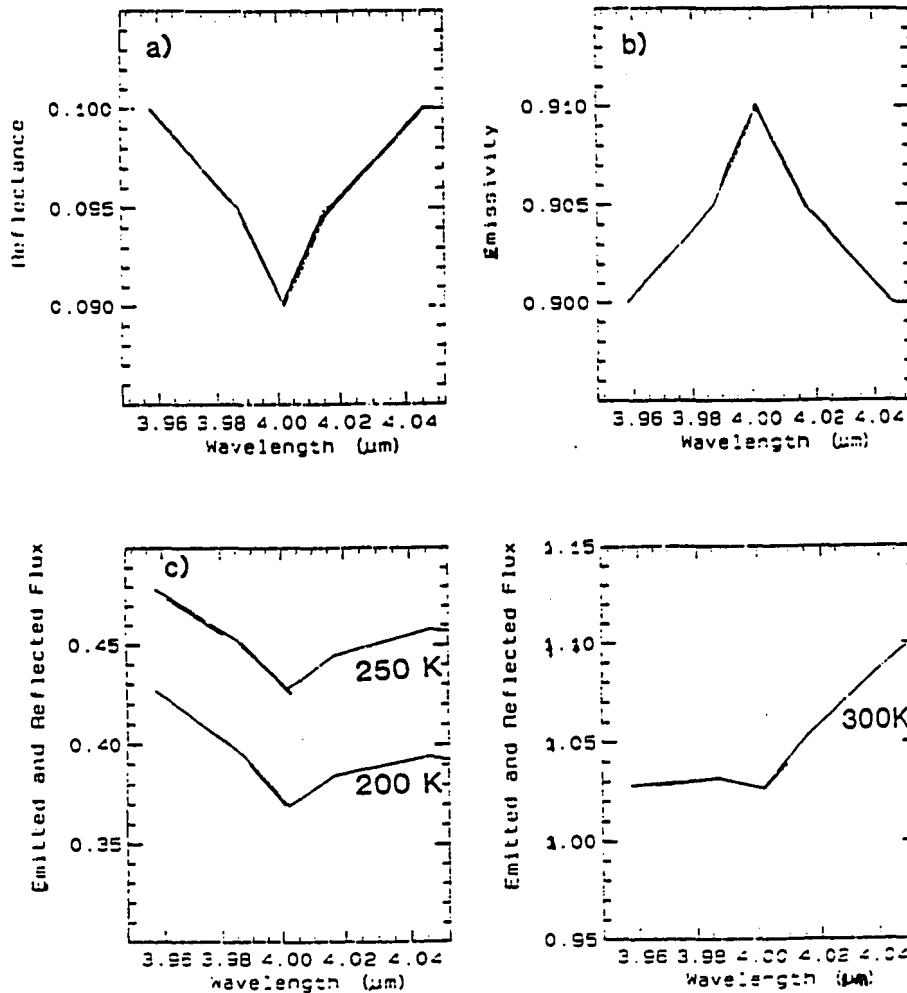


Figure 4.9. a) Synthetic band showing a 10% absorption band at 4.0 μm. The continuum level was approximated by scaling Martian reflectance data assuming a 3% reflectance near 3.0 μm. b) Emission corresponding to absorption band shown in 8a. c) Flux from the surface of Mars from both emitted and reflected light based on the emission and absorption shown in 8a and 8b. Solar flux arriving on the surface is based on terrestrial 4.0 μm flux values from Allen (1976) scaled to Mars. Emitted flux is from a gray body with emissivity given in 8b. Combined reflected and emitted flux is shown for three temperatures, 200K, 250K, and 300K.

Chapter 5.

Spectroscopy of Mars between 4.4 μm and 5.5 μm : Indications of Sulfate Minerals

I. Introduction

The geochemical evolution of the Martian surface has been a topic of interest for the last several decades. Viking data provided information on the oxide composition of the fine-grained material at two locations - Utopia and Chryse (e.g., Clark et al., 1982). However, oxide composition does not directly reveal mineralogy. Spectroscopy provides additional information on the composition of the surface. Specifically, spectroscopy between 4.4 μm and 5.1 μm can provide yield data on the sulfate mineralogy, abundance, and spatial distribution.

Previous spectroscopic work in the 4.4 μm to 5.1 μm region is extremely limited. Earth-based near-infrared spectroscopic observations in the 1950's, 1960's, 1970's, and early 1980's (e.g., Sinton, 1957; 1965; Moroz, 1965; Beer et al., 1971; Houck et al., 1973; McCord et al., 1982; Singer, 1982; Blaney and McCord, 1989a) all stopped at wavelengths shorter than or at the 4.2 μm CO₂ band, and thermal infrared measurements concentrated on wavelengths longer than 5.0 μm (e.g., Roush et al., 1989; Hanel et al., 1973). Spacecraft measurements from the Mariner 6 and 7 IR-spectrometer covered the wavelength region between 1.9 μm and 14.3 μm . However, calibration and instrumentation complications, the limited spatial coverage, and the complex atmospheric and thermal signatures have led to only first-order examination for information on the CO₂ atmosphere (Herr et al., 1969; T.Z. Martin, personal communication, 1989). The measurements presented here are the first earth-based high spectral resolution, high

signal-to-noise measurements which have undergone detailed examination for surface absorption features.

II. Observations

Telescopic measurements of Mars reported here were made on August 19, 1988 UT of Mars at the NASA IRTF facility. Spectra were obtained with the Cooled Grating Array Spectrometer (CGAS) which utilizes a thirty-two element InSb line array as described by Tokunaga et al. (1988). A grating with a resolution of $R=300$ was used. Measurements were made by taking data at two different grating positions, with an eleven-channel overlap between positions. Segment 1 covered $4.405 \mu\text{m} - 4.86 \mu\text{m}$, and segment 2 covered $4.67 \mu\text{m} - 5.13 \mu\text{m}$. Spectra were normalized to unity at $4.71 \mu\text{m}$ and were reduced using the star BS437 as a standard. A 2.7 arc-second aperture was used, producing a spot size 900 km in diameter at the sub-earth point. The measurements were taken as part of a sequence of measurements which also covered the wavelength region between $3.2 \mu\text{m}$ and $4.2 \mu\text{m}$ using three grating positions discussed in Blaney and McCord (1989b).

Location of the aperture on the disc of Mars was accomplished by boresighting using a bright star and measuring the half - power points of the signal to locate the center of the aperture in both right ascension and declination. An electronic crosshair was positioned to mark the center of the aperture. The crosshair on the video image of the telescopic focal plane image were video-taped for later reconstruction of the aperture locations on Mars. Boresighting was checked roughly every thirty minutes when standard star measurements were made. No noticeable drift in the location of the aperture was noticed during the course of the night.

Image locations were derived from the videotapes. The aperture locations are plotted on orthographic maps shown in Figures 1 and 2. Locations are referred to by letter and

named after the dominant geologic feature within the region covered by the aperture. The locations of the regions do not coincide with exact locations of the geologic feature named. The regions measured and whose locations are shown in Figures 1 and 2, exhibit a wide range in both age, and geological settings. The young Amazonian-age Tharsis volcanic region (areas *f* and *g*), as well as the Noachian-aged heavily cratered terrain (area *c* and *e*), were sampled. Measurements included both equatorial and high-latitude locations. Lower Chryse Planitia was included in measurement *h*. Nirgal Valles, a large valley network, was included in *a*. Regions *a* and *b* also included portions of Valles Marineris.

The data were reduced using the spectral data processing system SPECPR (Clark, 1980). The star BS437, a 0.97 magnitude G8III spectral type, was used as a standard. BS 437 followed thirty minutes behind Mars and a measurement scheme of thirty minutes on Mars, thirty on the standard was used. Table 1 shows the measurement sequence and observing information. Each Mars spectrum was reduced using a standard star observation within 0.1 airmass of the observation. Both Martian and standard star spectra were normalized to unity at 4.72 μm prior to dividing the spectra. Examination of the individual spectra showed that the sky was stable throughout the night and measurements varied smoothly with airmass. The data for the regions discussed are shown, normalized to one at 4.72 μm , in figure 3.

III. Thermal Modeling

The spectra of Mars in this wavelength region have significant contributions from thermal flux as well as reflected solar radiation. Additionally, Mars' albedo is unknown for these locations at wavelengths between 4.4 μm and 5.1 μm , which further complicates analysis. The data discussed, shown in figure 3, are normalized spectroscopic data, not spectrophotometric data (i.e., the measurements do not provide absolute flux or albedo information). Difference in channel-to-channel emitted and reflected light is the sole

information available. Figure 4 shows the flux available at the Martian surface from both solar radiation and black body radiation. The solar flux was calculated using solar irradiance data from Allen (1976) and assumes that Mars is at a distance of 1.52 AU from the sun. Thermal emitted flux was calculated assuming a black body at temperatures of 200 K, 220 K, 240 K, 250 K, 260 K, and 270 K. Note that the solar and black body flux levels are of comparable magnitudes at the longer wavelengths but that solar radiation is about 5 times larger than the emitted radiation for reasonable Mars temperatures at the shorter wavelengths. Therefore, unless the albedo of the Martian surface is extremely low, reflectance dominates the flux at the short wavelength end of the spectrum.

As albedo information on the Martian surface was unavailable, a laboratory study of Martian surface analogs were undertaken. The effects of surface reflectivity on the spectral shape was investigated by calculating the flux from the surface of two proposed surface components: basalt and palagonite. Basalt is the dominant form of igneous material based on geomorphic evidence (e.g., Greeley and Spudis, 1981) and the oxide composition of the fines at the Viking Lander sites (e.g., Toulmin et al., 1978). Palagonite is a spectral analog to the Martian surface in the visible and near-infrared (Evens and Adams, 1980; Singer, 1982)

Figure 5 shows the reflectance and emissivity of both basalt and palagonite. The basalt was from the Kilauea volcano in Hawaii and therefore of recent origin. The palagonite was collected from the 10,000 foot level on Mauna Kea and is a good spectral analog to Martian dust (Singer, 1982). The grain size was less than 34 microns dry sieved. Measurements were taken on a Nicolet 5SXC Fourier transform infrared spectrometer with diffuse reflectance attachment and made under a stream of air with CO₂ and H₂O removed using a mirror as a background. Measurements were made at a resolution of 2 cm⁻¹ and convolved to the lower resolution CGAS data. Mallinckrodt sublimed sulfur powder was also measured. The spectra of the basalt and palagonite were divided by that of the sulfur

to determine the reflectance. Nash (1986) showed that sublimed sulfur in the wavelength region between 4.4 μm and 5.1 μm is a spectrally featureless standard with a high reflectance. The design of the spectrometer used makes it difficult to determine reflectance levels with a high degree of precision as slight differences in sample height introduce changes in the amplitude of the signal. Additionally, the reflectance level of the sulfur has some degree of uncertainty due to packing. Therefore the reflectance levels shown here, while useful in making a qualitative investigation of the effects of reflectivity, should not be used in detailed calculations. For example, the albedo of a material could be said to be close to that of the palagonite but the reflection levels given here should not be used to derive optical constants for Hapke-theory modeling.

The emissivity was calculated by using Kirchoffs law :

$$E = 1 - R, \quad (5.1)$$

where E is the emissivity and R is the reflectance of the material. Note that both the palagonite and basalt are spectrally neutral and have reflection levels of about 22% and 32%, respectively, in this wavelength region.

The radiation coming from the Martian surface at any given wavelength is given by the equation

$$F_t = (R * F_s) + (E * F_b(T)), \quad (5.2)$$

where F_t is the total radiation flux leaving the Martian surface at a given wavelength, R is the surface reflectivity at that wavelength, F_s is the solar radiation at the given wavelength, E is the surface emissivity at that wavelength, and $F_b(T)$ is the radiation emitted from a black body at absolute temperature T.

Figure 6 shows the ratio of the sum of reflected and emitted radiation from basaltic and palagonitic surfaces divided by the solar spectrum (R) at surface temperatures of 200K, 220K, 240K, 250K, 260K, and 270K or

$$R = F_t(T) / F_s$$

for T = 200 K, 220 K, 240 K, 250 K, 260 K, and 270 K. (5.3)

Note that the differences between basalt and palagonite are sufficient to produce major differences in the curvature of the spectra, especially at wavelengths longer than 4.7 μm . This is better illustrated in figure 7 which shows R normalized to one at 4.4 μm . Notice that if the curvatures alone are considered to estimate the temperature of the surface the results would be differences of 15 - 20 degrees depending of whether a palagonite or basaltic surface is assumed. Figure 8 shows the normalized relative flux (R) for basalt at 270K, 260K, and 250K and for palagonite at 250K, 240K and 220K. Given the limited data, it would be impossible to distinguish between these possibilities, let alone determine an intermediate case such as a mixture of 1/2 palagonite, 1/2 basalt. Therefore, the unique determination of temperature based on the curvature of the spectra between 4.8 μm to 5.1 μm is not possible. Thermal modeling in wavelength regions where reflected solar radiation and thermal emission are of comparable magnitudes requires one of the following: the albedo must be known, the surface temperature must be known, or there must be measurements of the same region at different temperatures. As the data presented here do not meet the above qualifications, we will consider a range of appropriate temperatures when temperature is a variable. We will also focus on the wavelength region less than 4.7 μm where thermal contributions are minimized.

IV. Atmospheric Modeling

The Martian atmosphere has a large number of atmospheric absorptions from both CO and CO₂ in the wavelength region between 4.4 μm and 5.1 μm. Fortunately, spectra for the wavelength region between 3.2 μm and 4.2 μm (Blaney and McCord, 1989b) were collected concurrently, allowing for the measurement of both sides of the CO₂ band that extends from 4.2 μm to 4.4 μm as well as several weak bands caused by isotopically heavy CO₂ at 3.81 μm and 3.62 μm. Initial study of the 3.62 μm and the 3.81 μm bands by Encrenaz (1989) provided a starting place to model the CO₂ in 4.4 μm - 5.1 μm region. Estimating the CO abundance, however, is a more difficult problem.

The amount of CO present in the Martian atmosphere at the time of the measurements is unknown. Estimates can be made from measurements in the 2.3 μm region (Clark et. al., 1989) taken a few weeks after the measurements presented here, from infrared data collected by Connes et al. (1966), and from infrared and millimeter wavelength measurements by Encrenaz et al. (1989). The Clark et. al (1989) data is not a line-resolved measurement, and the 3.36 μm absorption feature band depth is not a sensitive indicator of CO abundance. Additionally, possible mineralogic absorptions in the 2.36 μm region may further complicate the determination of the amount of CO present. A few of the Clark et al. (1989) spectra do not have any sign of CO absorptions. The Connes measurement does resolve the CO line and provides a direct measurement of the CO abundance. Estimates using the Connes data have been made by Young and Young (1977), and yield a mole ratio of CO / CO₂ of 2.7×10^{-3} . The Connes measurement, was made over 30 years ago and CO abundance may be variable with time in the Martian atmosphere. Evidence of time variability comes from millimeter work which shows a latitudinal and solar time dependence in CO abundance (Encrenaz, 1989) and from an infrared based estimate of CO / CO₂ of 1.5×10^{-3} (Clark et al., 1989). We decided to treat CO abundance

as a variable with a nominal value CO / CO_2 of 2×10^{-3} . This value is intermediate between the Young and Young (1977) value and the Encrenaz (1989) value. We also examined the CO / CO_2 values of twice and half the nominal value.

The following six variables were considered in the modeling of the atmospheric transmission: 1) atmospheric pressure; 2) CO abundance; 3) path length through the atmosphere; 4) surface temperature; 5) temperature at 50 km; and 6) atmospheric scattering. A radiative transfer model for the Martian atmosphere developed by Encrenaz (Encrenaz, 1989) was used. The model requires as input the surface temperature, the temperature at 50 km, the surface pressure, the path length, and the CO path length and abundance. The temperature profile in the atmosphere is assumed to be linear in the lower atmosphere and isothermal above 50 km. Carbon monoxide is assumed to be well mixed in the Martian atmosphere. Calculations for CO_2 and CO transmission are done separately and combined in a second step. The model uses the GEISA atmospheric line catalog. The atmospheric model is calculated at 4 cm^{-1} resolution with 1 cm^{-1} sampling using a band model that includes pressure broadening. The model output was then run through a triangular filter program with the same resolution as CGAS. The resultant values from the filter are oversampled at 1 cm^{-1} and then interpolated using a cubic spline to the wavelengths observed with CGAS. Figures 9 - 12 show some representative models to illustrate the spectral behavior of the model as function of atmospheric pressure, path length, CO/CO_2 mixing ratio, and surface temperature change. Each of the component gases- CO_2 , CO - are shown separately and then in combination to illustrate the sensitivity of each parameter. Water vapor is ignored because it does not contribute spectrally in this wavelength region. As can be seen in figures 9 - 12, PCO_2 is the most sensitive parameter in these calculations, followed by airmass, and the CO/CO_2 ratio. Temperature effects on the model transmission spectra were negligible.

The general character of the model transmission was similar in all the cases examined. A steep rise out of the 4.2 μm - 4.4 μm CO₂ band occurred between 4.4 μm and 4.54 μm where the transmission reaches a maximum. Between 4.51 μm and 4.67 μm an absorption by the first of the two broad CO bands occurs. The region between 4.68 μm and 4.9 μm contains the second broad CO absorption and a number of sharp absorption features caused by CO₂ with band minima at 4.70 μm , 4.77 μm and 4.83 μm . The region between 4.9 μm and 5.1 μm has clear atmospheric transmission.

Perhaps the most serious omission in the Encrenaz model is the lack of atmospheric scattering in the calculation of band depth. This is probably most true in the saturated 4.2 μm to 4.4 μm CO₂ band. Additionally, any thermal flux from the surface would only make one pass through the atmosphere, compared with two passes for reflected light, causing a dependence of observed band depth with the amount of thermal flux. As discussed previously, the porportion of thermal to reflected flux is unknown. Therefore, the modeling of specific spectra is difficult. The largest discrepancies are at the wings of the 4.3 μm band and with the relative strengths of the bands around 4.7 μm . The model systematically gives broader and deeper features than would be predicted based on the Encrenaz (1989) modeling of the 3.8 μm region. We are unsure at this time the cause of the discrepancies but assume that the source is due to a combination of scattering and uncertainties in the amount of thermal flux. In the following discussion we use a 240K, 7mbar, CO / CO₂ = .002, airmass = 2.0 as our model atmosphere. These nominal values were determined by Encrenaz (1989) based on the strength of the 3.81 μm feature.

V. Detection of an Absorption Feature at $\sim 4.5 \mu\text{m}$ -- Indication of Sulfates

The standard modeled Mars spectrum discussed above is plotted over the spectrum from the Argyre region. Note that all the atmospheric absorption features discussed (shown with arrows) are clearly present in the telescopic data and that most features appear to be weaker than predicted by the model. The exception to this is the rise out of the $4.2 \mu\text{m} - 4.4 \mu\text{m}$ CO_2 absorption which has a much shallower slope in the telescopic data than in the model atmosphere spectrum. The sharp rise out of CO_2 band is present under all conditions except for atmospheric pressures of 1 mbar which is not realistic given the strengths of the other absorption features. Scattering and thermal flux act to fill in bands and could not be responsible for the slow gradual rise (Pollack personal communication, 1989, Crisp personal communication, 1989, Espiritio personal communication, 1989). In addition to this gradual slope, an inflection at $4.5 \mu\text{m}$ is present in all the spectra and is extremely well defined in the Eastern Solis Planum and Argyre spectra. These measurements indicate that a surface absorption, centered near $4.5 \mu\text{m}$, is present on the Martian surface.

The wavelength region between $4.4 \mu\text{m}$ and $5.1 \mu\text{m}$ contains sulfate absorptions, shown in figure 14 for anhydrite, gypsum, and MgSO_4 , with the the $2\nu_3$ vibrational overtone of the SO_4^{-2} anion being centered at $4.5 \mu\text{m}$. The sulfates were measured using the same instrumentation and procedure as the basalt and palagonite discussed previously. A grain size of less than $34 \mu\text{m}$ dry sieved was used.

The multiband structure seen in the sulfate spectra is produced by the metal cation complexing with the SO_4^{-2} and lowering the symmetry of the sulfate. The lower symmetry causes degeneracy in the ν_3 and ν_4 modes, and the appearance of the ν_1 and ν_2 modes that are not infrared active under the tetrahedral symmetry that the SO_4^{-2} anion. Unfortunately the Martian atmosphere cuts off the short wavelength portion of the

Unfortunately the Martian atmosphere cuts off the short wavelength portion of the absorption. The sulfates, shown in figure 14, are shown in figure 15 at the resolution and wavelength of the telescopic data. Note that there does not appear to be any of the structure associated with the sulfates shown in figures 14 and 15 present in the telescopic data.

A qualitative match to the wing of the CO₂ band can be made by multiplying the gypsum spectral reflectance with the model transmission of the atmosphere (figure 16). Note the presence of a 4.5 μm absorption duplicates the rise out of the CO₂ band very well. Gypsum, however, is probably not the sulfate on the Martian surface due to the second absorption at 4.75 μm which is not present in the Mars data.

The location of this feature at 4.5 μm, the 2ν₃ SO₄ overtone, is especially exciting as the Viking lander sites detected large quantities of sulfur (~7 wt% SO₃) in the Martian soils. The sulfur content was highly variable even at a local level. Sulfur abundance ranged from 5.9 wt% to 9 wt% SO₃ at Chryse and from 7.6 wt% to 8.5 wt% SO₃ at Utopia (Clark et al., 1982). Sulfur was present in the greatest concentrations in "clods" of material that broke apart, indicating a sulfate duracrust

The lack of structure in the absorption has two possible explanations. The first is that, because we are looking at a mixture of sulfate and other surface constituents the fine structure, except at 4.5 μm, is masked by these other spectrally neutral materials. However, the fine structure, at least in the sulfates measured, is of comparable strength to the 4.5 μm absorption, and to atmospheric features that are clearly seen. Considerable more modeling needs to be done of the spectra and the albedos in this wavelength range need to be determine before the total exclusion of this possibility can be made, but it unlikely that any of the sulfates measured - gypsum, anhydrite, or MgSO₄ - are major mineral species of the optical surface of Mars.

The second possibility is that the liganding of the cation with the sulfate anion is in a site that preserves its tetrahedral symmetry and so does not have the multiband structure

measured in the sulfates treated in figure 14. The mineralogy of sulfates formed in a Martian environment needs to be examined.

One of the oddest features of the Viking X-Ray Fluorescence experiment is the lack of correlation of sulfur content with any specific cation (Clark et al., 1982). Magnesium was assumed to be the cation due to its high abundance (Toulmin et al., 1977). However recent studies of veins of weathering products of Martian origin in EETA79001 (a SNC meteorite) indicate that the cation is calcium (Gooding et al., 1988). This is puzzling as the fine-grained material at the Viking lander site are considered to be calcium depleted relative to mafic materials (Toulmin et al., 1978, Warren, 1987). The calcium abundance is also directly comparable to the sulfur abundance so that any variation in sulfur content should also produce a corresponding variation in calcium abundance. A correlation of sulfur and calcium is not observed (Clark et al., 1982)

Only sulfate formation by volcanic aerosols (Settle, 1979) decouples the sulfate abundance from the surface composition. Formation of sulfates from stratospheric aerosols occurs on Earth in the interior portions of Antarctica (Campbell and Claridge, 1987). However, the role that ambient conditions and surface mineralogy play in determining the sulfate mineralogy is unknown.

VI. Spatial Variation in the 4.5 μm Band Depth -- Implications for Sulfate Distribution

In order to isolate atmospheric effects from surface absorptions we compared spectra which had the same 3.81 μm band depth. As discussed in Blaney and McCord (1989b) the 3.81 μm band in our data is caused by CO_2 with ^{16}O and ^{17}O . The isotopically heavy CO_2 absorption provides an indicator, independent of possible sulfate absorption, of the similarity of atmospheric conditions of the various spectra. Table 2 shows the 3.81 μm

band depth. The spectra for the regions Margaritifer Sinus, Valles Marineris, Argyre Basin, Eastern Solis Planum and Eastern Tharsis all have 3.81 μm band depth between 3.1% and 3.3%. The Margaritifer spectra, however, is of significantly lower signal-to-noise and will not be considered. Southern Chryse and the Southern Heavily cratered terrain have roughly the same 3.8 μm band depth, 4.0% and 3.9% band respectively, but the Chryse spectra has a relatively lower signal-to-noise like which makes the results of comparisons between the two ambiguous .

In comparing the Valles Marineris, Argyre Basin, Eastern Solis Planum and Eastern Tharsis spectra, the 4.5 μm inflection discussed above is probably the strongest indicator of sulfate abundance. In order of strength of deepest absorption to weakest the regions are ordered: 1. Eastern Solis Planum; 2. Argyre Basin; 3. Eastern Tharsis; and 4. Valles Marineris. A note of caution must be offered in taking this approach to estimating relative sulfate abundance as the strength of the 4.5 μm band could indicate not only different abundances but also changes in mineralogy and degree of crystallization. However, the four regions do follow a progression due to either sulfate abundance or chemistry and there is significant variation between regions shown in figure 17.

Blaney and McCord (1989b) described the slope into the 3 μm bound water band for the regions measured. Table 3 shows the strength of 4.5 μm feature and the hydration slope. No correlation exists between 3 μm band strength and 4.5 μm feature strength.

VII. Conclusions

The rise out of the 4.2 μm - 4.4 μm CO₂ band cannot be matched by solely atmospheric constituents. A surface absorption must be added at roughly 4.5 μm in order to decrease the reflectance rise and produce the 4.5 μm inflection which is present in the data. The known presence of sulfates on the Martian surface and the location of this feature

at the 2ν₃ overtone of the SO₄⁻² anion indicate that the surface absorption is probably caused by sulfates on the Martian surface. An exact match to a terrestrial sulfate mineral has not been made but it is suggested that the mineral has very weak structure and thus a high degree of symmetry . Significant variation exists between the spectra at 4.5 μm. In order of strength of deepest absorption to weakest the regions are ordered Eastern Solis Planum, Argyre Basin, Eastern Tharsis, and Valles Marineris for the four regions measured at similar Mars atmospheric conditions.

References

- Allen, C.W., *Astrophysical Quantities*, Altheon Press, London, England 310 p., 1976.
- Beer, R., R.H. Norton, and J.V. Martonchik, Astronomical infrared spectroscopy with a Connes-type interferometer: II. Mars, 2500-3500 cm⁻¹, *Icarus*, 15, 1-10, 1971.
- Blaney D.B., and T.B. McCord, An observational search for carbonates on Mars, *J. of Geophys. Res.*, 94, 10,159-10,166, 1989a.
- Blaney D.B. and T.B. McCord, Constraints on the climate and weathering histories of Mars from ground based spectroscopy between 3.2 μm and 4.2 μm. submitted to *J. Geophys. Res.*, June, 1989b.
- Clark, B.C., A.K. Baird, R.J. Weldon, D.M. Tsusaki, L. Schrabel, and M.P. Candelaria, Chemical Composition of Martian Fines, *J. Geophys. Res.*, 87, 10,059-10,068, 1982.
- Clark, R.N., A large scale interactive one dimensional array processing system, *Pub. A.S.P.*, 92, 221-224, 1980.
- Clark, R.N., R.B. Singer, and G. Swaze, Discovery of Globally abundant scapolite on Mars., submitted to *J. Geophys. Res.*, 1989.
- Connes, J., P. Connes, and M. Kaplan, Mars: New absorption bands in the spectrum. *Science*, 153, 739-740, 1966.
- Encranaz, T., On the atmospheric origin of weak absorption features in the infrared spectrum of Mars, submitted to *J. Geophys. Res.*, 1989.
- Evans, D.L. and J.B. Adams, Amorphous gels as possible analogs to Martian weathering products, Proc. Lunar Planet. Sci. Conf. 11th, 757-763, 1980.
- Greeley, R. and P. Spudis, Volcanism on Mars, *Rev. of Geophys. and Space Phys.*, 19, 13-41, 1981.
- Hanel, R.A., V.J. Kunde, B.J. Conrath, and J. Pearl, Mariner 9 infrared interferometer spectrometer (IRIS) reduced data records documentation, NASA TM-70504, 48pp, 1973.
- Herr K.C. and G.C. Pimental, Infrared absorptions near three microns recorded over the polar cap of Mars, *Science*, 166, 496-498, 1969.
- Houck, J.R., J.B. Pollack, C. Sagan, P. Schack, and J.A. Pecker, High altitude infrared spectroscopic evidence for bound water on Mars, *Icarus*, 18, 3, 470-479, 1973.

- McCord, T.B., R.N. Clark, and R.B. Singer, Mars: Near-infrared reflectance spectra of surface regions and compositional implication, *J. Geophys. Res.*, 87, 3021-3032, 1982.
- Moroz, V.I., The Infrared Spectrum of Mars (1 1.1 - 4.1 μ), *Soviet Astronomy*, 8, 273-281, 1964.
- Nash, D.B., Mid infrared reflectance spectra (2.3-22 μ m) of sulfur, gold, KBr, and MgO and halon, *Applied Optics*, 25, 2427-2433, 1986.
- Roush, T., J. Pollack, C. Stoker, F. Witteborn, J. Bregman, D. Wooden, and D. Rank (1989b) CO₃(²⁻) and SO₄(²⁻)-Bearing Anionic Complexes Detected in Martian Atmospheric Particulates, Presented at the Fourth International Conference on Mars, Tucson, Arizona, January, 1989.
- Singer, R.B. Spectral evidence for the mineralogy of high-albedo soils and dust on Mars, *J. Geophys. Res.* 87, 10159-1016, 1982.
- Sinton, W.M., Spectroscopic evidence for Vegetation on Mars, *Astrophys. J.*, 126, p.231-238, 1957.
- Sinton, W.M., On the Composition of the Martian Surface Materials, *Icarus*, 6, 222-228, 1967.
- Tokunaga, A.T., R.G. Smith, E. Irwin, Use of a 32-element reticon array for 1-5 micrometer spectroscopy, *Infrared Astronomy with Arrays*, Wynn-Williams and Becklin eds., p. 367-378, 1987.
- Toulmin, P., A.K. Baird, B.C. Clark, K. Keil, H.J. Rose, R.P. Christian, P.H. Evans, and W.C. Kelliher, Geochemical and mineralogical interpretation of the Viking inorganic chemical results, *J. Geophys. Res.*, 82, 4625-4634, 1977.
- Young, L. D. G. and A. T. Young, Interpretation of high-resolution spectra of Mars. IV. New calculations of the CO abundance. *Icarus*, 30, 75-79, 1977.

Table 5.1. Observing Information

Observation No.	Segment	Object	Region on Mars	Time (UT)	Airmass
1	1	Mars	Margaritifer	9:38	1.97
2	1	Mars	Margaritifer	9:40	1.94
3	2	Mars	Margaritifer	9:41	1.91
4	2	Mars	Margaritifer	9:43	1.88
5	2	Mars	Chryse	9:46	1.85
6	1	Mars	Chryse	9:50	1.80
7	2	BS437		10:09	1.81
8	1	BS437		10:16	1.73
9	2	Mars	Valles Mariner.	10:57	1.32
10	1	Mars	Valles Mariner.	11:03	1.30
11	1	Mars	Argyre	11:24	1.24
12	2	Mars	Argyre	11:28	1.23
13	2	BS437		11:43	1.21
14	1	BS437		11:51	1.19
15	2	Mars	Solis Planum	12:19	1.11
16	1	Mars	Solis Planum	12:23	1.11
17	2	Mars	E. Tharsis	12:34	1.09
18	1	Mars	E. Tharsis	12:38	1.09
19	2	BS437		12:58	1.05
20	1	BS437		13:06	1.05
21	2	Mars	S. Highlands	13:59	1.08
22	1	Mars	S. Highlands	14:05	1.08
23	2	Mars	W. Tharsis	14:26	1.10
24	1	Mars	W. Tharsis	14:30	1.10
25	2	BS437		14:49	1.01
26	1	BS437		15:02	1.02

Table 5.2. 3.81 μm Band Depth

<u>Location</u>	<u>Band Depth</u>
a) Margaritifer Sinus	3.3%
b) Valles Marineris	3.1%
c) Argyre Basin	3.2%
d) Eastern Solis Planum	3.2%
e) Heavily Cratered Terrain	3.9%
f) Eastern Tharsis	3.3%
g) Western Tharsis	2.5%
h) Southern Chryse	4.0%

Table 5.3. Slope between 3.2 μm and 3.6 μm (hydration state) as compared to 4.5 μm band strength.

Location	3.81 μm Band Depth	Slope (normalized reflectance/ μm)	Strength of 4.5 μm absorption feature (4 being strongest)
Valles Marineris	3.1%	0.71	1
Eastern Tharsis	3.3%	0.88	2
Argyre Basin	3.2%	0.73	3
Eastern Solis Planum	3.2%	0.75	4

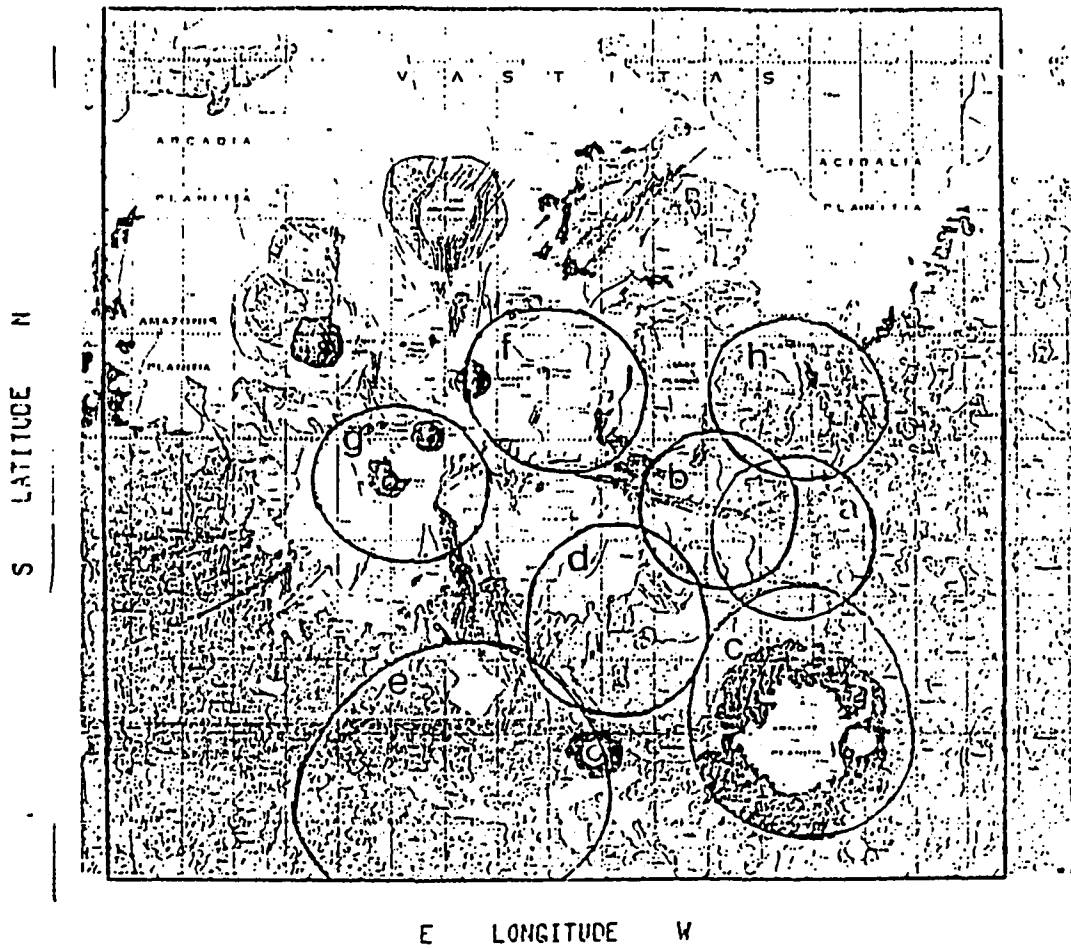


Figure 5.1. Locations of the eight regions observed . Aperture location was determined by measurement of boresited cross-hairs video-taped during the measurement then geometrically transformed to a mercator projection. Base map is Scott and Carr, (1977) geologic map of Mars.

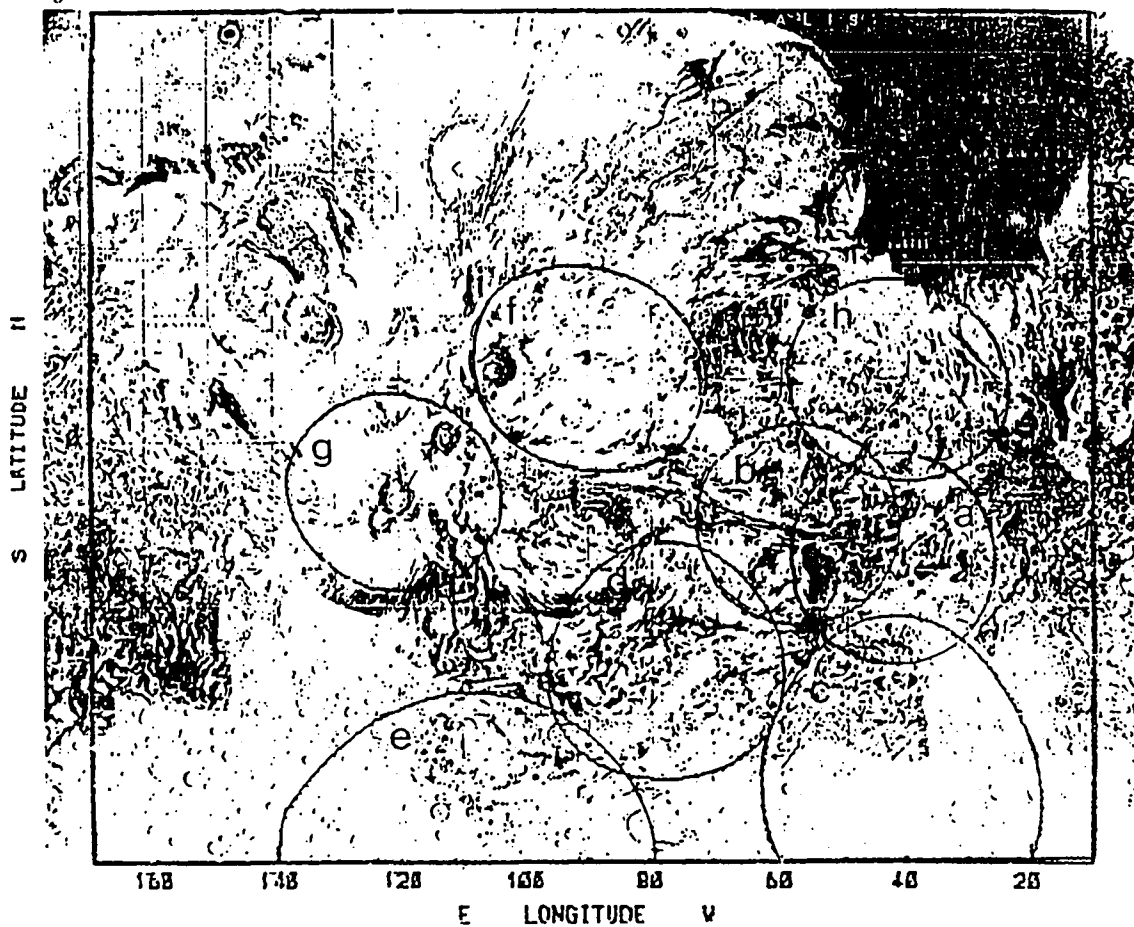


Figure 5.2. Locations of the eight regions observed . Aperture location was determined by measurement of boresited cross-hairs video-taped during the measurement then geometrically transformed to a mercator projection. Base map is USGS Map I-1535, (1985) showing shaded relief and surface markings.

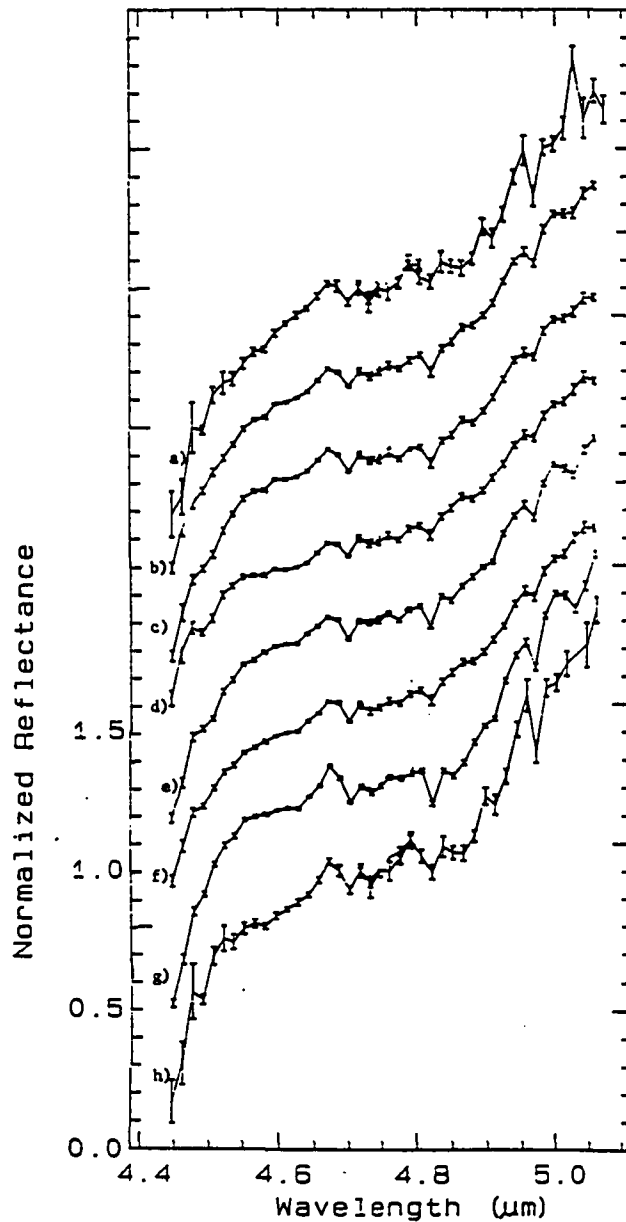


Figure 5.3. Spectra for eight ~900-km diameter regions on Mars reduced using the standard star BS437 and normalized to unity at 4.71 μm . The rough geographic locations are a) Margaritifer Sinus, Nirgal Valles, and Eastern Valles Marineris, b) Central Valles Marineris and Surroundings, c) Argyre Basin, d) Eastern Solis Planum, Ridged Plains, Heavily Cratered Terrain, e) Mid to High Latitude Heavily Cratered Terrain, f) Eastern Tharsis, g) Western Tharsis Montes, h) Southern Chryse and Outflow Channels. Locations of apertures are shown in Figures 1 and 2. Subsequent spectra are offset from each other by 0.2 units.

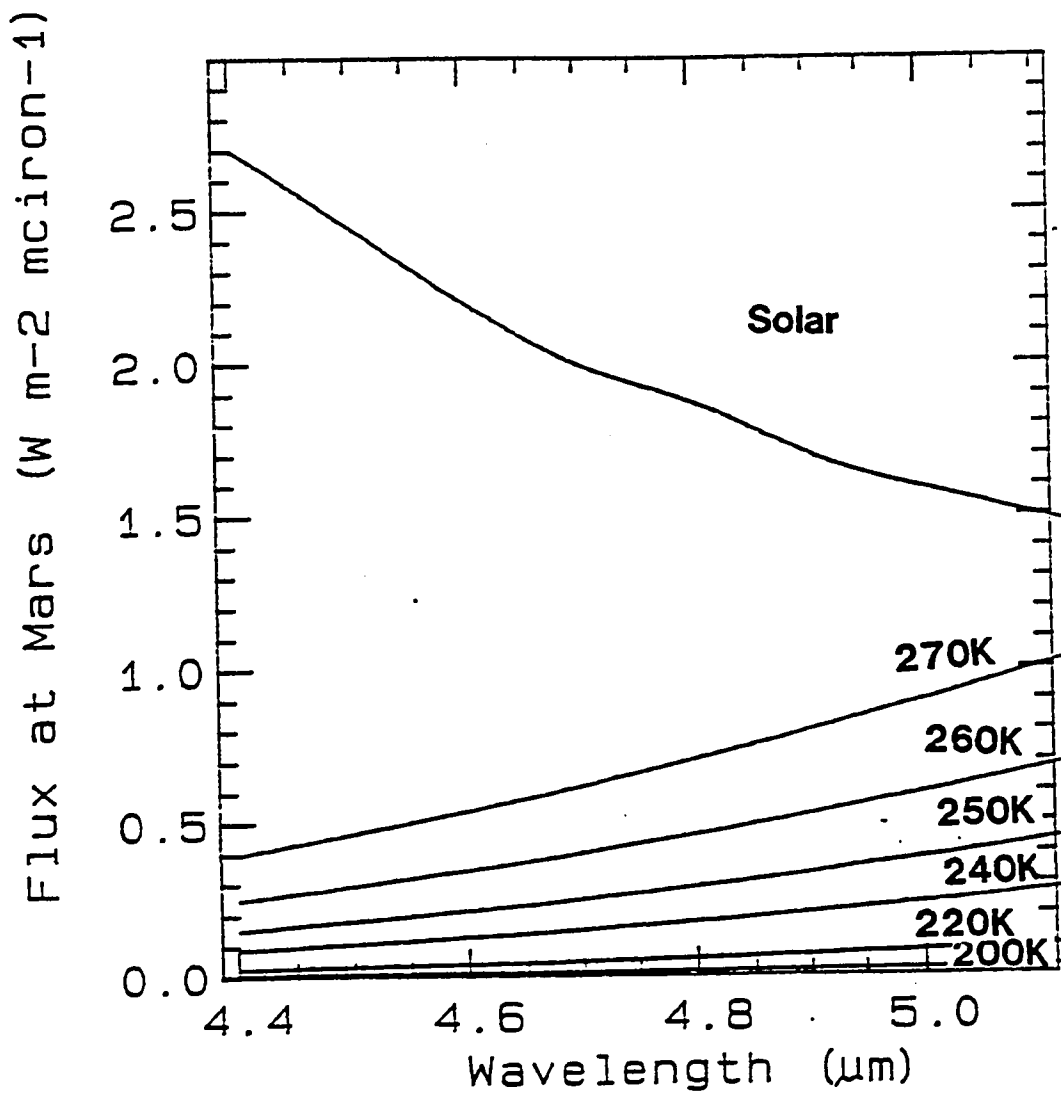


Figure 5.4. Comparison of solar flux and thermal flux at Mars. Mars flux is calculated using values from Allen (1976) scaled to a Mars - Sun distance of 1.52 AU. Thermal flux is calculated as being from a black body at temperature specified.

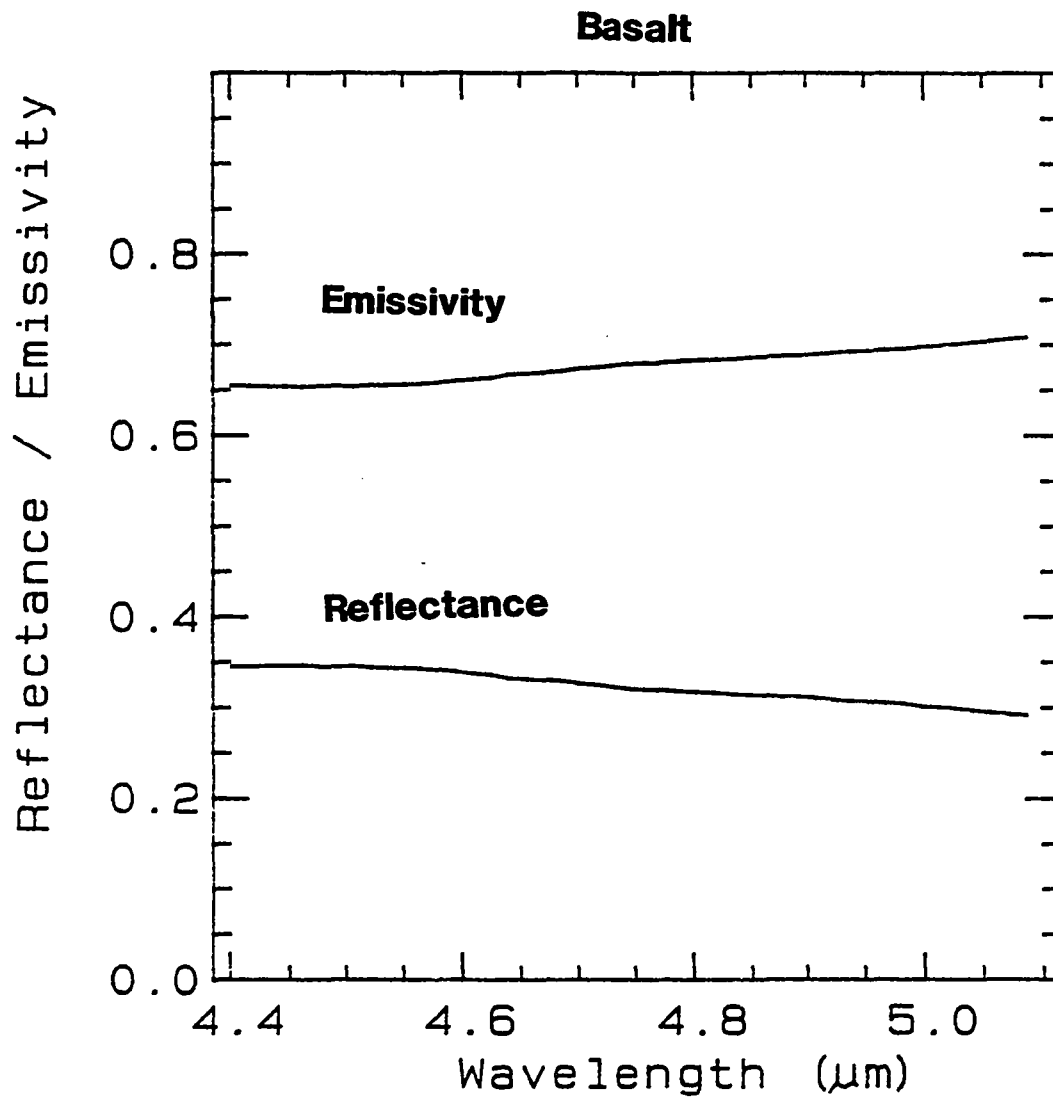


Figure 5.5a. Reflectance and emissivity of basalt (grain size $<34 \mu\text{m}$).

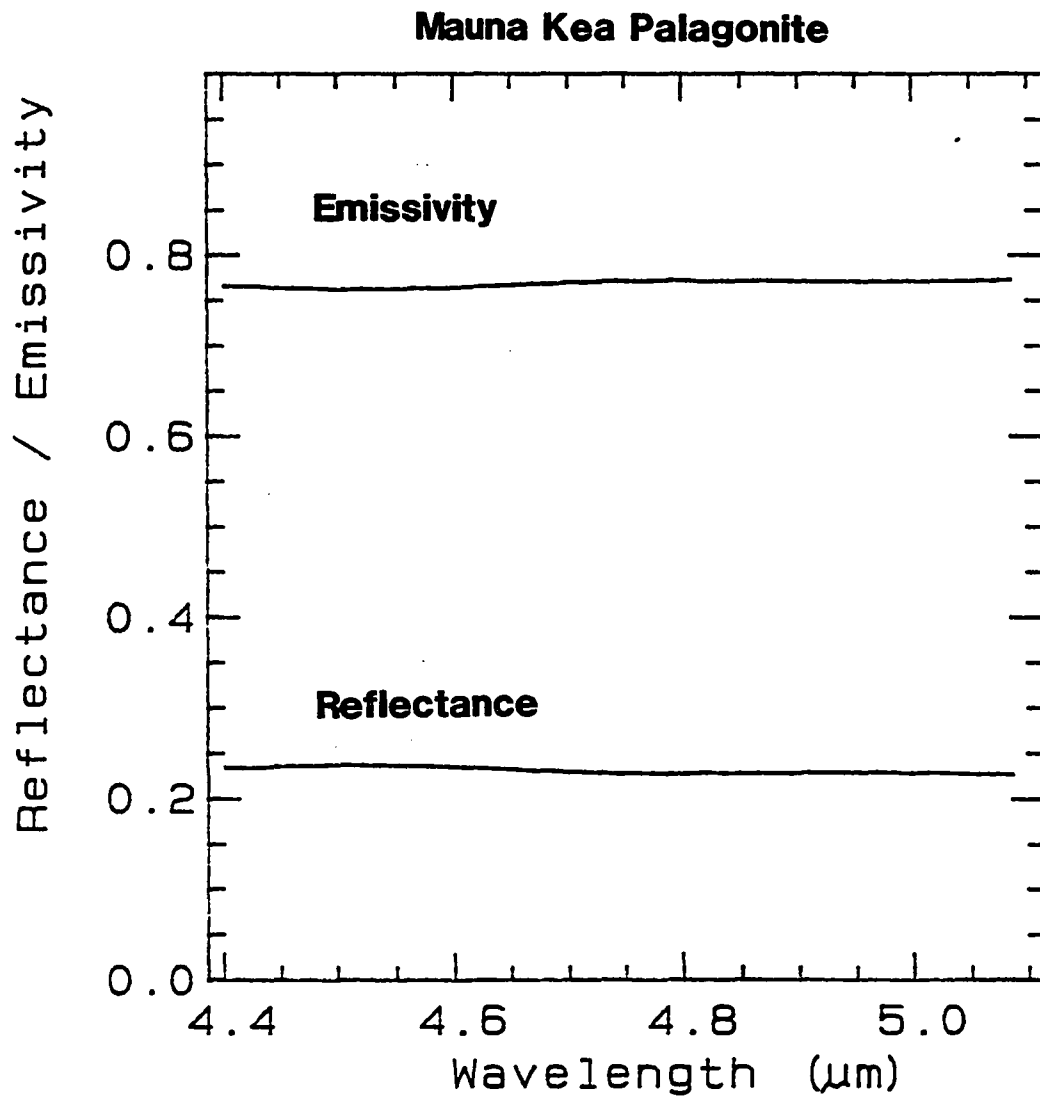


Figure 5.5b. Reflectance and emissivity of Mauna Kea palagonite (grain size $<34 \mu\text{m}$).

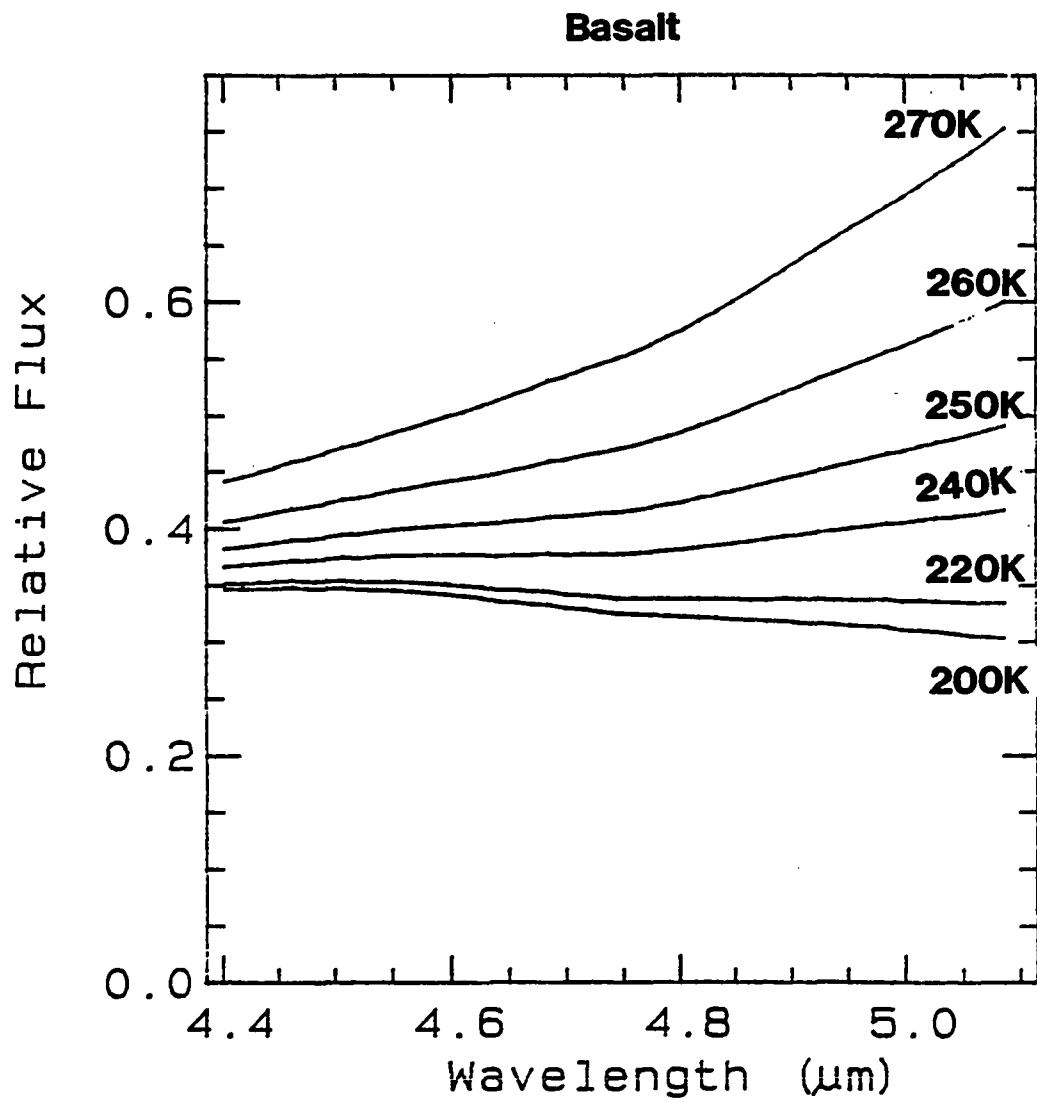


Figure 5.6a. Flux from a basaltic surface on Mars at temperatures ranging from 200 K - 270 K.

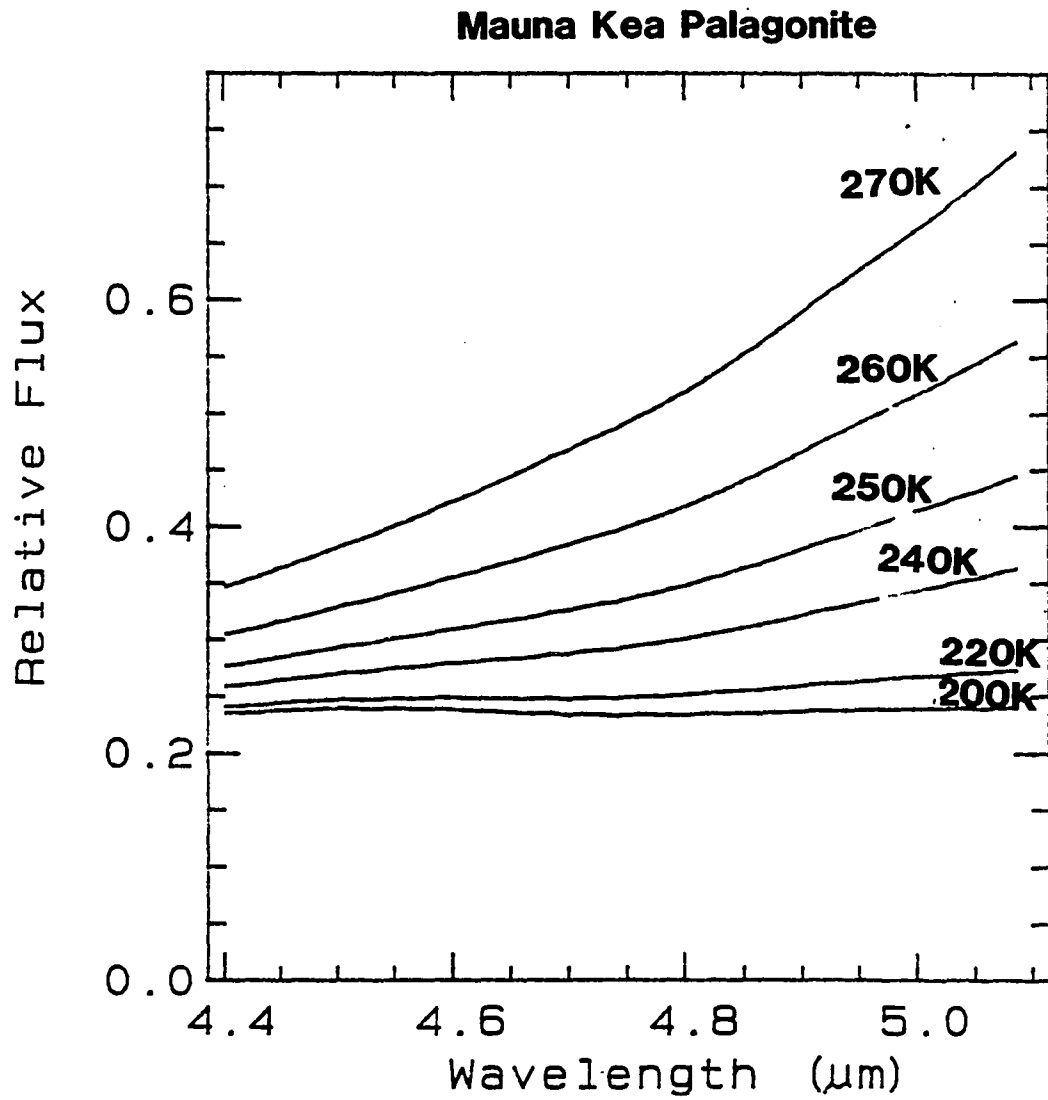


Figure 5.6b. Flux from a palagonite surface on Mars at temperatures ranging from 200K - 270K.

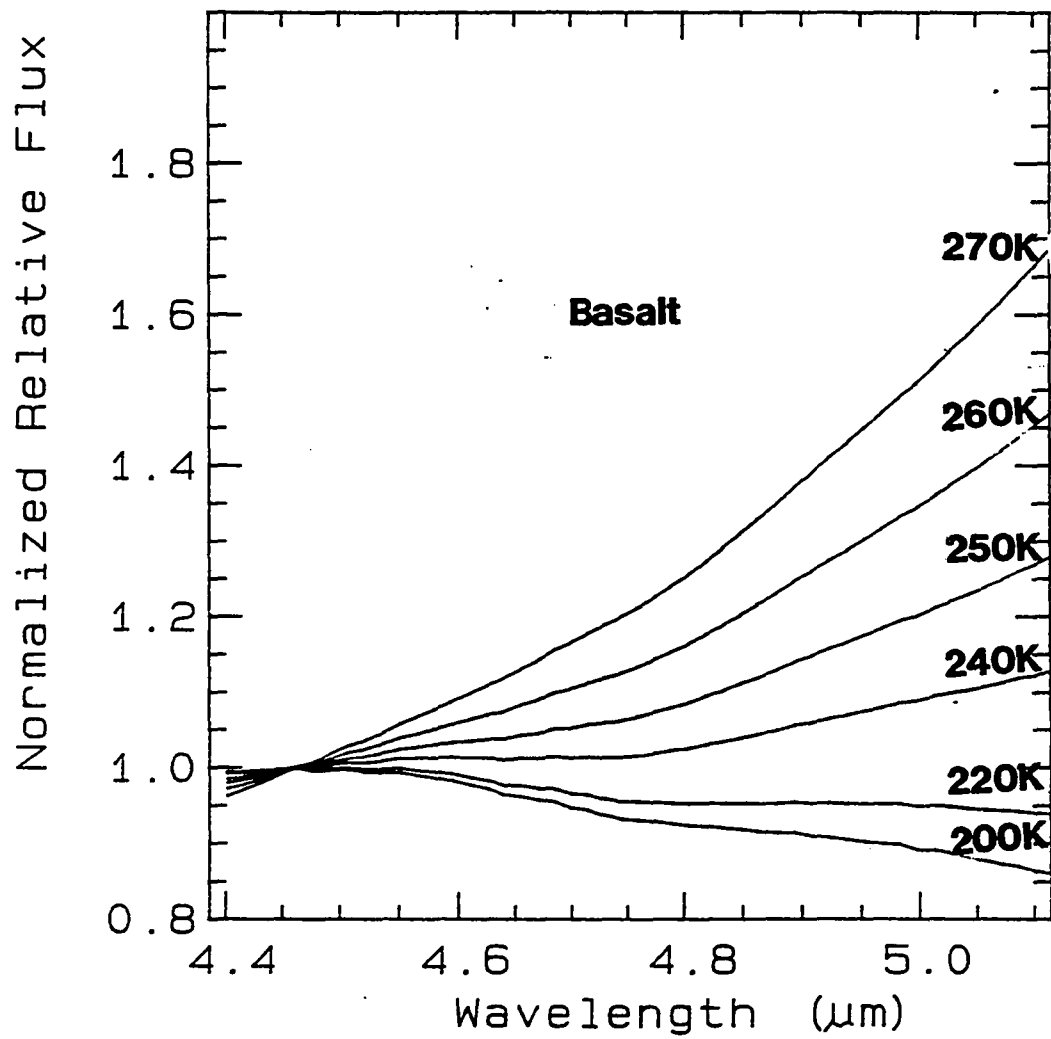


Figure 5.7a. Flux from a basaltic surface on Mars at temperatures ranging from 200 K - 270 K normalized to 1.0 at 4.46 μm.

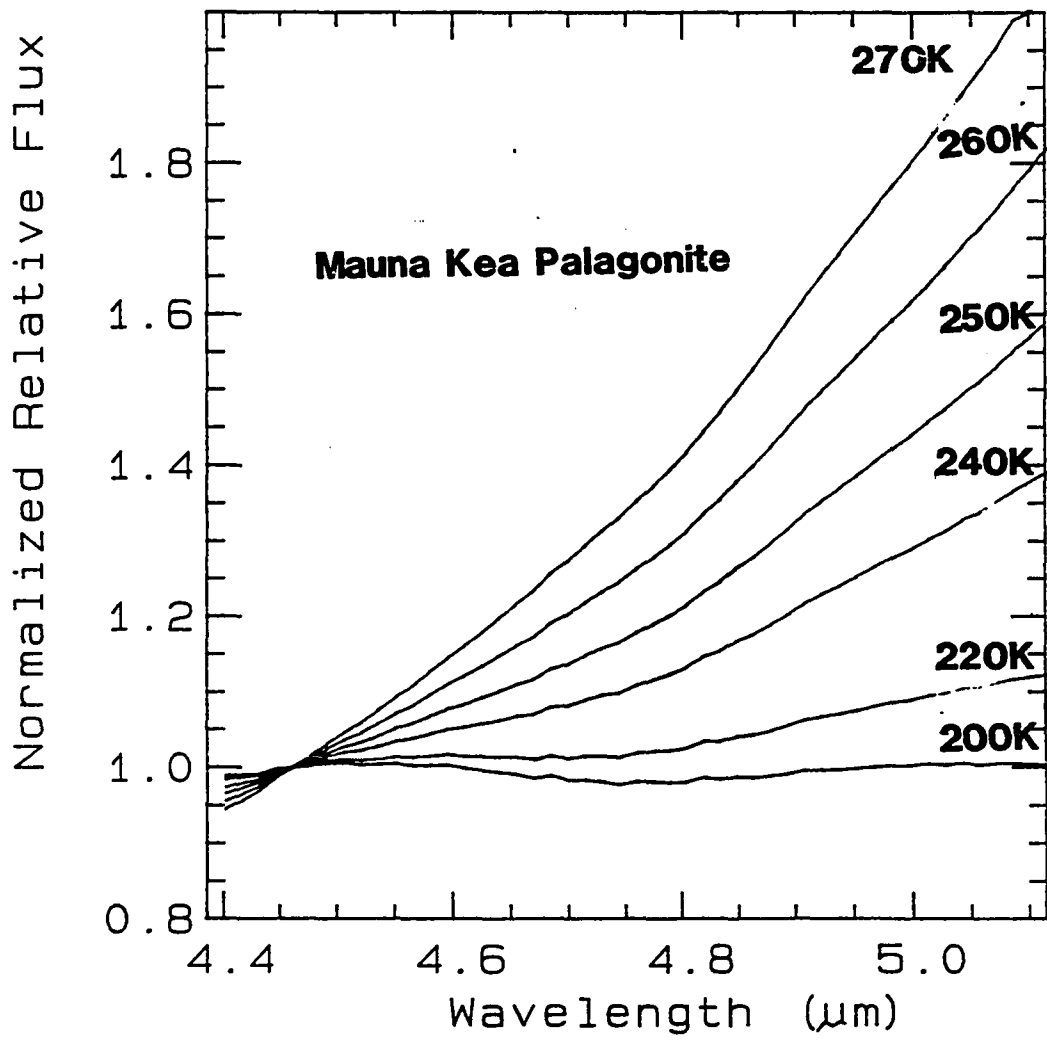


Figure 5.7b. Flux from a palagonite surface on Mars at temperatures ranging from 200 K - 270 K normalized to 1.0 at 4.46 μm.

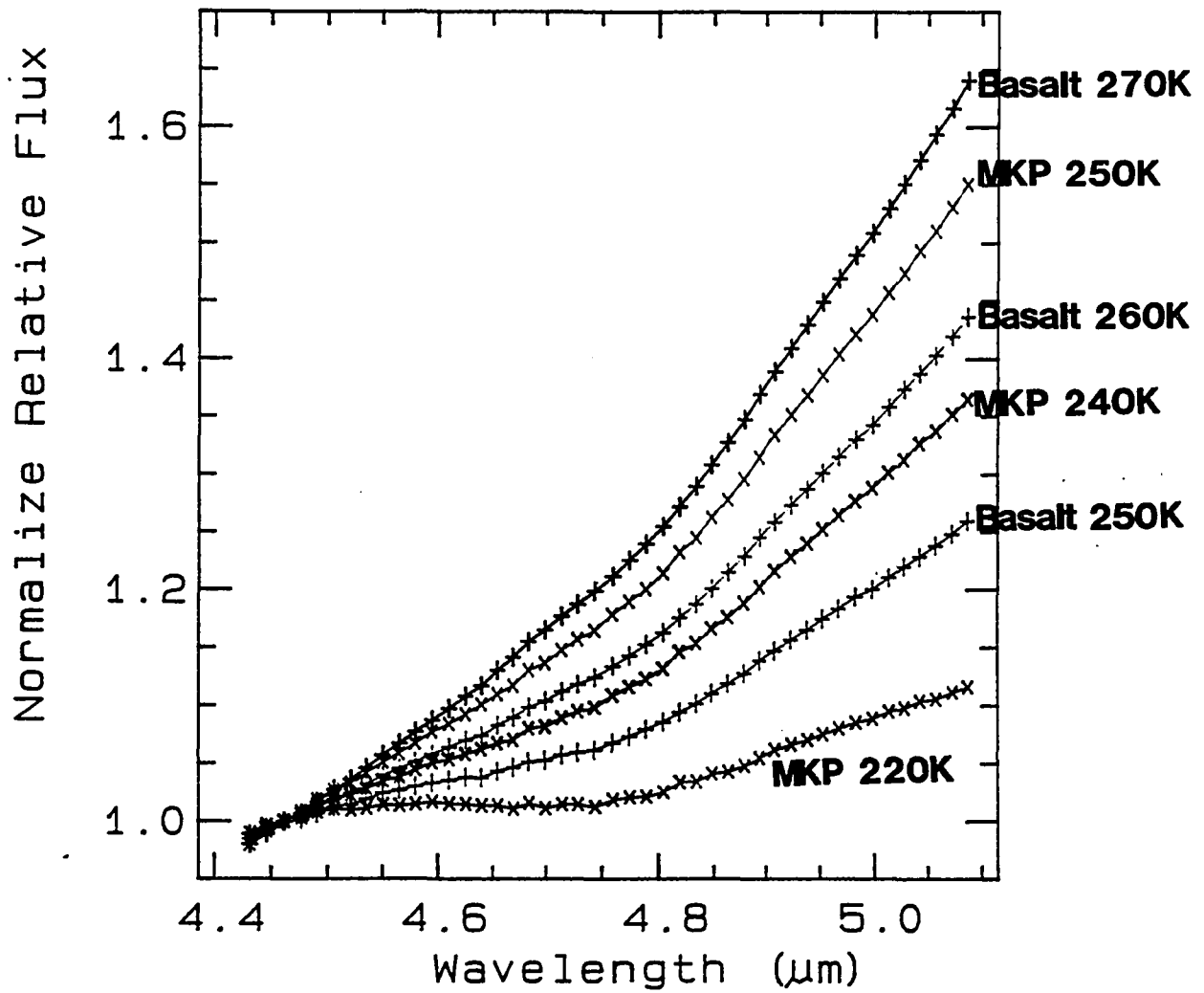


Figure 5.8. Flux from a basalt and a palagonite surface on Mars at temperatures ranging from 200K - 270K normalized to 1.0 at 4.46 μm illustrating the difficulties in thermal removal without knowing the albedo or temperatures.

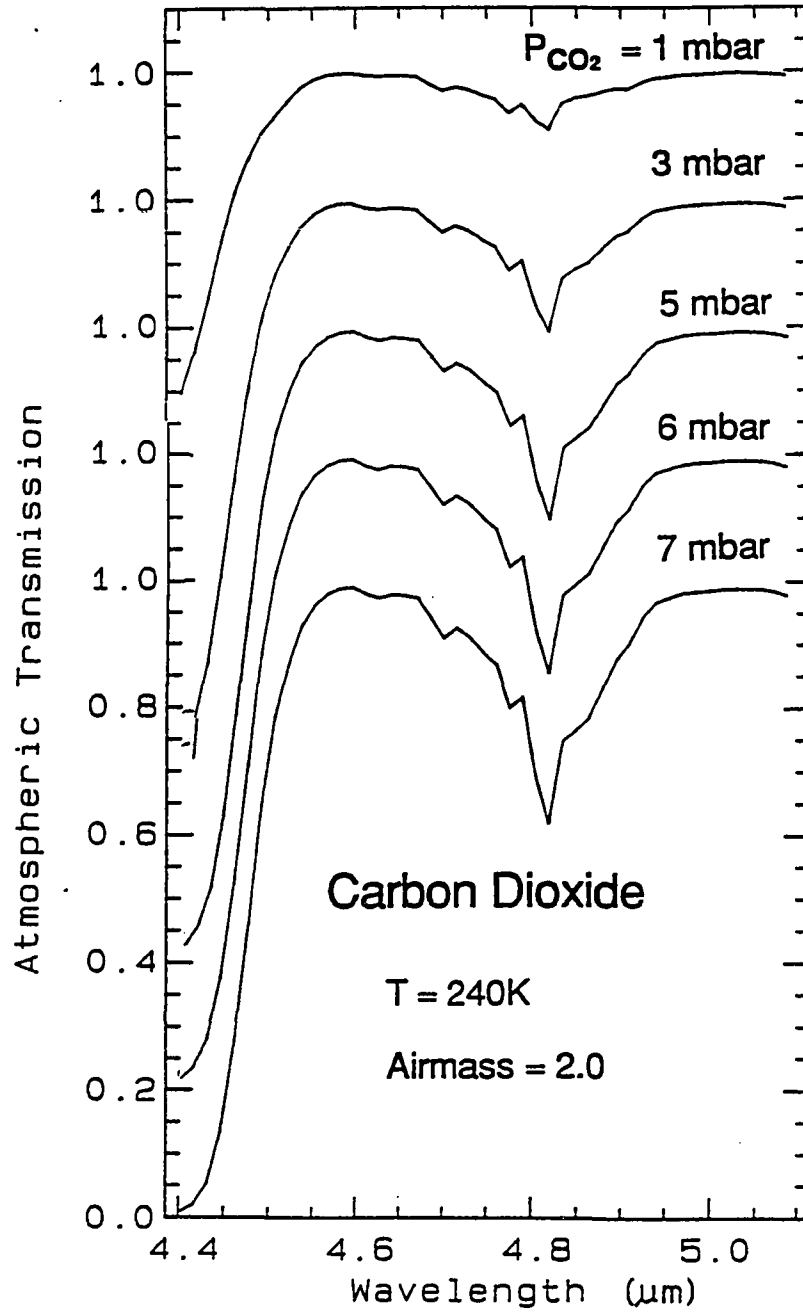


Figure 5.9a. Encrenaz model CO₂ transmission at P = 1, 3, 5, 6, and 7 mbar, T = 240 K, airmass = 2.0.

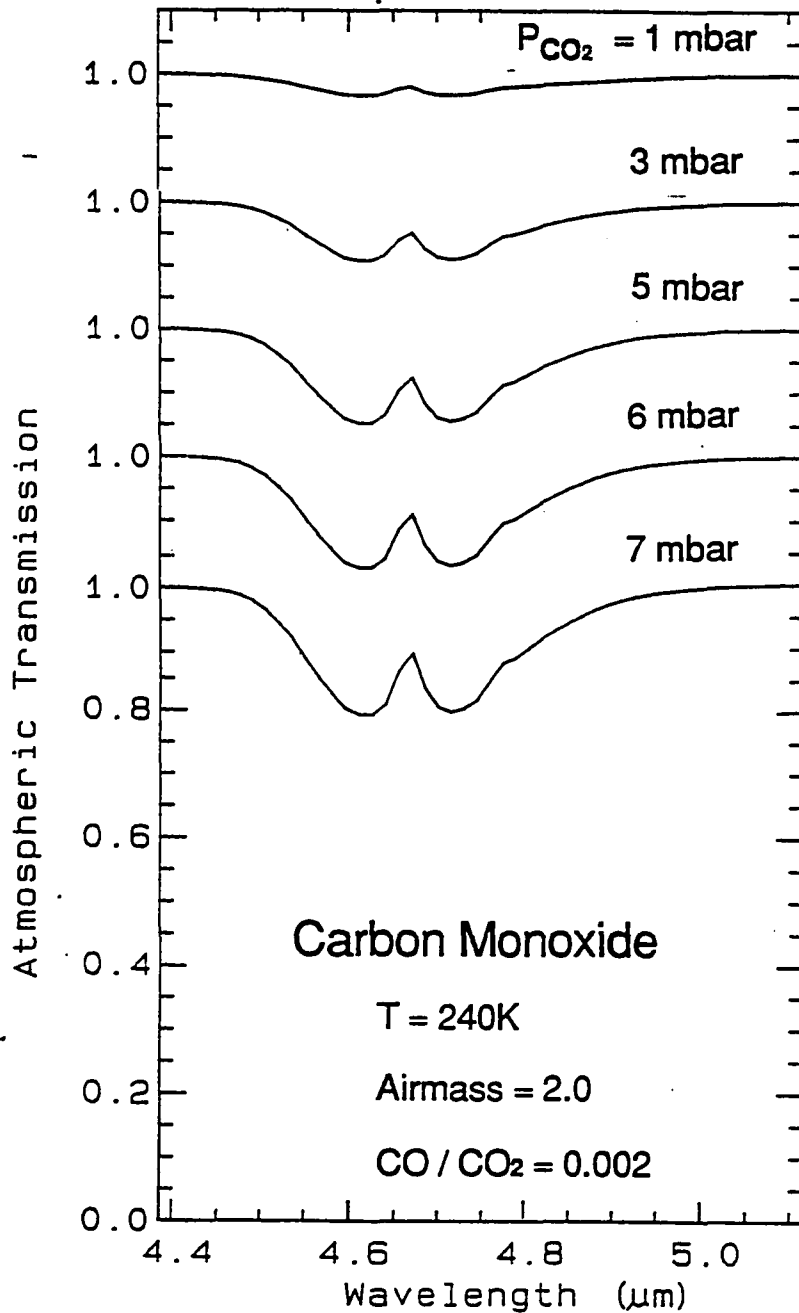


Figure 5.9b. Encrenaz model CO transmission at $P = 1, 3, 5, 6,$ and 7 mbar , $T = 240\text{K}$,
 airmass = 2.0, $\text{CO} / \text{CO}_2 = 0.002$.

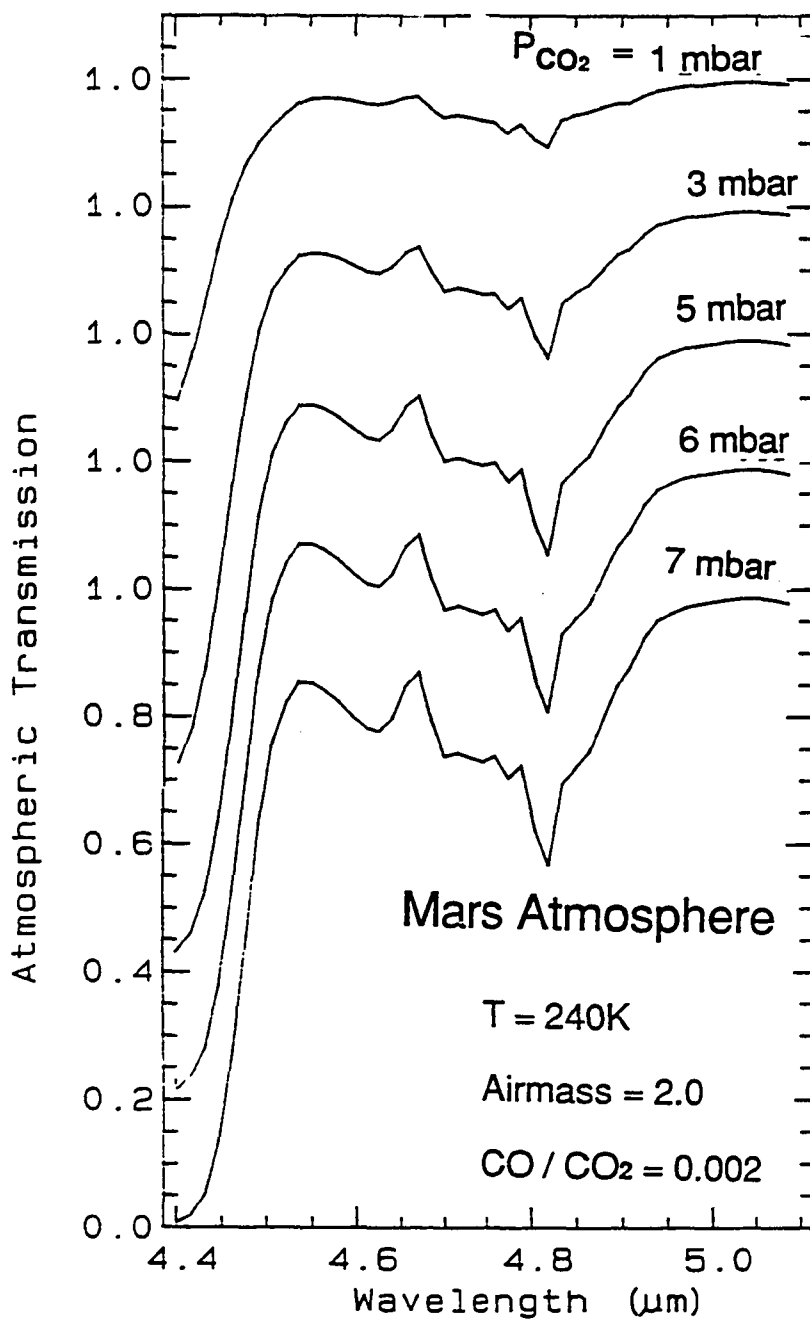


Figure 5.9c. Encrenaz model Mars atmospheric transmission at P = 1, 3, 5, 6, and 7 mbar, T = 240K, airmass = 2.0, CO / CO₂ = 0.002.

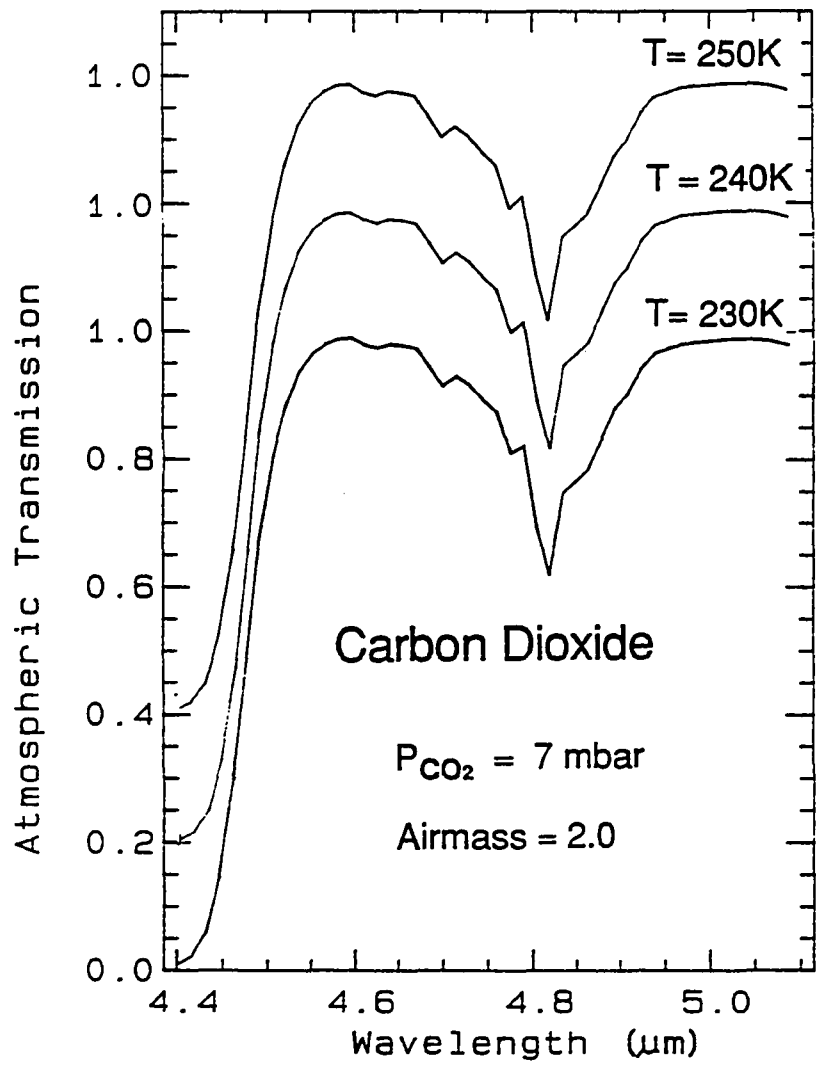


Figure 5.10a. Encrenaz model CO₂ transmission at P = 7 mbar, T = 230K, 240K, and 250K, airmass = 2.0.

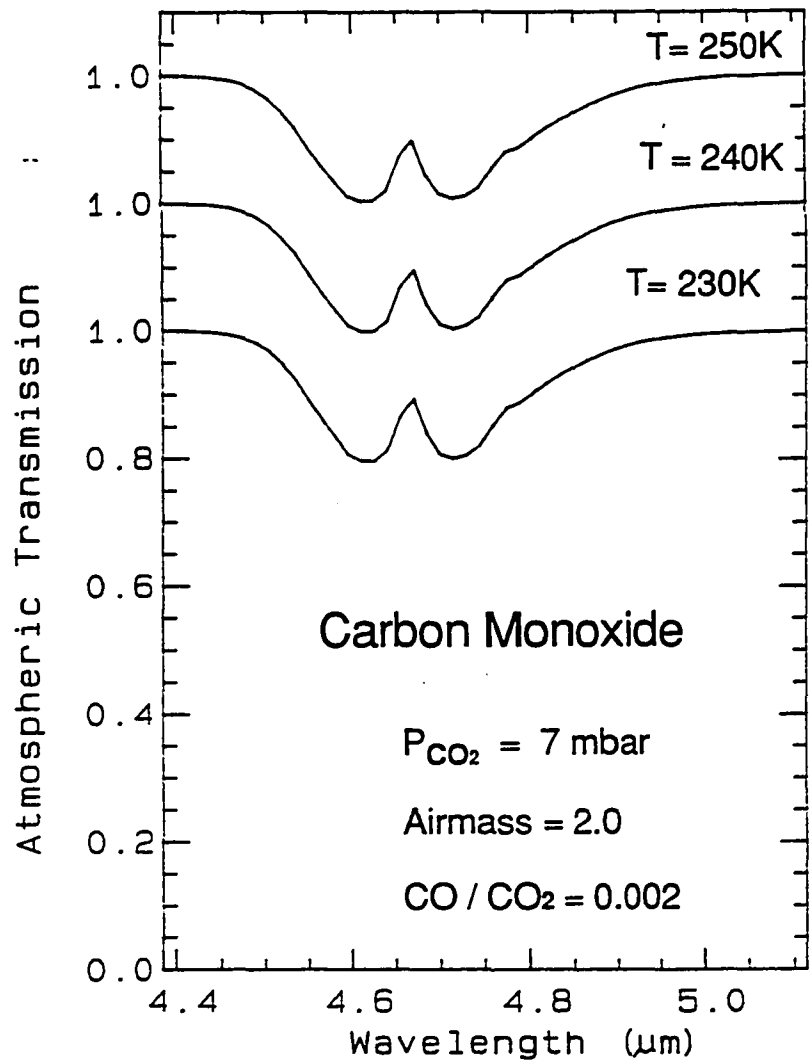


Figure 5.10b. Encrenaz model CO transmission at $P = 7 \text{ mbar}$, $T = 230\text{K}$, 240K , and 250K , airmass = 2.0, $\text{CO} / \text{CO}_2 = 0.002$.

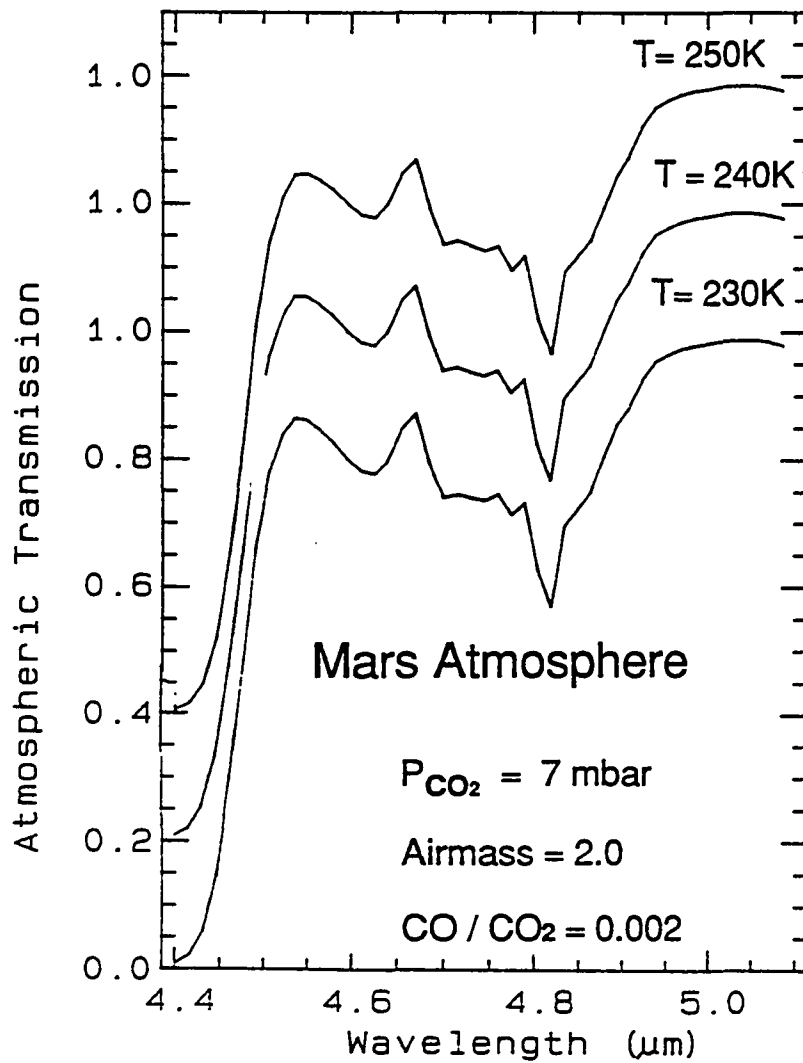


Figure 5.10c. Encrenaz model Mars atmospheric transmission at $P = 7 \text{ mbar}$, $T = 230\text{K}$, 240K , and 250K , airmass = 2.0, $CO / CO_2 = 0.002$.

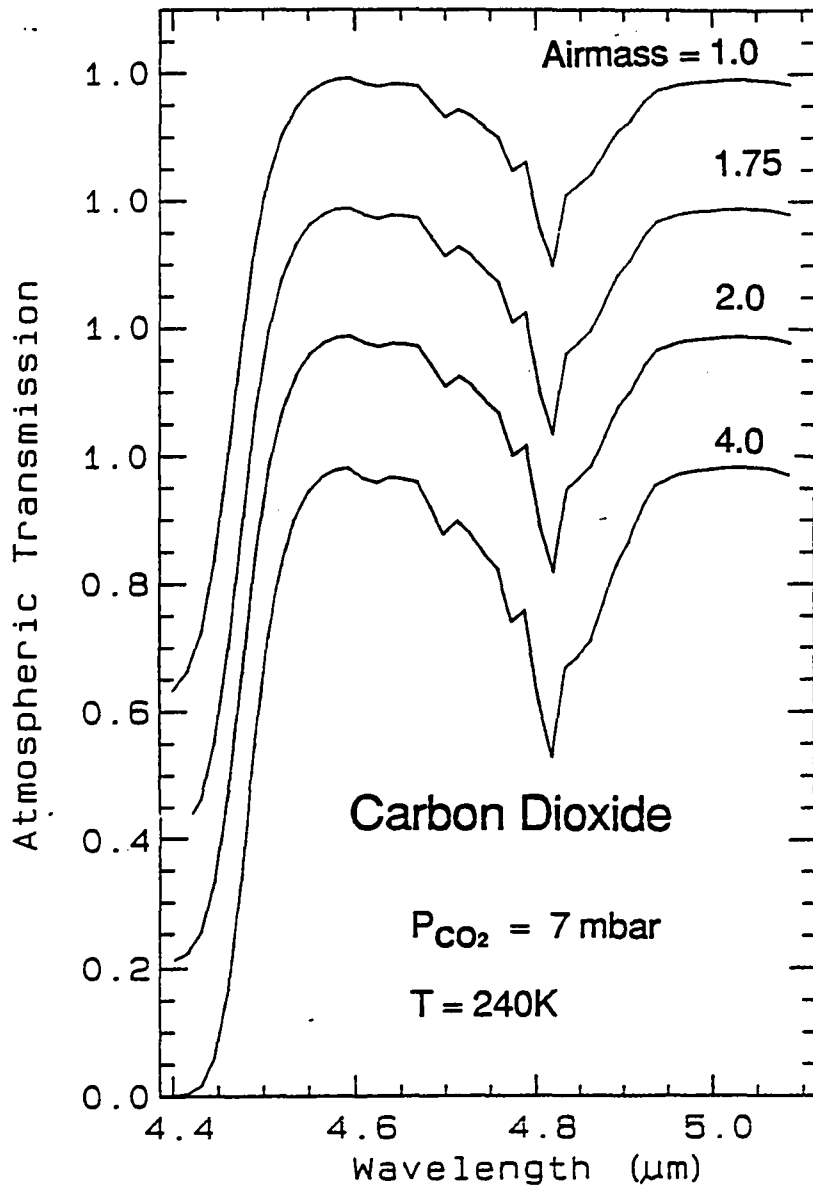


Figure 5.11a. Encrenaz model CO₂ transmission at P = 7 mbar, T = 240K, airmass = 1.0, 1.75, 2.0, and 4.0.

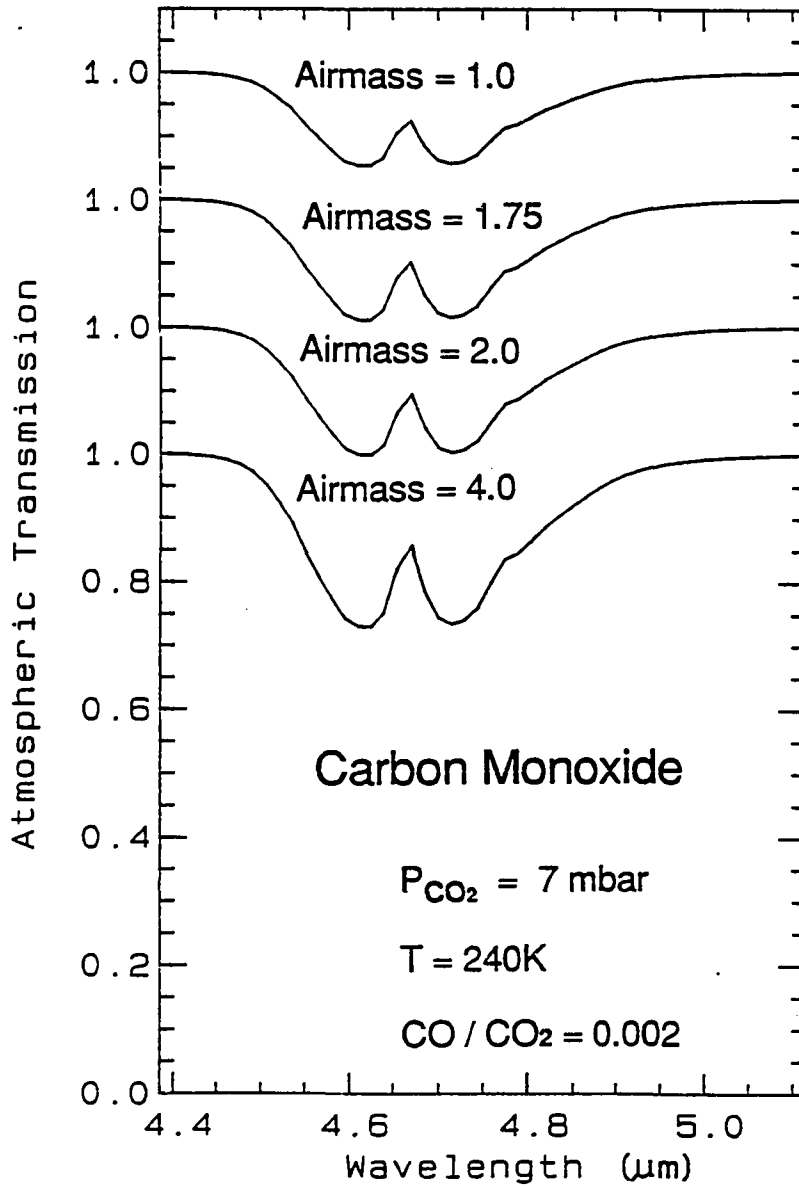


Figure 5.11b. Encrenaz model CO transmission at $P = 7 \text{ mbar}$, $T = 240\text{K}$, airmass = 1.0, 1.75, 2.0, and 4.0, $\text{CO} / \text{CO}_2 = 0.002$.

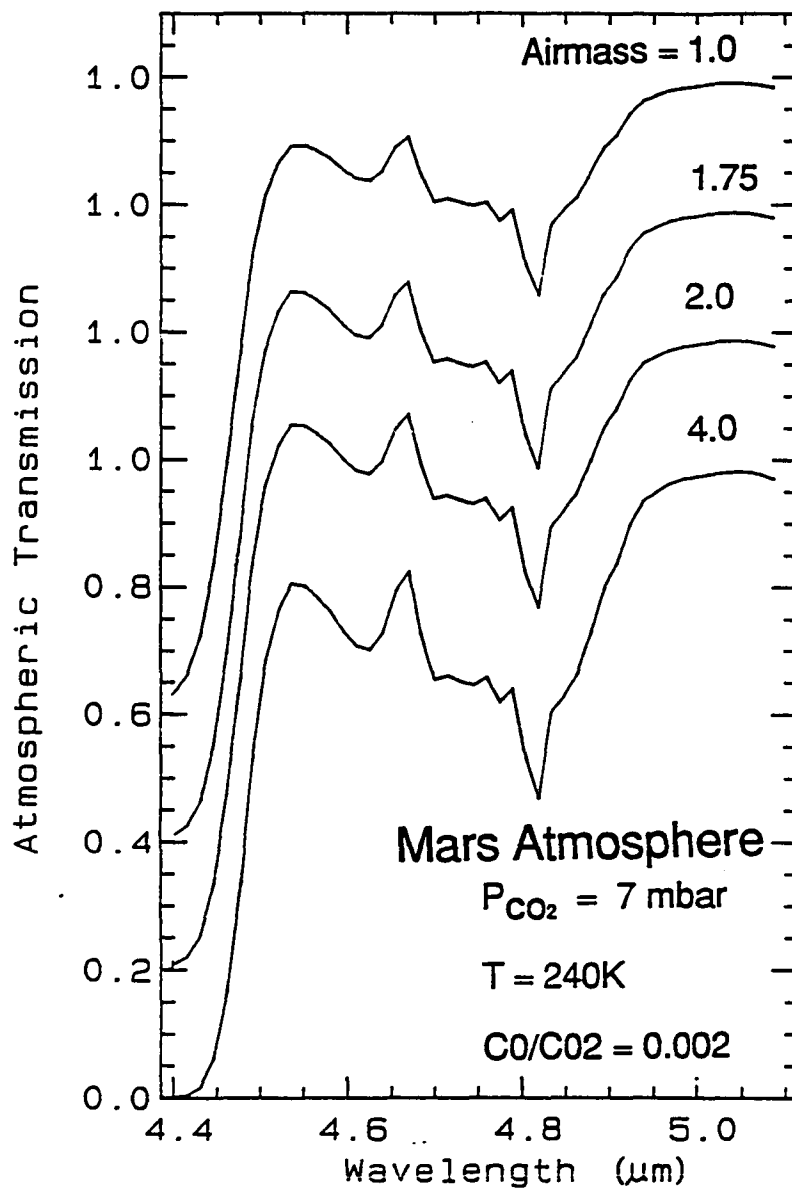


Figure 5.11c. Encrenaz model Mars atmospheric transmission at $P = 7 \text{ mbar}$, $T = 240\text{K}$, airmass = 1.0, 1.75, 2.0, and 4.0, $CO / CO_2 = 0.002$.

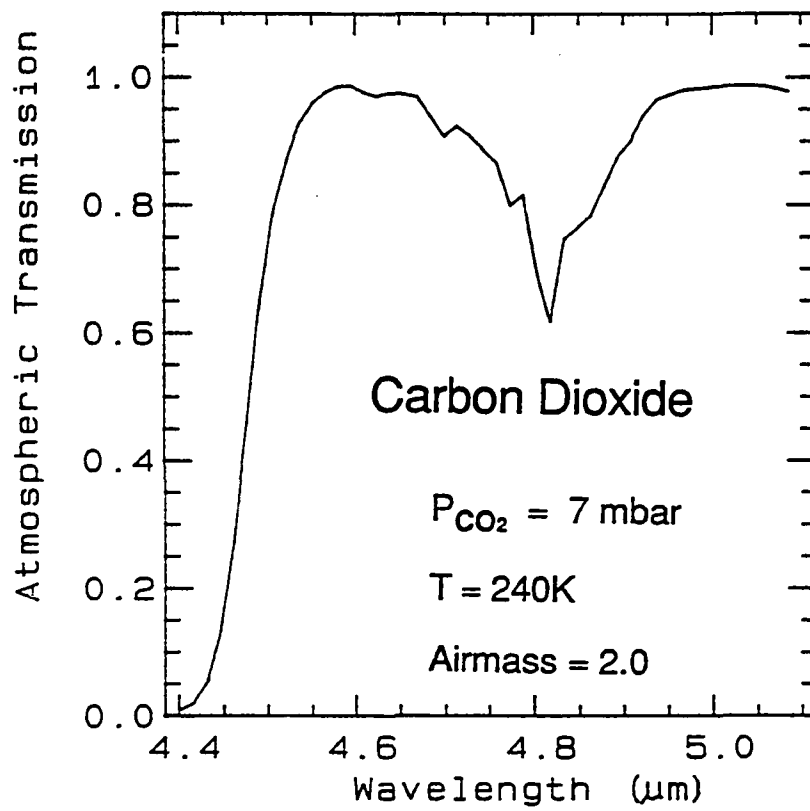


Figure 5.12a. Encrenaz model CO₂ transmission at P = 7 mbar, T = 240K, airmass = 2.0.

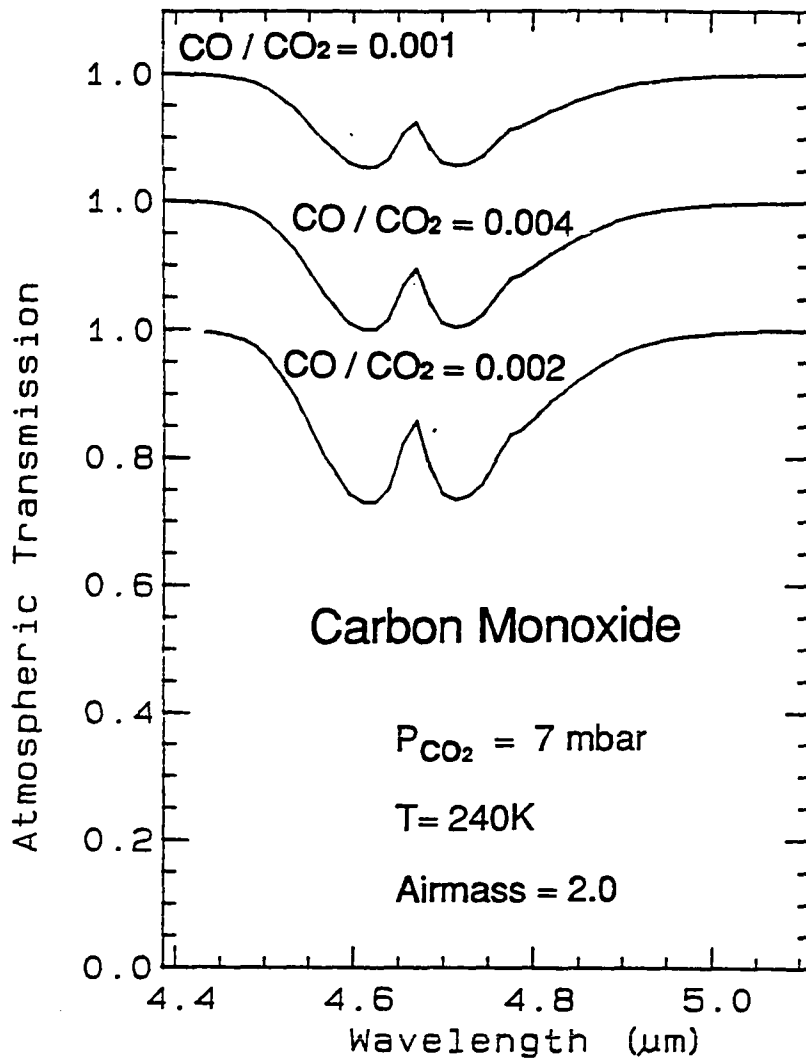


Figure 5.12b. Encrenaz model CO transmission at $P = 7 \text{ mbar}$, $T = 240\text{K}$, $\text{airmass} = 2.0$, $\text{CO} / \text{CO}_2 = 0.001, 0.002, 0.004$.

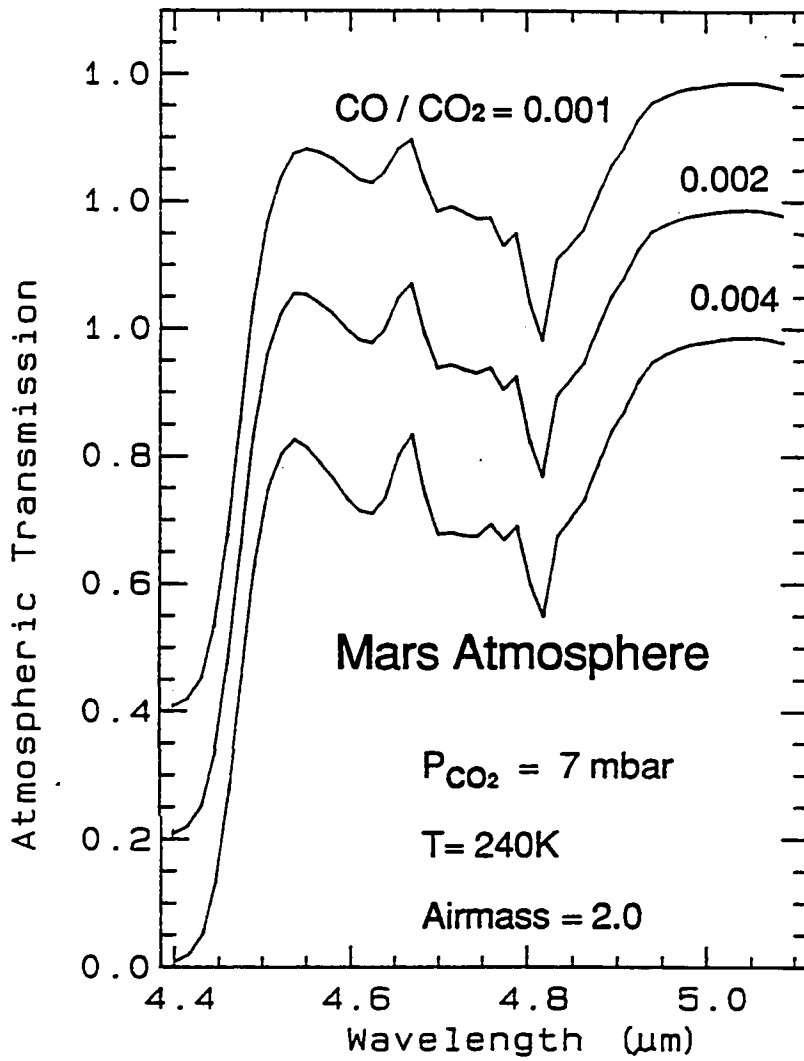


Figure 5.12c. Encrenaz model Mars atmospheric transmission at $P = 7$ mbar, $T = 240$ K, airmass = 2.0, $\text{CO} / \text{CO}_2 = 0.001, 0.002,$ and 0.004 .

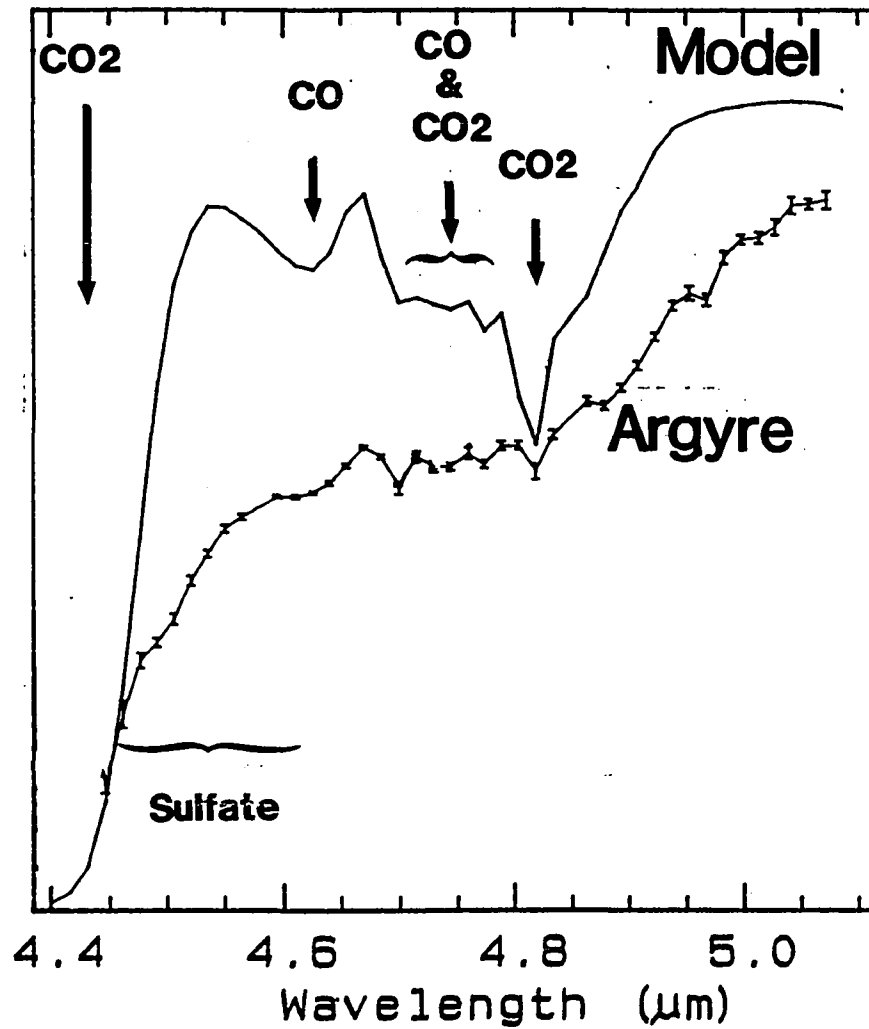


Figure 5.13. Representative spectra (Argyre region) and Mars model atmosphere of 7 mbar, 2 airmass, 240K, and CO / CO₂ with atmospheric and surface absorptions labeled.

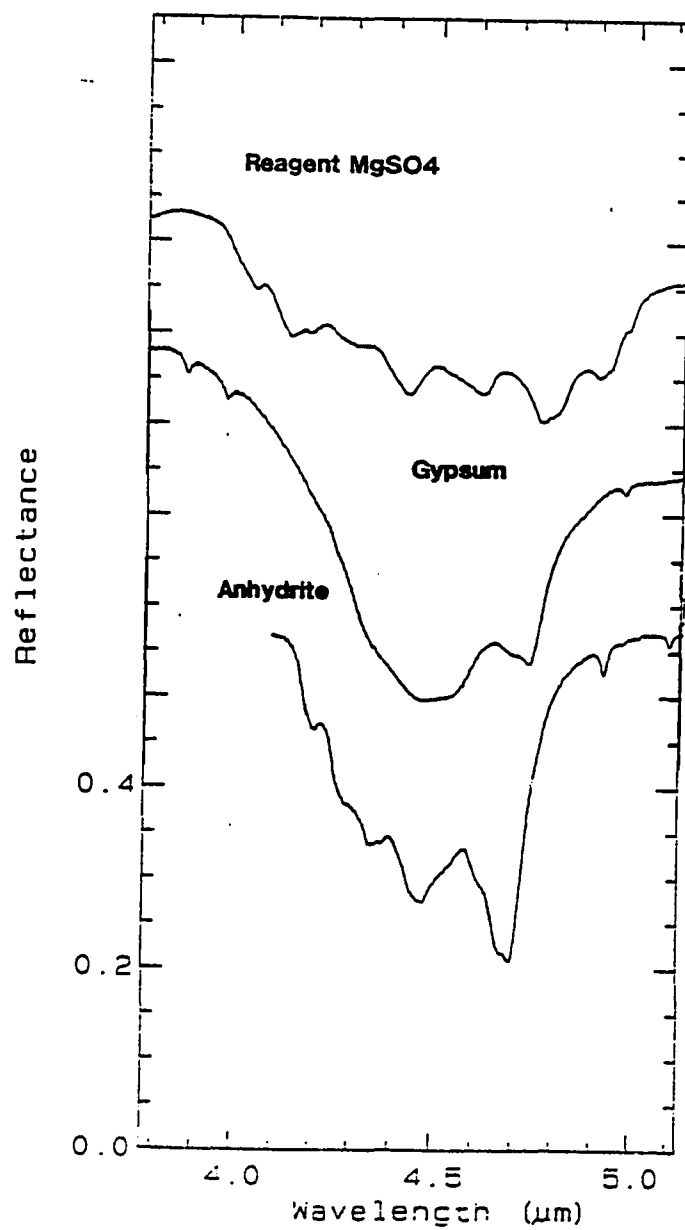


Figure 5.14. Reagent MgSO₄, gypsum, and anhydrite reflectance spectra. Spectra are relative to sulfur and have a grain size of <34 μm. Spectra measured at 2 cm⁻¹ resolution.

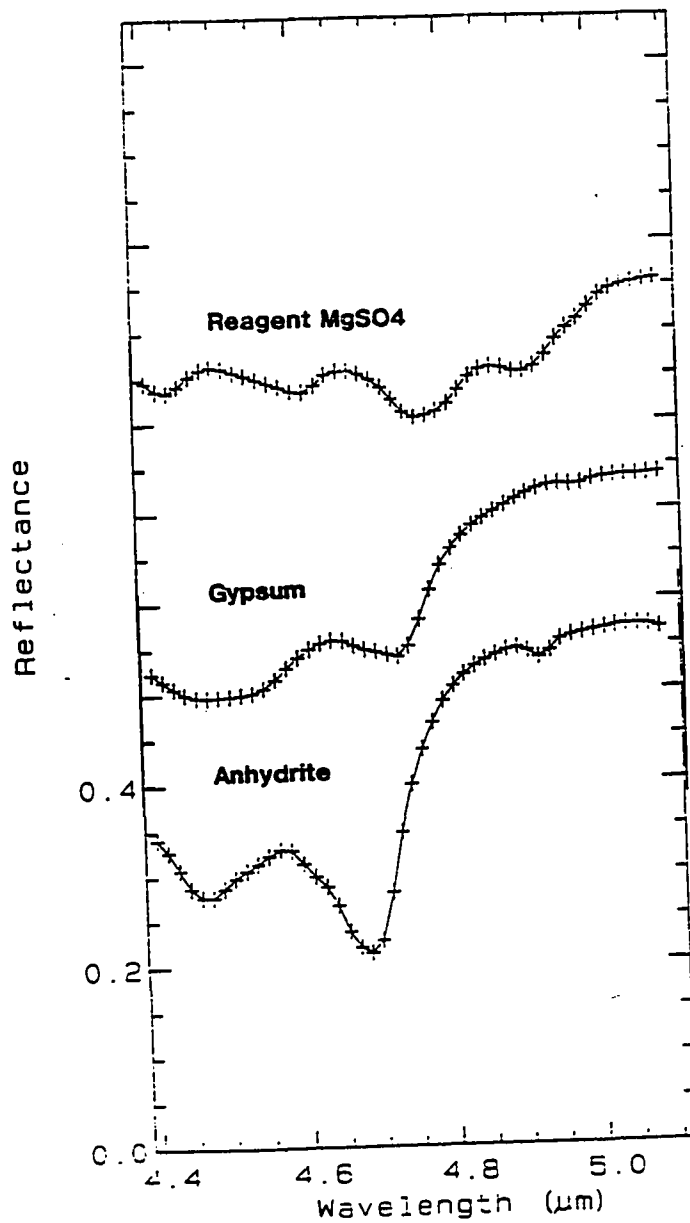


Figure 5.15. Reagent MgSO₄, gypsum, and anhydrite reflectance spectra. Spectra are relative to sulfur and have a grain size of <34 μm. Spectra convolved and interpolated to wavelengths of the telescopic observations.

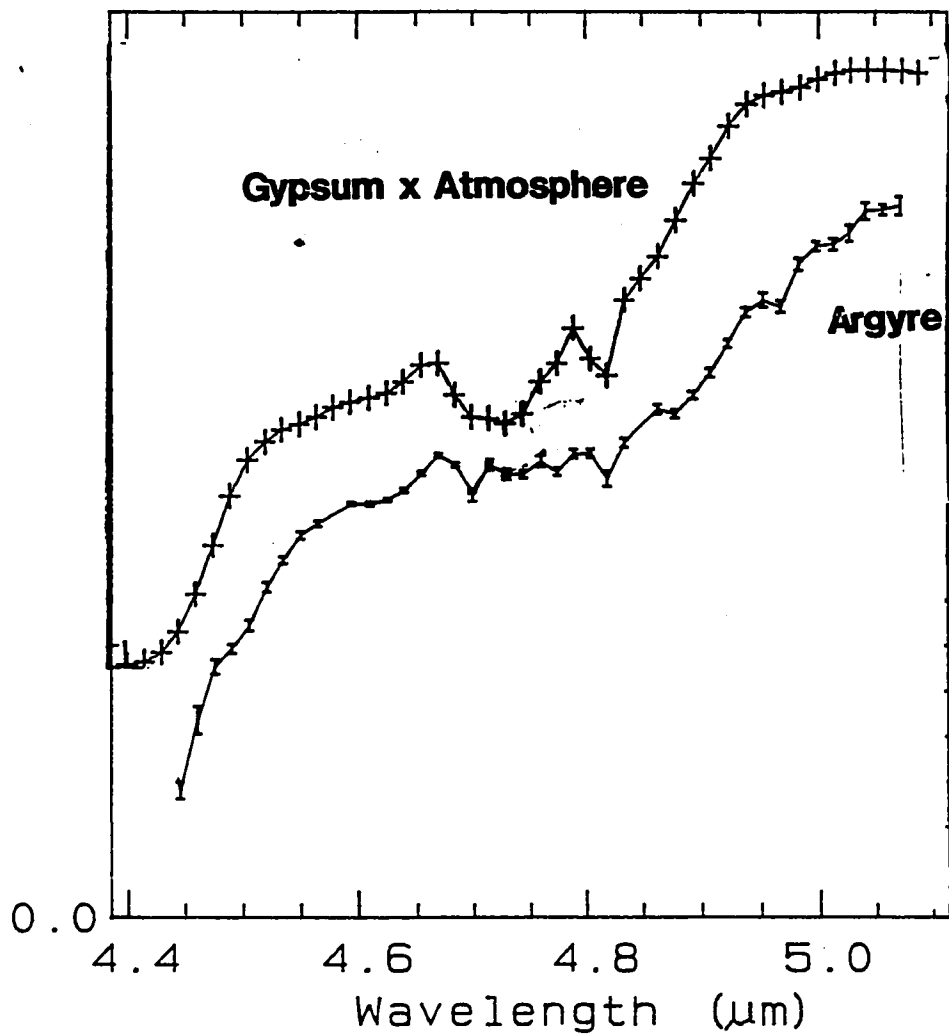


Figure 5.16. Gypsum multiplied by model atmospheric transmission (7 mbar, 240K, 2 airmass, C_0 / CO_2 0.002) over Argyre spectra. Illustrates the necessity of a 4.5 μm absorption to match the telescopic data.

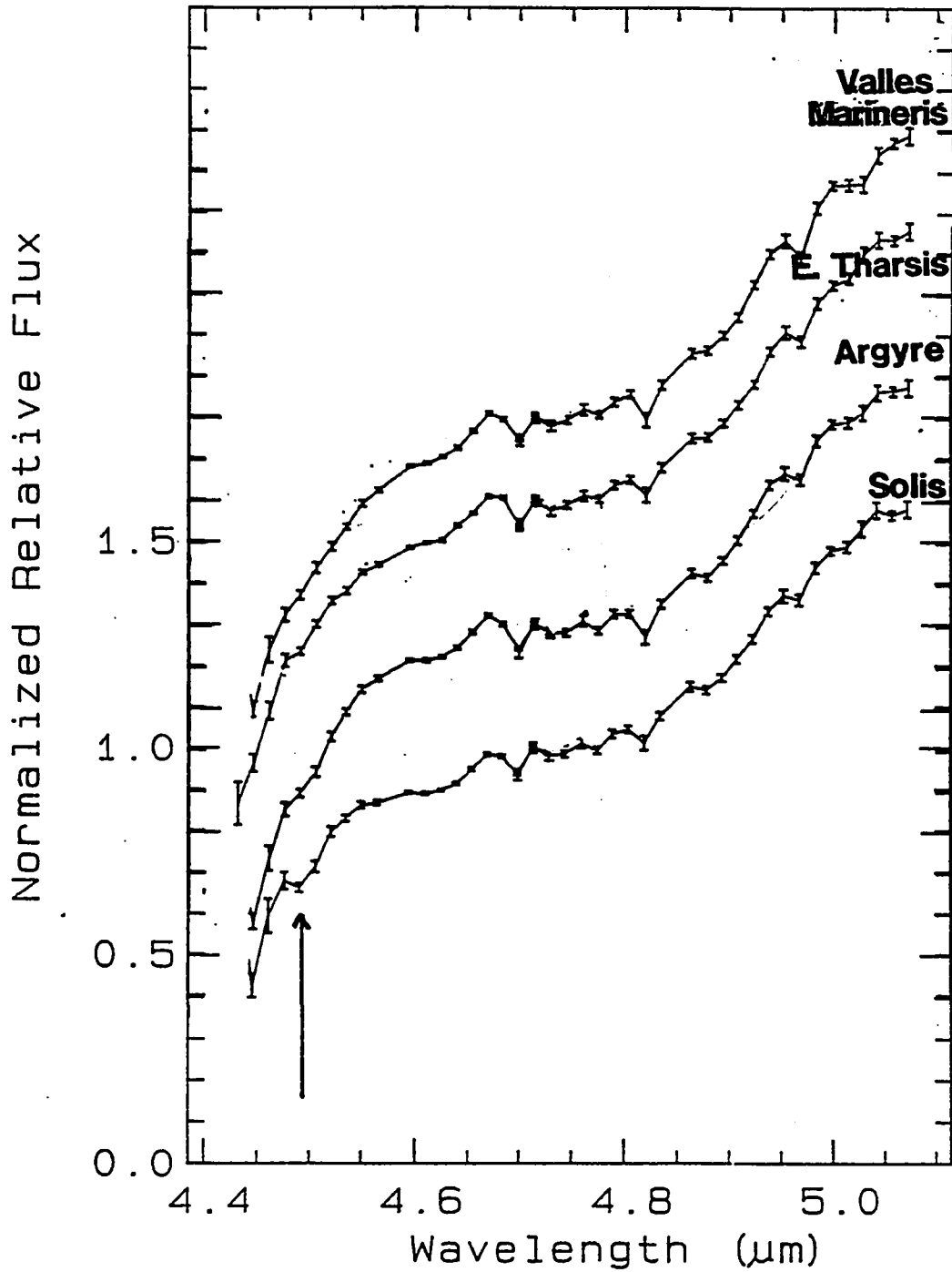


Figure 5.17. Spectra for four regions with similar $3.81 \mu\text{m}$ band depths. Regions are Eastern Solis Planum, Ridged Plains, Heavily Cratered Terrain; Argyre Basin; Eastern Tharsis; and Valles Marineris. Spectra are arranged in order of $4.5 \mu\text{m}$ band depth. Locations of apertures are shown in Figures 1 and 2. Subsequent spectra are offset from each other by 0.2 units.

Chapter 6.

Conclusions

Contrary to expectations from geochemical and climatic modeling of relatively large abundances of carbonates existing on the Martian surface, earth-based telescopic data from both the 1986 and 1988 oppositions indicate no sign of any $4\ \mu\text{m}$ carbonate absorption. Laboratory studies involving mixtures of Mauna Kea palagonite, a Martian soil analog, and various carbonates put upper limits of 3 - 5 wt% carbonate for regions measured in 1986 and 1 - 3 wt% carbonate for locations measured in 1988. The measurements presented cover terrains of all ages and types with the exception of regions in the Northern lowlands, which were not observable owing to viewing geometry limitations.

Low to non-existent carbonate abundances limits to a few weight percent the amount of weathering products formed as thermodynamically stable minerals under ambient conditions. Consequently, the fine-grained material on the Martian surface must have another origin, perhaps impact-generated ash or hydrothermally altered impact glass.

Carbonates formed during proposed clement climates early in Mars's history must be buried at depth, located in small regional deposits, removed from the optical surface by secondary weathering, such as decomposition by acidic sulfate solutions, or do not exist because a massive carbon dioxide atmosphere did not exist.

In addition to detection by the Viking landers, spectroscopic evidence for the presence of sulfates now exists. The rise out of the $4.2\ \mu\text{m}$ - $4.4\ \mu\text{m}$ CO_2 band cannot be matched by solely atmospheric constituents. A surface absorption must be added at roughly $4.5\ \mu\text{m}$ in order to decrease the reflectance rise and produce the $4.5\ \mu\text{m}$ inflection which is present in the data. The known presence of sulfates on the Martian surface and the location of this feature at the $2\nu_3$ overtone of the SO_4^{-2} anion indicate that the surface

absorption is probably caused by sulfates on the Martian surface. An exact match to a terrestrial sulfate mineral has not been made but it is suggested that the mineral has very weak structure and thus a high degree of symmetry . Significant variation exists between the spectra at 4.5 μm . In order of strength of deepest absorption to weakest, the regions are ordered Eastern Solis Planum, Argyre Basin, Eastern Tharsis, and Valles Marineris for the four regions measured at similar Martian atmospheric conditions.

Bibliography

- Allen C. C., J. L. Gooding, M. Jercinovic, and K. Keil, Altered basaltic glass: a terrestrial analog to the soil of Mars, *Icarus*, 45, 347-369, 1981.
- Allen C. C., J. L. Gooding, and K. Keil, Hydrothermally altered impact melt rock and breccia: contributions to the soil of Mars, *J. Geophys. Res.*, 87, 10,083-10101, 1982.
- Allen C.W., *Astrophysical Quantities*. London: University of London Athlone Press, 1976.
- Anders, E., and T. Owen, Mars and Earth: Origin and abundance of volatiles, *Science*, 198, 453-465, 1977.
- Arvidson, R.E., E.A. Guinness, S.W. Lee, Differential aeolian redistribution rate on Mars, *Nature*, 278, 533-555, 1979.
- Ashwal, L.D., J.L. Warner, and C.A. Wood, SNC meteorites: Evidence against asteroidal origin, *Proc. Lunar and Planet. Sci. Conf. 13th, Part 1, J. Geophys. Res.* 87, suppl., A393-A400, 1982.
- Baird, A.K., P. Toulmin, B.C. Clark, H.J. Rose, K. Keil, R.P. Christian, and J.L. Gooding, Mineralogic and petrologic implications of Viking geochemical results from Mars: Interim report, *Science*, 194, 1288-1293, 1976.
- Becker, R.H., and R.O. Pepin, The case for a Martian origin of the shergottites: Nitrogen and noble gases in EETA 79001, *Earth and Planet. Sci. Lett.*, 69, 225-242, 1984.
- Beer, R., R.H. Norton, and J.V. Martonchik, Astronomical infrared spectroscopy with a Connes-type interferometer: II. Mars, 2500-3500 cm⁻¹, *Icarus*, 15, 1-10, 1971.

- Biemann, K., J. Oro, P. Toulmin, L.E. Orgel, O. Nier, P.M. Anderson, P.G. Simmonds, D. Floy, A.V. Diaz, R. Rushneck, J.E. Biller, and A.L. Lafleur, The search for organic substances and inorganic volatile compounds in the surface of Mars, *J. Geophys. Res.*, 82, 4641-4658, 1977.
- Blaney D.B., and T.B. McCord, An observational search for carbonates on Mars, *J. of Geophys. Res.*, 94, 10,159-10,166, 1989a.
- Blaney D.B. and T.B. McCord, Constraints on the climate and weathering histories of Mars from ground based spectroscopy between 3.2 μm and 4.2 μm . submitted to *J. Geophys. Res.*, June, 1989b.
- Burns, R.G., Ferric sulfates on Mars. *Proc. Seventeenth Lunar Planet. Sci. Conf., Part 2, J. Geophys. Res.*, 92, E570-E574, 1987.
- Burns, R.G., Gossans on Mars, *Proc. of the 18th Lunar and Planetary Sci. Conf.*, 713-721, 1988.
- Campbell, I.B., and G.G.C. Claridge, *Antarctica: Soils, Weathering Processes and Environment, Developments in soil science 16*, Elsevier Science Pub. B.V., New York, N.Y., 1987.
- Carr, M. H., Stability of streams and lakes on Mars. *Icarus* , 56, 476-495, 1983.
- Carr, M. H., Mars: A water-rich planet? *Icarus* ,68, 187-216, 1986.
- Carr, M. H., Recharge of the early atmosphere of Mars by impact-induced release of CO_2 . *Icarus*, in press, 1989.
- Carr, M. H., and Clow, G. D., 1981. Martian channels and valleys: Their characteristics, distribution and age. *Icarus*, 48, 91-117, 1981.
- Clark B.C., S.L. Keniey, D.L. O'Brien, G.R. Huss, R. Mack, and A.K. Baird, Heterogeneous phase reactions of Martian volatiles with putative regolith minerals. *J. Mol. Evol.*, 14, 91-102, 1979.

- Clark, B.C., A.K. Baird, P. Toulmin, H.J. Rose, K. Keil, A.J. Castro, W.C. Kelliher, C.D. Rowe, and P.H. Evans, Organic analysis of martian surface samples at the Viking landing sites, *Science*, 194, 1976.
- Clark, B.C. and P.C. Van Hart, The salts of Mars, *Icarus*, 45, 370-378, 1981.
- Clark, B.C., A.K. Baird, R.J. Weldon, D.M. Tsusaki, L. Schrabel, and M.P. Candelaria, Chemical Composition of Martian Fines, *J. Geophys. Res.*, 87, 10,059-10,068, 1982.
- Clark, R.N., A large scale interactive one dimensional array processing system, *Pub. A.S.P.*, 92, 221-224, 1980.
- Clark, R.N., R.B. Singer, and G.A. Swayze, Discovery of Globally-distributed Scapolite on Mars, 4th International Conference on Mars, 82-83, 1989.
- Colthup, N. B., L. H. Daly, and S. E. Wiberleym, *Introduction to Infrared and Raman Spectroscopy*, Academic Press, Inc., New York, New York, 523p., 1975.
- Connes, J., P. Connes, and M. Kaplan, Mars: New absorption bands in the spectrum. *Science*, 153, 739-740, 1966.
- Dreibus, G., and H. Wanke, Accretion of the earth and inner planets, *Proc. 27th Int. Geol. Congr. Moscow*, 11, 1-11, 1984.
- Dreibus, G., and H. Wanke, Comparison of Cl/Br and Br/I ratio in terrestrial samples and SNC meteorites, *Proc. Workshop on The Evolution of the Martian Atmosphere*, Technical Report, 86-07, 13-14, Lunar and Planetary Institute, Houston, TX, 1986.
- Encranaz, T., On the atmospheric origin of weak absorption features in the infrared spectrum of Mars, submitted to *J. Geophys. Res.*, 1989.
- Evans, D.L. and J.B. Adams, Amorphous gels as possible analogs to Martian weathering products, *Proc. Lunar Planet. Sci. Conf. 11th*, 757-763, 1980.

- Fanale, F.P., Martian volatiles; Their degassing history and geochemical fate. *Icarus*, 28, 179-202, 1976.
- Fanale, F.P., and W.A. Cannon, Mars: CO₂ absorption and capillary condensation on clays--Significance for volatile storage and atmospheric history, *J. Geophys. Res.*, 84, 8404-8415, 1979.
- Fanale, F.P., J.R. Savail, W.B. Banerdt, and R.S. Saunder, The regolith-atmosphere-cap system and climate change, *Icarus*, 50, 381-407, 1982.
- Fanale, F.P., J.R. Savail, A.P. Zent, and S.E. Postawko, Global distribution and migration of subsurface ice on Mars, *Icarus*, 67, 1-18, 1986.
- Fanale, F.P., J. B. Pollack, M. H. Carr, R. O. Pepin, and S. E. Postawko, Epochal climate change on Mars, *Mars Book*, University of Arizona Press, submitted 1989.
- Farmer V.C. (ed.), *The Infrared Spectral of Minerals*, Mineralogical Society of London, Monograph 4, London England, 539p., 1974.
- Gary, M., R. McAfee, and C.L. Wolf (Eds), *Glossary of Geology*, American Geologic Institute, Washington, D. C., 1974.
- Goetz, A.F.H., B.N. Rock, and L.C. Rowan, Remote sensing for exploration: An overview, *Econ. Geol.* 78, 573-590, 1983.
- Gooding, J.L., Chemical Weathering on Mars. Thermodynamic Stability of Primary Minerals (and there Alteration Porducts) from Mafic Igneous Rocks, *Icarus*, 33, 483-513, 1978.
- Gooding, J.L., S.J. Wentworth, and M.E. Zolensky, Calcium Carbonate and sulfate of possible extraterrestrial origin in the EETA 79001 meteorite, *Geochim. et. Cosmochim. Acta*, 52, 909-915, 1988.
- Greeley, R. and P. Spudis, Volcanism on Mars, *Rev. of Geophys. and Space Phys.*, 19 , 13-41, 1981.
- Encranaz, T., On the atmospheric origin of weak absorption features in the infrared

spectrum of Mars, submitted to *J. Geophys. Res.*, 1989.

Evans, D.L. and J.B. Adams, Amorphous gels as possible analogs to Martian weathering products, *Proc. Lunar Planet. Sci. Conf. 11th*, 757-763, 1980.

Greeley, R. and P. Spudis, Volcanism on Mars, *Rev. of Geophys. and Space Phys.*, 19, 13-41, 1981.

Hanel, R.A., V.J. Kunde, B.J. Conrath, and J. Pearl, Mariner 9 infrared interferometer spectrometer (IRIS) reduced data records documentation, NASA TM-70504, 48pp, 1973.

Hawke, B. R., P. G. Lucey, P. D. Spudis, P. D. Owensby, Impact structures as crustal probes, (abstract), *Lunar and Planetary Science XX*, 389-390, Lunar and Planetary Institute, Houston, Texas, March 1989.

Herr K.C. and G.C. Pimental, Infrared absorptions near three microns recorded over the polar cap of Mars, *Science*, 166, 496-498, 1969.

Houck, J.R., J.B. Pollack, C. Sagan, P. Schack, and J.A. Pecker, High altitude infrared spectroscopic evidence for bound water on Mars, *Icarus*, 18, 3, 470-479, 1973.

Huguenin, R.L., and L. Harris, Accreted H₂O inventory on Mars, *Proc. Workshop on the Evolution of the Martian Atmosphere*, Honolulu, *Technical Report*, 86-07, 19-22, Lunar and Planetary Institute, Houston, TX, 1986.

Hunt, G.R. and J.W. Salisbury, Visible and near-infrared spectra of minerals and rocks, I, Silicate minerals, *Mod. Geol.* 1, 283-300 (1970).

Kieffer, S.W., and C.H. Simonds, The role of volatiles and lithology in the impact cratering process, *Rev. of Geophys. and Space Phys.*, 18, 143-181, 1980.

Masursky, H., J.M. Boyce, A.L. Dial, G.G. Schaber, and M.E. Strobell, Formation of martian channels, *J. Geophys. Res.*, 82, 4016-4038, 1977.

- McCord, T.B., R.N. Clark, and R.B. Singer, Mars: Near-infrared reflectance spectra of surface regions and compositional implication, *J. Geophys. Res.*, **87**, 3021-3032, 1982.
- McElroy, M.B., T.Y. Kong, and Y.L. Yung, Photochemistry and evolution of Mars' atmosphere: A Viking perspective, *J. Geophys. Res.*, **82**, 4379-4388, 1977.
- McKay, C.P., and S.S. Nedeli, Are there carbonate deposits in the Valles Marineris, Mars?, *Icarus*, **73**, 142-148, 1988.
- McSween, H.Y., SNC Meteorites: Clues to Martian petrologic evolution?, *Rev. Geophys.*, **23**, 391-416, 1985.
- Morgan, J.W., and E. Anders, Chemical composition of Mars, *Geochim. Cosmochim. Acta.*, **43**, 60-76, 1979.
- Moroz, V.I., The Infrared Spectrum of Mars (1.1 - 4.1 μ), *Soviet Astronomy*, **8**, 273-281, 1964.
- Nakamoto, Kuzuo, *Infrared Spectra of Inorganic and Coordination Compounds*, John Wiley and Sons, Inc., New York, New York, 328p., 1963.
- Nash, D.B., Mid infrared reflectance spectra (2.3-22 μ m) of sulfur, gold, KBr, and MgO and halon, *Applied Optics*, **25**, 2427-2433, 1986.
- Neukum, G. and K. Hiller, Martian Ages, *J. Geophys. Res.*, **86**, 3097-3121, 1982.
- Phinney, W.C., C.H. Simonds, A. Cochran, and P.E. McGee, West Clearwater, Quebec impact structure II, Petrology, *Proc. Lunar Sci. Conf. 9th.*, 2659-2693, 1978.
- Piere, D.C., Martian Valleys: Morphology, distribution, age, and origin, *Science*, **210**, 895-897, 1980.
- Pieters, C. M., Stratigraphy of the lunar crust, (abstract), *Lunar and Planetary Science XX*, 848-849, Lunar and Planetary Institute, Houston, Texas, March 1989.

- Pimmetel G. C., P.B. Forney, and K.C. Herr, Evidence about Hydrate and Solid Water in the Martian Surface from the 1969 Mariner Infrared Spectrometer, *J. Geophys. Res.*, 79, 1623-1634, 1974.
- Pollack, J. B., Climate change on the terrestrial planets. *Icarus* 37, 479-553, 1979.
- Pollack, J.B., and D.C. Black, Implications of the gas compositional measurements of Pioneer Venus for the origin of planetary atmospheres, *Science*, 205, 56-59, 1979.
- Pollack, J. B., and Yung, Y. L., Origin and evolution of planetary atmospheres. *Ann. Rev. Earth Planet. Sci.* 8, 425-487, 1980.
- Pollack, J. B., Kasting, J. F., Richardson, S. M., and Poliakov, K., The case for a wet warm climate on early Mars. *Icarus* ,71, 203-224, 1987.
- Postowko S.E. and W.R. Kuhn, Effects of the greenhouse gases (CO₂, H₂O, and SO₂) on Martian paleoclimate. *J. Geophys. Res.*, 82, 4635-4639, 1986.
- Roth, L.E., R.S. Saunders, and G. Schubert, Mars: Seasonally variable radar reflectivity (abstract), *Lunar and Planetary Science XVI*, 712-713, Lunar and Planetary Institute, Houston, TX, 1985.
- Roush, T.L., D. Blaney, T.B. McCord, R.B. Singer, Carbonates on Mars: Searching the Mariner 6 and 7 IRS measurements (abstract), *Lunar and Planetary Science XVII*, 732-733, Lunar and Planetary Institute, Houston, Texas, 1986.
- Roush, T., J. Pollack, C. Stoker, F. Witteborn, J. Bregman, D. Wooden, and D. Rank (1989b) CO₃(²⁻)- and SO₄(²⁻)-Bearing Anionic Complexes Detected in Martian Atmospheric Particulates, Presented at the Fourth International Conference on Mars, Tucson, Arizona, January, 1989.

- Roush, T., J. Pollack, C. Stoker, F. Witteborn, J. Bregman, D. Wooden, and D. Rank (1989b) CO₃(²⁻)- and SO₄(²⁻)-Bearing Anionic Complexes Detected in Martian Atmospheric Dust, Submitted to 20th Lunar and Planetary Science Conference, Lunar and Planetary Institute, Houston, Texas, March, 1989.
- Scott, D. H., and M. H. Carr, *Geologic Map of Mars*, U. S. Geol. Survey, Misc. Inv. Map I-1083, 1978.
- Schultz, P., The Martian atmosphere before and after the Argyre impact, *Proc. Workshop on The Evolution of the Martian Atmosphere*, Honolulu, *Tech. Report 86-07*, 38-39, Lunar and Planetary Institute, Houston, TX, 1986.
- Settle, M., Formation and deposition of volcanic sulfate aerosols on Mars, *J. Geophys. Res.*, *84*, 8,343-8,354, 1979.
- Sharp, R.P., Mars: Fretted and chaotic terrains, *J. Geophys. Res.*, *78*, 4073-4083, 1973a.
- Sharp, R.P., Mars Troughed terrain, *J. Geophys. Res.*, *78*, 4063-4072, 1973b.
- Sharp, R.P., Mars: South polar pits and etche terrain, *J. Geophys. Res.*, *78*, 4222-4230, 1973c.
- Sidorov Yu. I. and M. Yu Zolotov, Weathering of Martian surface rocks. In S.K. Saxena (ed.), *Chemistry and Physics of Terrestrial Planets*, Adv. Geochem. Vol. 6, Springer-Verlag, New York, p. 191-223, 1986.
- Singer, R.B. Spectral evidence for the mineralogy of high-albedo soils and dust on Mars, *J. Geophys. Res.* *87*, 10159-1016, 1982.
- Sinton, W.M., Spectroscopic evidence for Vegetation on Mars, *Astrophys. J.*, *126*, p.231-238, 1957.
- Sinton, W.M., On the Composition of the Martian Surface Materials, *Icarus*, *6*, 222-228, 1967.

- Soderblom, L. S., Kriedler, T. J., and Masursky, H., 1973. Latitudinal distribution of a debris mantle on the martian surface. *J. Geophys. Res.* 78, 4117-4122.
- Soderblom L.A. and D.B. Wenner (1978) Possible fossil water liquid-ice interfaces in the martian crust, *Icarus*, 34, 622-637.
- Spencer and Croft, *MECA Workshop on the Evolution of the Martian Atmosphere*, LPi Technical Report 86-07, p.40-41, 1986.
- Spencer, J.R. , F.P. Fanale, and J.E. Tribble, Karst on Mars? Origin of Closed Depressions in Valles Marineris by Solution of Carbonates in Groundwater Sulfuric Acid, in *Fourth Int. Conf. on Mars, Tuscon Az, Jan 10-13*, p.193-194, 1989.
- Squyres, S. W., Early Mars: Wet and warm, or just wet? (abstract). *Fourth International Conference on Mars. Tucson, AZ., Tuscon Az, Jan 10-13*, p.193-194, 1989a.
- Squyres, S. W., Early Mars: Wet and warm, or just wet? (abstract), *Lunar and Planetary Science XX*, 1044-1045, Lunar and Planetary Institute, Houston, Texas, March 1989b.
- Squyres, S. W., and Carr, M. H., 1986. Geomorphic evidence for the distribution of ground ice on Mars. *Science*, 231, 249-252.
- Stahle, V., and J. Ottemann, Ries-Forschungsbohrung 1973: Zeolithisierung der glaser in suevit und petrographic der Beckensuevite und gangbreccian, *Geol. Bavarica*, 75, 191-217, 1977.
- Stoffler, D., U. Ewald, R. Ostertag, and W.U. Reimold, Research drilling Nordlingen 1973, (Ries) composition and texture of polymict impact breccias, *Geol. Bavarica*, 75, 163-190, 1977.
- Stolper, E.M., and H.Y. McSween Jr., Petrology and origin of the shergottite meteorites, *Geochim. Cosmochim. Acta.*, 43, 1475-1498, 1979.

- Tokunaga, A.T., R.G. Smith, E. Irwin, Use of a 32-element reticon array for 1-5 micrometer spectroscopy, *Infrared Astronomy with Arrays*, Wynn-Williams and Becklin eds., p. 367-378, 1987.
- Toulmin, P., A.K. Baird, B.C. Clark, K. Keil, H.J. Rose, R.P. Christian, P.H. Evans, and W.C. Kelliher, Geochemical and mineralogical interpretation of the Viking inorganic chemical results, *J. Geophys. Res.*, 82, 4625-4634, 1977.
- U.S. Geol. Survey, *Shaded Relief Map of Eastern Mars*, U.S. Geol. Survey Map I-1535, 1985.
- Wallace, D., and C. Sagan, Evaporation of ice in planetary atmospheres: Ice covered rivers on Mars, *Icarus*, 39, 385-400, 1979.
- Walsh, P.A., D.L. Blaney, and T.B. McCord, Martian surface analogs: Laboratory spectral studies in the mid infrared. *Mars Evolution of Volcanism, Tectonism and Volatiles Meeting*, Napa Valley, CA, December, 1987.
- Walsh, P.A., *A Spectroscopic Study of Mars Surface Analogs*, master thesis, University of Hawaii at Manoa, defense pending 1989.
- Warren, P.H., Mars Regolith versus SNC Meteorites: Possible Evidence for Abundant Crustal Carbonates, *Icarus*, 70, 153-161, 1987.
- Watkins, G.H., and J.S. Lewis, Evolution of the atmosphere of Mars as the result of asteroidal and cometary impacts, *Proc. Workshop on the Evolution of the Martian Atmosphere*, Honolulu, *Technical Report, 86-07*, 46-47, Lunar and Planetary Institute, Houston, TX, 1986.
- Yung, Y.L., and M.B. McElroy, Fixation of nitrogen in the prebiotic atmosphere, *Science*, 203, 1002-1004, 1979.
- Young, L. D. G. and A. T. Young, Interpretation of high-resolution spectra of Mars. IV. New calculations of the CO abundance. *Icarus*, 30, 75-79, 1977.

Zent, A.P., and F.P. Fanale, Possible Mars brines: Equilibrium and kinetic considerations, *J. Geophys. Res.*, 91, D439-D445, 1986.

Zisk, S.H., and P.J. Mouginis-Mark, Anomalous region on Mars: Implications for near-surface liquid water, *Nature*, 44, 735-738, 1980.